

# Dynamic System Analysis of Receptor Interaction and Effectuation Mechanisms of Digoxin in the Rat Heart

## Dissertation

Zur Erlangung des akademischen Grades  
*doctor rerum naturalium* (Dr. rer. nat)

vorgelegt der

Mathematisch-Naturwissenschaftlich-Technischen Fakultät  
der Martin-Luther-Universität Halle-Wittenberg

von Myoungki Baek, MS.  
geb. 02. 09. 1970 in Daejon, Südkorea

Gutachter:

1. Prof. Dr. Michael Weiss
2. Prof. Dr. Reinhard Neubert
3. Prof. Dr. Richard Süverkrüp

Halle (Saale), den 06. 04. 2005

**urn:nbn:de:gbv:3-000008190**

[<http://nbn-resolving.de/urn/resolver.pl?urn=nbn%3Ade%3Agbv%3A3-000008190>]



# Table of Contents

1. Introduction	
1.1 Cardiac glycosides .....	1
1.2 Physiology of cardiac muscle .....	4
1.3 Inotropic response of cardiac glycosides .....	6
1.3.1 Inhibition of Na <sup>+</sup> ,K <sup>+</sup> -ATPase .....	6
1.3.2 Role of Na <sup>+</sup> /Ca <sup>2+</sup> Exchanger .....	7
1.4 Disease states .....	10
1.5 PK/PD modeling .....	11
1.6 Purpose .....	14
2. Materials and Method	
2.1 Materials .....	16
2.2 Isolated perfused heart .....	17
2.3 Experimental protocol .....	19
2.4 Hypertrophy inducement .....	19
2.5 Sepsis inducement .....	20
2.6 Determination of digoxin in perfusate .....	20
3. Model development and data analysis	
3.1 Mechanistic model of digoxin .....	21
3.1.1 Myocardial uptake and binding processes .....	21
3.1.2 Kinetics of receptor binding and cellular effectuation .....	23
3.2 Data analysis .....	25
3.3 Statistics .....	29
4. Results and Discussion	
4.1 Cardiac uptake of digoxin .....	30
4.2 Receptor binding kinetics of digoxin .....	31
4.3 Generation of cellular response to digoxin .....	34
4.4 Model validity .....	36

4.5 Effect of external Ca <sup>2+</sup> and NCX inhibition .....	39
4.5.1 Measurement of outflow concentration and cardiac performance .....	39
4.5.2 PK/PD parameter estimation .....	42
4.5.3 Simulated response characteristics .....	46
4.5.4 Functional receptor heterogeneity .....	49
4.5.5 Receptor occupancy-response relationship .....	50
4.5.6 Effect of external calcium concentration .....	51
4.5.7 Effect of NCX inhibition by KB-R7943 .....	52
4.6 Effect of leftventricular hypertrophy on uptake, receptor binding and inotropic response of digoxin .....	54
4.6.1 Baseline cardiac function in normal and hypertrophied rats .....	54
4.6.2 Outflow concentration and inotropic response to digoxin .....	55
4.6.3 Model analysis .....	56
4.6.4 Capacity and affinity of digoxin binding sites .....	60
4.6.5 Occupancy-response relationship .....	61
4.7 Endotoxin induced alterations in inotropic effect of digoxin .....	68
4.7.1 Baseline cardiac function in normal and sepsis rats .....	68
4.7.2 Outflow concentrations and inotropic response to digoxin .....	70
4.7.3 Capacity and affinity of digoxin .....	71
4.7.4 Occupancy-response relationship .....	75
5. Summary .....	79
6. Zusammenfassung und Ausblick .....	81
7. References .....	83

Publications

Acknowledgement

Curriculum Vitae

## List of Abbreviations

AIC	Akaike information criterion
ANOVA	Analysis of variance
AT	Atrial
AUC	Area under the concentration-time curve
AUEC	Area under the effect-time curve
CHF	Congestive Heart Failure
CPP	Coronary perfusion pressure
CVR	Coronary vascular resistance
EC	Excitation-Contraction
GEN-IC	Generalized information criteria
HR	Heart rate
IL	Interleukin
ISO	Isopreterenol
KBR	KB-R7943
LPS	Lipopolysaccharides
LSC	Liquid Scintillation Counter
LSC	Liquid Scintillation Counter
LV	Left ventricular
LVDP	Left ventricular developed pressure
LVEDP	Left ventricular end-diastolic pressure
LVSP	Left ventricular systolic pressure
MAP	Maximum a posteriori probability
NCX	Na <sup>+</sup> /Ca <sup>2+</sup> Exchanger
PK/PD	Pharmacokinetics/Pharmacodynamics
RV	Right ventricular
SNLR	Simultaneous nonlinear regression
SR	Sarcoplasmic reticulum
TNF	Tumor Necrosis Factor

## 1. INTRODUCTION

### 1.1 Cardiac glycosides

The cardiac glycosides are an important class of naturally occurring drugs which actions include both beneficial and toxic effects on the heart, and have played an outstanding role in the therapy of congestive heart failures (CHF) since William Withering codified their use in his classic monograph on the efficacy of the leaves of the common foxglove plant (*Digitalis Purpurea*) in 1785 (Willius, 1941). The terms ‘cardiac glycoside’ or ‘digitalis’ are used throughout to refer to any of steroid or steroid glycoside compounds that exert characteristic positively inotropic effect on the heart.

The cardiac glycosides are composed of two structural features; the sugar (glycoside) and the non-sugar (aglycon) moieties.

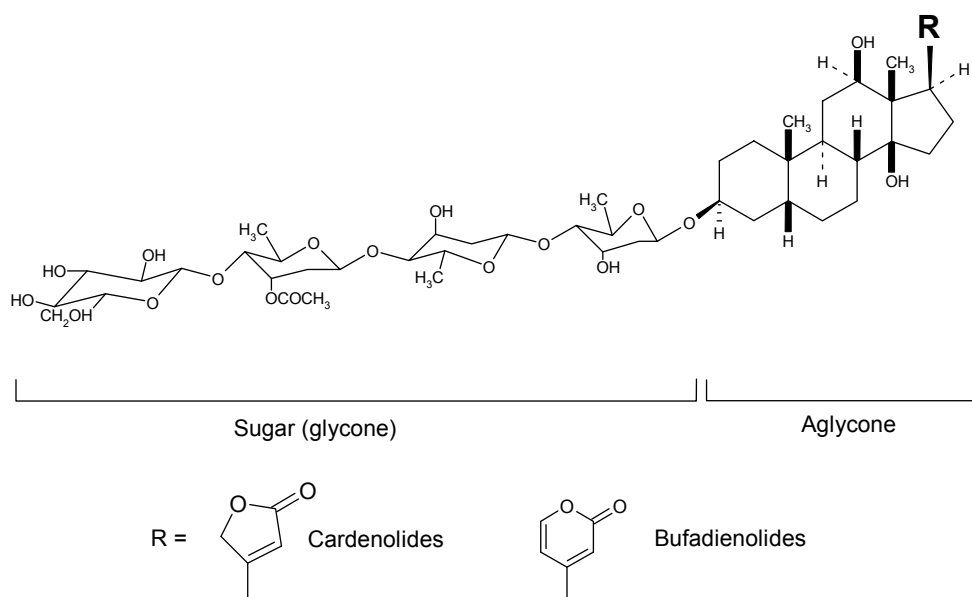


**Figure 1.** Chemical structure of cardiac glycosides.

The R group at the 17-position defines the class of cardiac glycosides, and two classes have been observed in nature, Cardenolides and Bufadienolides according to their chemical structure (Fig. 1). *Digitalis Purpurea*, *Digitalis lanata*, *Strophanthus gratus* and *Strophanthus kombe* are the major source of cardiac glycosides and digoxin, digitoxin, and ouabain (G-strophanthin) are well known cardiac glycosides.

Digoxin, which is extracted from *Digitalis lanata*, is one of the cardiac glycosides, a closely related group of drugs having in common specific effects on the myocardium.

Digoxin is described chemically as (3 $\beta$ ,5 $\beta$ ,12 $\beta$ )-3-[O-2,6-dideoxy- $\beta$ -D-ribo-hexopyranosyl-(1 $\rightarrow$ 4)-O-2,6-dideoxy- $\beta$ -D-ribo-hexopyranosyl-(1 $\rightarrow$ 4)-2,6-dideoxy- $\beta$ -D-ribo-hexopyranosyl]oxy]-12,14-dihydroxy-card-20(22)-enolide. The chemical structure of digoxin is shown in Fig. 2, its molecular formula is C<sub>41</sub>H<sub>64</sub>O<sub>14</sub>, and its molecular weight is 780.95.

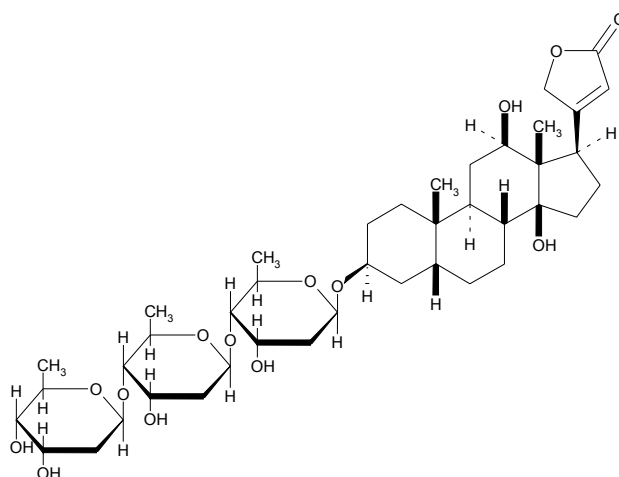


**Figure 2.** Chemical structure of digoxin.

Digoxin is clinically used for treatment of congestive heart failure (CHF), slows the ventricular rate in tachyarrhythmias such as atrial fibrillation, atrial flutter, supraventricular tachycardia. Digoxin is a one representative therapeutic drug monitor (TDM) drug due to its narrow therapeutic window, the therapeutic range of digoxin is 0.5 ~ 1.5 ng/ml. And minimal effect concentration is about 0.5 ng/ml and toxic adverse effect generating concentration is about 2.5 ng/ml. In general, following drug administration, a 6 ~ 8 hours tissue distribution phase is observed. This is followed by a much more gradual decline in the serum concentration of the drug, which is dependent on the elimination of digoxin from the body. Digoxin is concentrated in tissue (binding to Na<sup>+</sup>,K<sup>+</sup>-ATPase of skeletal muscle) and therefore has a large apparent volume of distribution, and approximately 25 % of digoxin in the plasma is bound to protein, only a small percentage (16 %) of digoxin is metabolized.

## 1. Introduction

Digoxin inhibits  $\text{Na}^+, \text{K}^+$ -ATPase, an enzyme that regulates the quantity of sodium and potassium inside cells. Inhibition of the enzyme leads to an increase in the intracellular concentration of sodium and thus (by stimulation of  $\text{Na}^+/\text{Ca}^{2+}$  exchange) to an increase in the intracellular concentration of calcium (Fig. 3); in other words, intracellular  $\text{Ca}^{2+}$  availability for contractile protein results in an increase in positive inotropy (Levi et al., 1994).

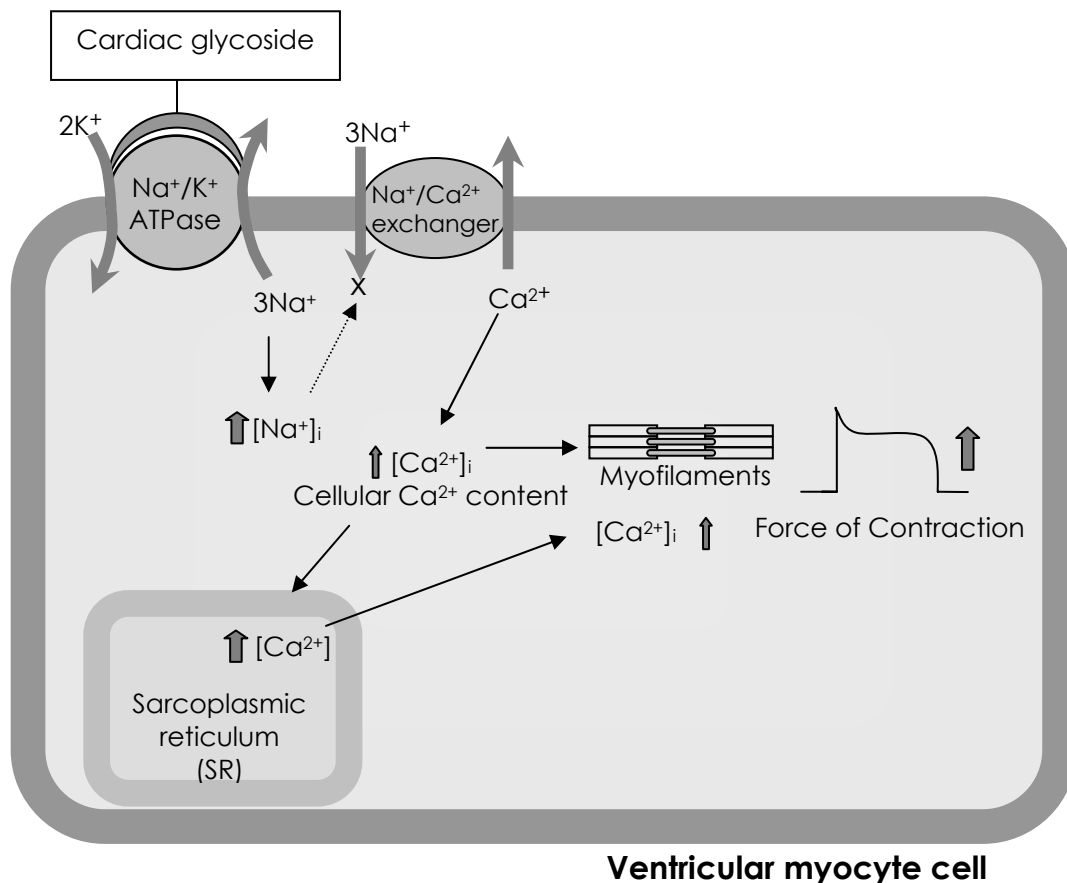


**Figure 3.** A schematic diagram to illustrate the effect of a cardiac glycoside in a heart muscle cell.



### 1.2 Physiology of cardiac muscle

The contractile mechanism in cardiac muscle depends on some proteins, myosin, actin, troponin, and tropomyosin and it has contractile mechanism that is activated by the action potential. The initial rapid depolarization and the overshoot (phase 0) are due to a rapid increase in sodium conductance via  $\text{Na}^+$  channel opening and upstroke ends as  $\text{Na}^+$  channels are rapidly inactivated. The initial rapid repolarization (phase 1) is due to inactivation of  $\text{Na}^+$  channel and  $\text{K}^+$  channel rapidly open and close causing a transient outward current. The subsequent prolonged plateau (phase 2) is due to a slower but prolonged opening of voltage-gated  $\text{Ca}^{2+}$  channels, that results in slow inward current that balances the slow outward leak of  $\text{K}^+$ . Final repolarization (phase 3) is due to closure of the  $\text{Ca}^{2+}$  channel and prolonged opening of  $\text{K}^+$  channels, this restores the resting potential (phase 4). The action to this point is a net gain of  $\text{Na}^+$  and loss of  $\text{K}^+$ . This imbalance is corrected by  $\text{Na}^+, \text{K}^+$ -ATPase.

Cardiac glycosides increase cardiac contractions by inhibiting the  $\text{Na}^+, \text{K}^+$ -ATPase in cell membrane of the muscle fibers. The resultant increase in intracellular  $\text{Na}^+$  increases the efflux of  $\text{Na}^+$  in exchange for  $\text{Ca}^{2+}$  via  $\text{Na}^+/\text{Ca}^{2+}$ -exchanger in cell membrane. The development of contraction force depends on intracellular free  $\text{Ca}^{2+}$  concentration, and the physiological contraction generates both isometric force, i.e., ventricular pressure, and rapid shortening to eject blood. The role of  $\text{Ca}^{2+}$  in excitation and contraction coupling, depolarization due to opening of  $\text{Na}^+$  channels activates the  $\text{Ca}^{2+}$  channels and it is the resulting influx of  $\text{Ca}^{2+}$  from the extracellular fluid that triggers release of  $\text{Ca}^{2+}$  from the sarcoplasmic reticulum (SR). The strength of cardiac contraction is changed by altering the amplitude or duration of the  $\text{Ca}^{2+}$  transient. And then,  $\text{Ca}^{2+}$  must be removed from the cytosol to lower intracellular free  $\text{Ca}^{2+}$  concentrations and allows relaxation (Fig 3). This is achieved by several routes, the quantitative importance of which varies between species. In rabbit ventricular myocytes, more like to that of human, the SR  $\text{Ca}^{2+}$ -ATPase pump removes 70% of the activator  $\text{Ca}^{2+}$ , and  $\text{Na}^+/\text{Ca}^{2+}$  exchanger (NCX) removes 28%, leaving only about 1% each to be removed by the sarcolemmal  $\text{Ca}^{2+}$ -ATPase and mitochondrial  $\text{Ca}^{2+}$  uniporter. The activity of SR  $\text{Ca}^{2+}$ -ATPase is higher in rat ventricle than in rabbit and human, and  $\text{Ca}^{2+}$  removal through  $\text{Na}^+/\text{Ca}^{2+}$  exchanger is lower, resulting in a balance of 92% for SR  $\text{Ca}^{2+}$  ATPase, 7% for NCX and 1% for the slow system, removed by sarcolemmal  $\text{Ca}^{2+}$ -ATPase and mitochondrial uniport. Thus,

## 1. Introduction

mouse and rat ventricle (which also show very spikelike action potentials) poorly mimic human with respect to the quantitative balance of cellular  $\text{Ca}^{2+}$  flux (Fig. 4).

Cardiac glycosides are widely used in the treatment of congestive heart failure because the inhibition of  $\text{Na}^+, \text{K}^+$ -ATPase ( $\text{Na}^+$  pump), which serves as a functional receptor for digitalis, results in an increase in positive inotropy. Binding of digitalis drugs, such as digoxin, to the catalytic  $\alpha$ -subunit inhibits the sodium pump and increases intracellular  $\text{Ca}^{2+}$  availability for contractile proteins with stimulation of  $\text{Na}^+/\text{Ca}^{2+}$  exchanger (NCX).

The rat is known to be rather insensitive to cardiac glycosides due to its higher intracellular  $\text{Na}^+$  concentration. Repke et al., (1965) found that species variations in susceptibility to cardiac glycosides correspond to variations in the susceptibility of the cardiac  $\text{Na}^+, \text{K}^+$ -ATPase to these drugs. Rat heart  $\text{Na}^+, \text{K}^+$ -ATPase activity is half-maximally inhibited by ouabain in a concentration of  $5.9 \times 10^{-5}$  M whereas this value for the enzyme for human heart is  $2.5 \times 10^{-9}$  M.

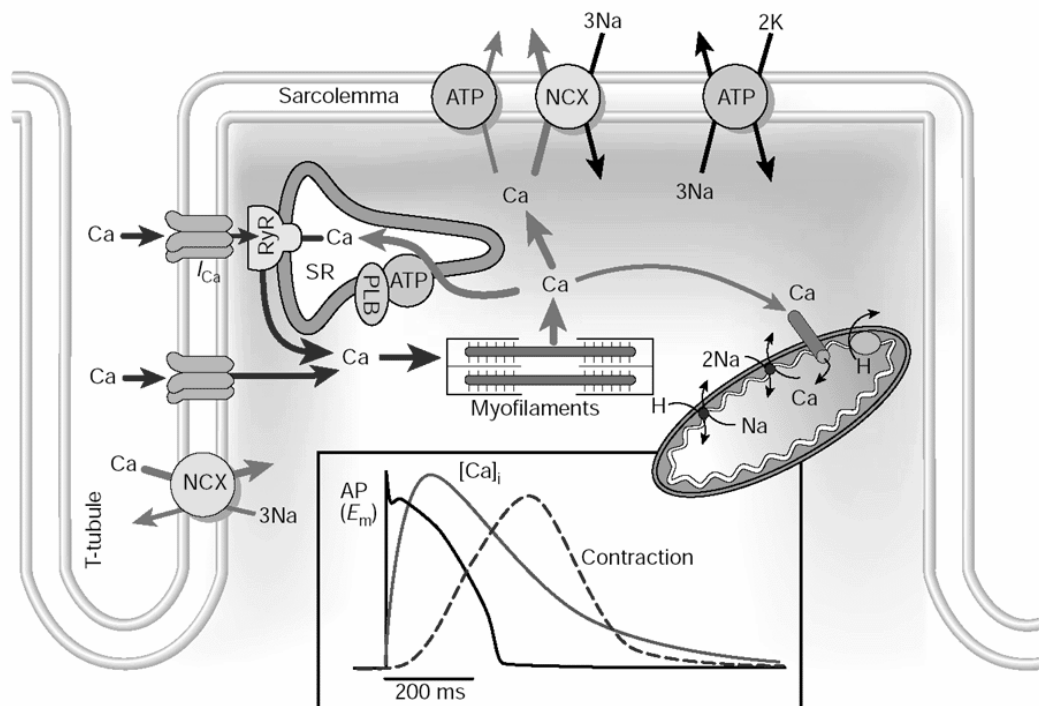


**Figure 4.** General scheme of  $\text{Ca}^{2+}$  cycle in a cardiac ventricular myocyte. (from D.M. Bers 2002).

And it is well known that both rat and mouse hearts are unique compared to all other species where intracellular  $\text{Na}^+$  is higher; at a concentration of calcium in the range used by the authors, both species exhibit a negative force-frequency, a very short action potential and a marked insensitivity to cardiac glycosides (Serikov et al., 2001; Chevalier et al., 1987; Capogrossi et al., 1986). All of the latter are due to a major difference in the distribution of intracellular calcium, with most of the calcium derived from the SR in rat and mouse heart as opposed to all other mammalian species. Further upon stimulation or twitches, the rat and mouse hearts accrue calcium while the rabbit and guinea pig extrude calcium. Therefore, the rat heart is already “loaded” with calcium during stimulation. In order to measure normal physiological and pharmacological responses, it is necessary to utilize much lower concentrations of calcium in perfusion media.

### 1.3 Inotropic response of cardiac glycosides

#### 1.3.1 $\text{Na}^+, \text{K}^+$ -ATPase

The  $\text{Na}^+, \text{K}^+$ -ATPase is a heteromeric protein consisting of  $\alpha$  and  $\beta$  subunits.  $\text{Na}^+, \text{K}^+$ -ATPase is also called sodium pump, and it is the protein that is responsible for establishing and maintaining the electrochemical gradient for  $\text{Na}^+$  and  $\text{K}^+$  ions across the plasma membrane of mammalian cells. In the heart, the  $\text{Na}^+, \text{K}^+$ -ATPase has additional importance as the target for cardiac glycosides which are used in the treatment of heart failure and atrial fibrillation. By blocking the catalytic activity of the enzyme, cardiac glycosides increase intracellular  $\text{Na}^+$  concentration at least locally, which leads to an increased  $\text{Ca}^{2+}$  content of the cell via  $\text{Na}^+/\text{Ca}^{2+}$  exchanger and enhanced contractility. While the  $\alpha$  subunit of the  $\text{Na}^+, \text{K}^+$ -ATPase contains the amino acids involved in catalytic function and the ion, nucleotide and cardiac glycoside binding sites, the function of the  $\beta$  subunit is not completely understood. The  $\beta$  subunit is essential, however, for the normal activity of the enzyme and is involved in the transport of the functional  $\text{Na}^+ - \text{K}^+$ -ATPase to the plasma membrane. Several isoforms of the  $\text{Na}^+, \text{K}^+$ -ATPase have been identified for both  $\alpha$  ( $\alpha_1$ ,  $\alpha_2$ ,  $\alpha_3$ , and  $\alpha_4$ ) and  $\beta$  subunits ( $\beta_1$ ,  $\beta_2$ , and  $\beta_3$ ), which are expressed in a tissue specific manner. While  $\alpha_1$

isoform is expressed in most tissue,  $\alpha_2$  is predominant in skeletal muscle and can be detected in the brain and heart (Wang et al., 1996), whereas  $\alpha_3$  is found in excitable tissue and  $\alpha_4$  was found in testis. Similarly,  $\beta_1$  appears to be ubiquitously expressed, whereas the  $\beta_2$  and  $\beta_3$  isoforms are mostly found in neural tissue, skeletal muscle or lung and liver. In the human heart,  $\alpha_1$ ,  $\alpha_2$ , and  $\alpha_3$  together with  $\beta_1$  and a low level of  $\beta_2$  are expressed in a region specific manner. In the adult rat heart, mainly two receptor isoforms,  $\alpha_1$  and  $\alpha_2$ , are expressed exhibiting low and high affinity, respectively for digitalis (McDonough et al., 1995; Sweadner, 1993; Verdonck et al., 2003).  $\text{Na}^+, \text{K}^+$ -ATPase isoforms can differ greatly in their affinity for cardiac glycosides.

Binding of digitalis drugs, such as digoxin, to the catalytic  $\alpha$ -subunit inhibits the sodium pump and increases intracellular  $\text{Ca}^{2+}$  availability for contractile proteins. The cardiac actions of digitalis glycosides and the “pump-inhibition hypothesis” have been critically reviewed (Eisner and Smith, 1992; Levi et al., 1994). In the rat, consecutive inhibition of the  $\alpha_2$ - and the  $\alpha_1$ - isoforms of  $\text{Na}^+, \text{K}^+$ -ATPase with high and low affinity, respectively, for ouabain, induces positive inotropic effect over wide dose range (Grupp et al., 1985; Sweadner, 1993; McDonough et al., 1995; Schwartz et al., 2001). Despite fundamental new insights obtained in the last decades at the enzyme and cellular level by biochemical and electrophysiological studies, but there is limited knowledge about the functional role of  $\text{Na}^+, \text{K}^+$ -ATPase isoforms in the intact heart. Although recent evidence suggests that the  $\alpha_2$ -isoform may have a special function in the regulation of intracellular  $\text{Ca}^{2+}$  (Blaustein and Lederer, 1999; James et al., 1999), implying that only this single isoform mediated the glycoside action, this view is still controversial (Gao et al., 1995; Kometiani et al., 2001; Schwartz et al., 2001).

### 1.3.2 Role of $\text{Na}^+/\text{Ca}^{2+}$ exchanger

The  $\text{Na}^+/\text{Ca}^{2+}$  exchanger (NCX) is a major regulator of intracellular  $\text{Ca}^{2+}$  in many types of cells and plays a particularly important regulatory function in cardiac myocytes (Reuter et al., 2002). In normal cardiac myocytes, the electrogenic NCX extrude calcium (forward mode three  $\text{Na}^+$  in and one  $\text{Ca}^{2+}$  out) contributing significantly to muscle relaxation. Thus, under steady state conditions,  $\text{Ca}^{2+}$  influx, primarily through L-type  $\text{Ca}^{2+}$  channels during systole, is matched by  $\text{Ca}^{2+}$  efflux (via NCX and to a less

extent by sarcolemmal  $\text{Ca}^{2+}$  pump) during diastole. As a result, there is no net increase or decrease in intracellular free  $\text{Ca}^{2+}$  concentration. However, during ischemic conditions, intracellular calcium rises dramatically leading to  $\text{Ca}^{2+}$  overload that precipitates cellular dysfunction. Alteration in NCX function can contribute to the ischemically-induced calcium overload. As a consequence of ATP depletion, the  $\text{Na}^+, \text{K}^+$ -ATPase can no longer function properly and cellular  $\text{Na}^+$  levels increase. Elevations in intracellular sodium reverse the direction of the NCX so that sodium is extruded and calcium is taken up by the cell. This increased calcium entry and the resulting membrane current may lead to afterdepolarizations that trigger ventricular arrhythmias. Therefore, suppression of the NCX may be beneficial, reducing calcium overload and enhancing the electrical stability of the heart.

NCX extrude ~ 30 % of the  $\text{Ca}^{2+}$  required to activate the myofilaments in rabbit, guinea pig, and human ventricles but a much smaller portion (7 %) in rat and mouse ventricles. The mammalian NCX forms a multigene family of homologous proteins comprising 3 isoforms: NCX1, NCX2, and NCX3. These isoforms share ~ 70 % amino acid identity in the overall sequences and thus presumably have a very similar molecular structure. NCX1 is the first NCX cloned and is highly expressed in cardiac muscle and brain and to a less extent in many other tissues. NCX2 and NCX3 are not expressed in adult rat hearts at the protein level, the density of NCX1 per unit membrane capacities is 2 to 4 fold larger in guinea pig and hamster myocytes than in rat myocytes. Immunocytochemically, NCX1 is located in the T-tubule membrane as well as in the peripheral sarcolemmal and the intercalated disks in rat and guinea pig ventricular myocytes.

The  $\text{Na}^+/\text{Ca}^{2+}$  exchanger (NCX) is a cation transporting protein present in the plasma membrane of animal cells. NCX transports three  $\text{Na}^+$  in exchange for one  $\text{Ca}^{2+}$  and that is electrogenic; the function of the exchanger is controlled by the gradients for  $\text{Na}^+$  and  $\text{Ca}^{2+}$  across the cell membrane and membrane potential. In normal cardiac myocytes, NCX plays an important role in  $\text{Ca}^{2+}$  homeostasis. NCX functions in a forward mode, in which  $\text{Na}^+$  enters the cell and  $\text{Ca}^{2+}$  is extruded. The rate of  $\text{Ca}^{2+}$  extrusion by NCX is much greater than by the sarcolemmal  $\text{Ca}^{2+}$  pump, and Bridge et al. (1990) have shown that NCX extrudes the amount of  $\text{Ca}^{2+}$  that enters the cell via the L-type  $\text{Ca}^{2+}$  channel as  $\text{Ca}^{2+}$  current, thus maintaining  $\text{Ca}^{2+}$  homeostasis on a beat-to-beat basis. As NCX extrudes  $\text{Ca}^{2+}$  and thus lowers  $\text{Ca}^{2+}$  from its peak, it contributes to relaxation in parallel

with  $\text{Ca}^{2+}$  uptake by the sarcoplasmic reticulum (SR)  $\text{Ca}^{2+}$ -ATPase. The extent to which NCX contributes to the decline of the  $\text{Ca}^{2+}$  transient varies between species because the relative balance between the activities of these two  $\text{Ca}^{2+}$  removal systems is influenced by their level of expression, the  $[\text{Na}^+]_i$ , and the duration of the action potential. In rats and mice, which have a high level of activity of the SR  $\text{Ca}^{2+}$ -ATPase and a relatively high  $[\text{Na}^+]_i$ , NCX is responsible for only  $\sim 10\%$  of relaxation. In rabbits, which have a lower  $[\text{Na}^+]_i$  and SR  $\text{Ca}^{2+}$ -ATPase activity, NCX contributes more significantly to the decline of the  $\text{Ca}^{2+}$  transient, especially during the terminal phase of the transient.

NCX can also produce  $\text{Ca}^{2+}$  influx by operating in the reverse mode. Electrochemical considerations indicate that early after the upstroke of the action potential, before a rise in intracellular  $[\text{Ca}^{2+}]_i$  occurs because of  $\text{Ca}^{2+}$ -induced  $\text{Ca}^{2+}$  release,  $\text{Ca}^{2+}$  influx on the exchanger will occur.  $\text{Ca}^{2+}$  influx can also occur after the decline of the  $[\text{Ca}^{2+}]_i$  transient if the duration of the action potential is long. The magnitude of this influx is dependent on the magnitude and rate of rise of the  $[\text{Ca}^{2+}]_i$  transient, the density of NCX in the sarcolemmal membrane, and the  $[\text{Na}^+]$  adjacent to NCX in the subsarcolemmal space, which is influenced by the  $\text{Na}^+$  pump activity and  $I_{\text{Na}}$  as well as by the bulk cytosolic  $[\text{Na}^+]$ . The functional importance of reverse-mode NCX ( $\text{Ca}^{2+}$  influx) has been debated. This mode of NCX function has been proposed to increase the content of  $\text{Ca}^{2+}$  in SR, it modulates the effectiveness of the L-type  $\text{Ca}^{2+}$  channel current in inducing  $\text{Ca}^{2+}$  release, and directly induces  $\text{Ca}^{2+}$  release, although other experimental work does not support a significant role for NCX-induced  $\text{Ca}^{2+}$  release in excitation-contraction (EC) coupling.

KB-R7943 (KBR), Carbamimidothioic acid, 2-[4-[(4-nitrophenyl)methoxy]phenyl]ethyl ester monomethanesulfonate,  $\text{C}_{16}\text{H}_{17}\text{N}_3\text{O}_3\text{S} \cdot \text{MeSO}_3\text{H}$ , and its molecular weight is 427.5 (Fig. 5), is an amphiphilic molecule that contains a positively charged isothioureia group at neutral pH ( $\text{pK}_a = 10$ ). KB-R7943 is developed by Kanebo KK, and target indications are ischemia, reperfusion injury, and heart arrhythmia. It inhibits the outward  $\text{Ca}^{2+}$  transport more than potentially than the inward transport under unidirectional flow conditions; however, inward and outward  $\text{Ca}^{2+}$  transport were inhibited equally under bidirectional conditions. The drug was a competitive to external calcium, and the inhibition was reversible with recovery half life of about 30s. KBR dose-dependently inhibited the whole cell NCX current recorded in rat and guinea pig.

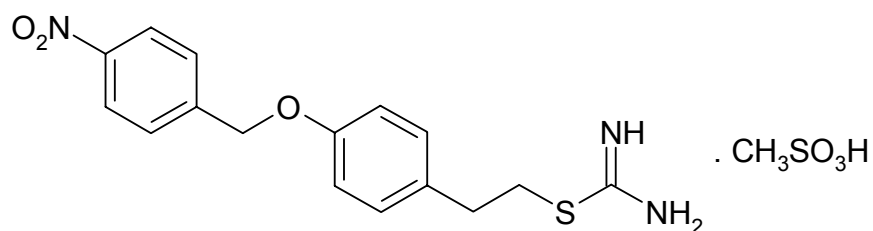


**Figure 5.** Chemical structure of KB-R7943.

#### 1.4 Disease states

Cardiac hypertrophy, i.e., enlargement of individual myocytes that result in an increase in cardiac mass, is part of the process of remodeling of a heart under longterm stress and is an effective phenotypic adaptation to compensate for increased left ventricular wall stress. Increased wall stress has several independent causes, physical training hypertension or the presence of scar tissue after a myocardical infarction. In pathological situations, cardiomyocyte hypertrophy is a mechanism to compensate for the loss of individual cardiomyocytes due to necrosis, unregulated cell death and/or apoptosis, regulated cell ceath. This process often accompanied by fibrosis resulting in increased stiffness may ultimately evolve the overcompensation and out stage heart failure.

It is known that chronic infusion of  $\alpha$ ,  $\beta$ -stimulant, norepinephrine, and the  $\beta$ -stimulant, isoprenaline induces cardiac hypertrophy accompanied with enhanced fibrosis among cardiac interstitial cells (Boluyt et al., 1995; Zierhut and Zimmer, 1989). In 1959, Rona et al. (1959) first recommended the use of isoproterenol (ISO) at repeated daily doses for the production of a model of cardiac disease with increased heart weight. Taylor and Tang (1984) later reported that maximum cardiac growth can be reached on the 8th day of subcutaneous ISO administration at a dose of 0.3 mg/kg bodyweight. Thereafter, repeated subcutaneous ISO administration became an accepted method for the induction of cardiac hypertrophy. Benjamin et al. (1989) have shown no remarkable difference in

myocardial hypertrophy whether the route of ISO administration is bolus subcutaneous injection or via an osmotic minipump. One of the commonly used surgical interventions for pressure-overload induced hypertrophy in rat is coarction of the ascending aorta, *i.e.* aortic banding. Aortic banding is an excellent model system to evaluate the process of development of left ventricular hypertrophy in response to hemodynamic stress. Furthermore, after several months, a subset of animals progresses into heart failure.

Sepsis is an often fatal disease with mortality rates of 30 % for mild to moderate sepsis and up to 82 % for severe sepsis and septic shock. Depression of myocardial contractility constitutes an important feature of human septic shock (Court et al., 2002; Levy and Deutschman, 2004). Exposure to endotoxin, lipopolysaccharides (LPS) present in the outer portion of the cell wall of gram-negative bacteria, can result in fever, systemic inflammation and shock. Sepsis is systemic inflammatory response syndrome due to a presumed or known site of infection.

Sepsis can occur as a result of infection of any body site as a primary blood stream infection. Bacteria are the pathogens most commonly associated with the development of sepsis, although fungi, viruses, and parasite do cause sepsis. The pathophysiology of sepsis is initiated by the outer membrane components of both gram-negative organisms (lipopolysaccharide, endotoxin) and gram-positive organisms (lipoteichoic acid, peptidoglycan).

Attempts to study the pathophysiology of sepsis have often involved animal models. Gram-negative bacteria have been shown to induce sepsis and septic shock in animals, thus resulting in a number of cardiovascular squeals. Rats receiving endotoxin from *Escherichia coli* in the dorsal subcutaneous space or intraperitoneal space exhibit a depression of cardiac function. Sepsis-induced cardiac dysfunction is apparent *in vitro*, both in terms of peak systolic pressure development and cardiac output, over a wide range of left ventricular volumes.

### **1.5 Pharmacokinetics and Pharmacodynamics Modeling**

The objectives of pharmacokinetics are to study the time course of drug and metabolite concentrations or amount in the biological fluids, tissue and excreta, to investigate the



time course of pharmacological response and to build a suitable model to interpret such data. In other words, if pharmacokinetics is the movement of drugs, pharmacodynamics is the action of drug. Pharmacodynamics can be defined as the study of the biological effects of the interaction between drugs and biological systems (Holford et al., 1981).

A pharmacokinetics/pharmacodynamics (*PK/PD*) model is a mathematical description of this relationship (Fig. 6); the model parameters provide information about intrinsic drug properties. The model links the concentration-time profiles as assessed by pharmacokinetics to the intensity of observed response as quantified by pharmacodynamics. Thus, the resulting integrated *PK/PD* model allows the description of the complete time course of drug effect in response to drug therapy. The knowledge of the combined *PK/PD* model and the parameter estimates allows prediction of concentration vs. time and effect vs. time profiles for different dosing regimen.

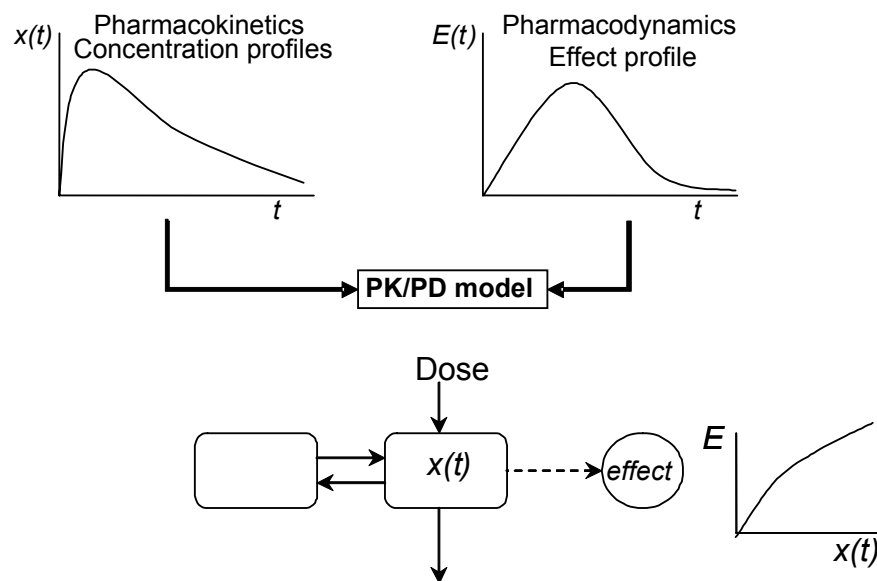


**Figure 6.** Structure of the *PK/PD* modeling.

Mechanism-based *PK/PD* modeling, a mechanistic model, as the name implies, should have as many features of the primary system built into it as observations or data will allow. Such a model should be consistent with the observed behavior of the system; further, it should be predictive of the system's future behavior or behavior under perturbation. One must have some knowledge of the primary system in terms of

structural connectivity and functional mechanisms. As emphasized by Van Der Graaf et al., (1998) and Derendorf et al., (1999), the need for a more mechanism-based approach in *PK/PD* modeling is increasingly being recognized. Receptors are the most important targets for therapeutic drugs. In the past decades, the enormous progress in the area of molecular biology has yield many new insight in the structure and functions of receptors. As a biological system analysis, mechanism based *PK/PD* modeling can donate the characterization in a mechanic and strict quantitative manner of the functioning of the integral biological system *in vivo* (Fig 7). For example, *PK/PD* in perfused heart (Weiss and Kang, 2002), receptor trafficking, and cellular signaling mechanisms can be incorporated to the model (Mager and Jusko, 2001b).

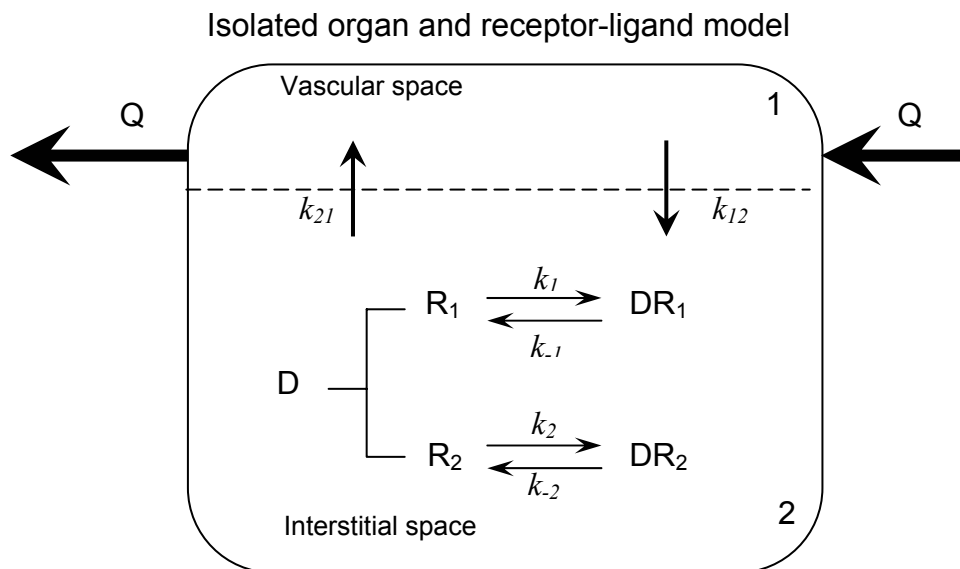


**Figure 7.** Model diagram of isolated organ and receptor-ligand model.

### 1.6 Purpose

It is now widely accepted that the cardiac glycosides exert their positive inotropic effect through an inhibition of  $\text{Na}^+, \text{K}^+$ -ATPase: the  $\text{Na}^+, \text{K}^+$ -ATPase controls the cytoplasmic  $\text{Na}^+$  concentration, which in turn determines  $\text{Ca}^{2+}$  concentration via the  $\text{Na}^+/\text{Ca}^{2+}$  exchanger (NCX). In the adult rat heart, mainly two receptor isoforms,  $\alpha_1$  and  $\alpha_2$ , are expressed exhibiting low and high affinity, respectively, for digitalis. However, the in vivo functional roles of the  $\alpha_1$ - and then  $\alpha_2$ -isoform of the  $\text{Na}^+, \text{K}^+$ -ATPase in mediating this inotropism in rat hearts and the effect of external calcium concentration are still a matter of debate. Likewise, although it appears clear that  $\text{Na}^+/\text{Ca}^{2+}$  exchanger is essential for the action of cardiac glycosides, the quantitative role of NCX in this process is poorly understood in the whole heart.

Cardiac hypertrophy induced by increased workloads is associated with alterations in myocardial  $\text{Na}^+, \text{K}^+$ -ATPase concentrations. Previous, some studies with different rat hypertrophy models showed clear evidence of a decrease of  $\alpha_2$   $\text{Na}^+, \text{K}^+$ -ATPase mRNA and protein levels in cardiac left ventricle, whereas the expression of the predominant  $\alpha_1$  isoform remained unchanged. It was suggested that deinduction of  $\alpha_2$   $\text{Na}^+, \text{K}^+$ -ATPase gene expression is a pressure-overload transcriptional response mechanism in both humans and rats. However, the functional consequences of such remodeling processes are poorly understood, especially when information is solely based on biochemical studies. Thus, the fact that cardiac glycosides exert their positive inotropic effects by inhibiting the  $\text{Na}^+$  pump raises the question of how this shift in  $\text{Na}^+, \text{K}^+$ -ATPase isoforms affects receptor binding kinetics and action of digitalis. Furthermore, it remains uncertain whether the diminished positive inotropic effect of cardiac glycosides can be explained by this change in sodium pump expression.

Depression of myocardial contractility constitutes an important feature of human septic shock. Myocardial dysfunction has been also demonstrated in experimental animal models following administration of endotoxin, a lipopolysaccharide (LPS) component of the outer membrane of gram-negative bacteria. It is hardly surprising for a syndrome as complex as sepsis that despite valuable information recently obtained from such experimental studies the underlying cellular mechanisms have not been fully defined.

Much less is known, however, about the inotropic response to cardiac glycosides under these conditions.

The purpose of this study was to examine the influence of alterations in calcium in perfusate as well as the effect of the NCX inhibitor KBR on the processes that underlie inotropic actions of digoxin in the perfused normal rat heart, namely myocardial uptake, receptor binding ( $\text{Na}^+/\text{K}^+$ -ATPase inhibition) and postreceptor events. To understand the action of cardiac glycosides, quantitative description of the processes involved is needed. To this end, a mechanism-based mathematical model was developed for describing the uptake kinetics, receptor interaction, and positive inotropic effect of digoxin in the single-pass isolated perfused rat heart. Using this model to analyze transient outflow concentration and inotropic response data of digoxin, it was possible to estimate model parameters characterizing receptor binding and cellular response generation of digoxin. Added that, the function of the  $\text{Na}^+,\text{K}^+$ -ATPase has not been previously studied in cardiac hypertrophy induced by a continuous infusion of isoprenaline (ISO) and sepsis induced by endotoxin injection. With this background, we have designed experiments in hearts of isoprenaline-pretreated rats and endotoxin-pretreated sepsis rats to study the effect of left ventricular hypertrophy on myocardial uptake and receptor binding kinetics ( $\text{Na}^+,\text{K}^+$ -ATPase inhibition) and positive inotropic effect of digoxin. The inotropic effect of digoxin in a rat model of hypertrophy and endotoxin-induced myocardial dysfunction and the functional receptor heterogeneity and the differences between effects elicited at the receptor and postreceptor level in disease state were investigated. In view of the changes of NCX activity in cardiac hypertrophy and NCX function endotoxic shock, it was considered whether NCX inhibition by KB-R7943 would influence digoxin action in disease state.

## 2. MATERIALS AND METHODS

### 2.1 Materials

[<sup>3</sup>H]-Digoxin (37Ci/mmol) was purchased from Perkin-Elmer Life Sciences Inc. (Boston, USA) and [U-<sup>14</sup>C]-Sucrose (660mCi/mmol) was purchased from Amersham Bioscience UK Limited. Digoxin (12β-hydroxydigitoxin, C<sub>41</sub>H<sub>64</sub>O<sub>14</sub>), (-)-Isoproterenol (+)-bitartrate salt (C<sub>11</sub>H<sub>17</sub>NO<sub>3</sub>·C<sub>4</sub>H<sub>6</sub>O<sub>6</sub>), Lipopolysaccharides (from *Escherichia coli*: serotype 055:B5) were purchased from Sigma-Aldrich Chemie GmbH (Steinheim, Germany). KB-R7943 was kindly donated from Nippon Organon KK and all other chemicals and solvents were of the highest grade available.

ALZET micro-osmotic pump (DURECT Corp. USA) was used for inducement of hypertrophy; ALZET model 1003D (1.0 ± .15μl/hr, 3 days, 90 ± 10μl).

Perfused rat heart experiment system configuration.

HSE-Harvard Isolated Heart Size 3 & ISOHEART software  
 ISOTEC pressure transducer and HSE-Harvard PLUGSYS system  
 M3 LAUDA pump (type MS) LAUDA DR.R. WOBSEER GmbH & Co., KG  
 IVAC-50ml syringe pump (IVAC P4000) MEDIZINTECHNIK GMBH  
 ISMATEC MS-REGLO pump  
 Graphtec Linearecorder mark 8 (WK3500)

Krebs-Henseleit buffer solution composition.

	M.W. (g/mol)	Concentrations (mmol/l)
NaCl	58.44	118.00
KCl	74.56	4.70
CaCl <sub>2</sub> ·2H <sub>2</sub> O	147.02	1.50
MgSO <sub>4</sub> ·7H <sub>2</sub> O	246.48	1.66
NaHCO <sub>3</sub>	84.01	24.88
KH <sub>2</sub> PO <sub>4</sub>	136.09	1.18
Glucose	198.17	5.55
Sod. pyruvate	110.00	2.00
BSA	N.A.	0.1 %
Aerating gas		95%O <sub>2</sub> -5% CO <sub>2</sub>
pH		7.4

### 2.2 Isolated perfused heart

Wistar rats (280 – 320 g) were used in this study. Surgery on the rat was performed using general anesthesia and artificial ventilation. Sodium pentobarbital was injected as a bolus at concentration of 50 mg/kg. Following the onset of anesthesia, rats were fixed on an appropriate operating table and 500 IU of heparin was pre-treated with i.v. injection to prevent blood coagulation in blood vessels. A cannula was bound into the trachea for ventilation, and the skin is incised by a longitudinal cut from the middle of abdomen up to the throat. Then, the abdomen is opened up to the diaphragm. The diaphragm is cut off the ribs following the anterior part of the inferior thoracic aperture. The thorax is cut open on the left and right side following the bone-cartilage-border on a line parallel to the sternum starting at the diaphragm and proceeding as far cranial as to the first rib. The complete anterior thoracic wall is turned upwards over the rat's head and the sternum is split from the xiphoid process exactly in the middle. The ribs are cut as far lateral as possible and the two thorax halves are turned upwards. The pericardium is removed as far as its attachment at the vascular system and any connective tissue around the ascending aorta is discarded. An aortic cannula filled with perfusate was rapidly inserted into the aorta and the pulmonary artery was incised to allow outflow of perfusate. Retrograde perfusion was started with an oxygenated perfusate consisted of Krebs-Henseleit buffer solution, pH 7.4.

A latex balloon attached to the end of a steel catheter was placed in the left ventricular through mitral valve. The catheter and the balloon are filled with a mixture of ethanol and water (50:50), and the other end is linked to the amplifier module (HSE-Harvard PLUGSYS) via a pressure transducer. The balloon is inflated with water to create a diastolic pressure of 5 to 6 mmHg. Langendorff apparatus is depicted in Figure 8. The heart is perfused with a Krebs-Henseleit buffer at 37°C with a 60 mmHg pressure. After stabilization, the system is changed to constant flow condition maintaining a coronary flow of  $9.5 \pm 0.4$  ml/min. The hearts are beating spontaneously at an average rate of  $270 \pm 20$  beats/min.

Left ventricular (*LV*) pressure and heart rate (*HR*) are continuously monitored by means of the balloon. Coronary perfusion pressure (*CPP*) is regulated by a perfusion pressure control module and measured by a pressure transducer connected to the aortic infusion cannula. A physiological recording system (Hugo Sachs Elektronik, March, Germany)

## 2. Materials and Method

is used to monitor left ventricular systolic pressure (*LVSP*), left ventricular enddiastolic pressure (*LVEDP*), maximum and minimum values of rate of left ventricular pressure development ( $LVdP/dt_{max}$  and  $LVdP/dt_{min}$ ), heart rate and coronary perfusion pressure.

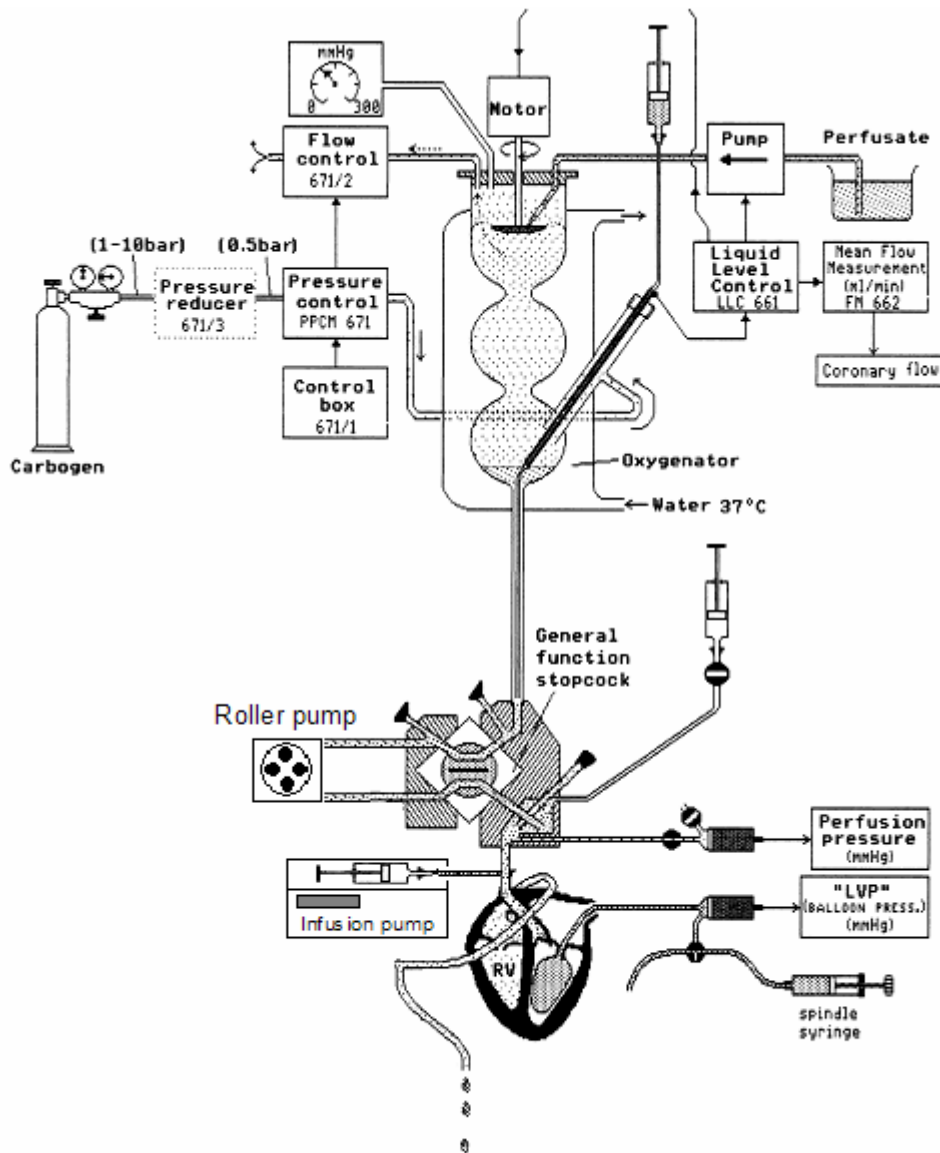
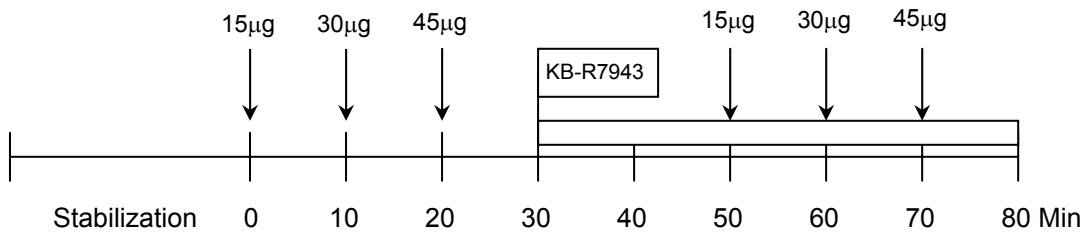


**Figure 8.** Langendorff apparatus for isolated perfused heart. (modified from Operating Instructions for the experimental apparatus isolated heart size 3 type 830, Hugo Sachs Elektronik).

### 2.3 Experimental protocol

The following experiments were performed in two groups of hearts ( $n = 5$  in each) with calcium concentrations in perfusate of 0.5 and 1.5 mM, respectively. After 20-min periods of equilibration, three doses (15, 30, and 45  $\mu\text{g}$ ) of [ $^3\text{H}$ ]-digoxin were administered as 1-min infusions, permutating the sequence of doses with an interval of 15 min. Infusion was performed into the perfusion tube close to the aortic cannula using an infusion device. Outflow samples were collected every 5 s for 2 min and every 30s for the next 5 min (total collection period, 7 min) and the cardiac response was measured. After an equilibration period of 10 min, these experiments were repeated in the presence of KBR (0.1  $\mu\text{M}$ ) in perfusate (starting 15 min after perfusion with KBR-containing buffer).

In selected experiments, [ $\text{U-}^{14}\text{C}$ ]-Sucrose (2  $\mu\text{Ci}/10$  ml, 0.3  $\mu\text{M}$ ) was simultaneously administered as 1-min infusion with digoxin. Outflowing perfusate were collected as same protocol that of digoxin for 7 mins, and it was analyzed with Liquid Scintillation Counter. The outflow samples were kept frozen at  $-20^\circ\text{C}$  until analysis.



### 2.4 Hypertrophy inducement

Cardiac hypertrophy was induced in male Wistar rats weighing 280 to 330 g ( $n = 5$ ) by treatment with isoprenaline for 4 days. The control group received vehicle infusion ( $n = 5$ ). Delivery of isoprenaline was achieved by implanting a mini-osmotic pump filled with sterilized isoprenaline solution or vehicle (0.1 % ascorbic acid). The mean pumping rate was  $1.06 \pm 0.04$   $\mu\text{l}/\text{hr}$  and mean fill volume was  $93.8 \pm 4.5$   $\mu\text{l}$ . The mini-osmotic pump was implanted underneath of the neck skin under ether anesthesia.



## 2. Materials and Method

---

Isoprenaline was continuously infused at a rate of 2.4 mg/kg/day over 4 days. At the end of infusion treatment, animals were anaesthetized with sodium pentobarbital (50 mg/kg, i.p.) and the hearts were excised under the condition of trachea ventilation. After finishing the perfusion experiment, the heart was separated into atrial (*AT*), right ventricular (*RV*), and left ventricular (*LV*) sections. Hypertrophy was monitored by the ratio of myocardial wet weight (each section) to body weight.

### 2.5 Sepsis inducement

Sepsis was carried out by a single intra peritoneal injection of 4 mg/kg LPS (Lipopolysaccharides from *Escherichia coli*: serotype 055:B5), and normal saline (0.9 % NaCl) was injected to the other animal group as a control (sham). 4 hours after injection, the heart was excised for isolated heart experiment. Before excision of the heart, rectal temperature of rat was measured with electronic thermometer.

### 2.6 Determination of digoxin in perfusate

The outflow samples were kept frozen at -20 °C until analysis. For determination of [<sup>3</sup>H]-digoxin concentration in the perfusate, 200 µl of collected outflow sample was transferred to a scintillation vial and 2 ml of cocktail (Lumasafe™ Plus) was added. After vigorous mixing, the radioactivity was measured with a liquid scintillation counter (Perkin-Elmer Instruments, Shelton, CT).

### 3. MODEL DEVELOPMENT AND DATA ANALYSIS

#### 3.1 Mechanistic model of Digoxin

##### 3.1.1. Myocardial uptake and binding processes

The cardiac distribution spaces of digoxin; the vascular, interstitial and cellular, were represented by compartments as shown in the model structure (Fig. 9). This comprehensive approach to analyze myocardial uptake and receptor binding of digoxin has been combined with a model that links  $\text{Na}^+, \text{K}^+$ -ATPase to inotropic response (circle in Fig. 9).

The corresponding differential equations describing changes in the amounts of digoxin in the mixing, capillary, and interstitial compartment as well as in the two compartments representing the two saturable binding sites after infusion of digoxin at the inflow side of the heart (perfused at flow  $Q$  in single-pass mode) are given by Eqs. 1 to 5.

$$dD_0(t) / dt = -(Q/V_0)D_0(t) + RATE \quad (1)$$

$$dD_{vas}(t) / dt = -(Q/V_{vas} + k_{vi}) D_{vas}(t) + k_{iv} D_{is}(t) + (Q/V_0)D_0(t) \quad (2)$$

$$dD_{is}(t) / dt = k_{vi} D_{vas}(t) - k_{iv} D_{is}(t) - [k_1 (R_{tot,1} - DR_1(t)) + k_2 (R_{tot,2} - DR_2(t))] C_{is}(t) + k_{-1} DR_1(t) + k_{-2} DR_2(t) \quad (3)$$

$$dDR_1(t) / dt = k_1 [R_{tot,1} - DR_1(t)] C_{is}(t) - k_{-1} DR_1(t) \quad (4)$$

$$dDR_2(t) / dt = k_2 [R_{tot,2} - DR_2(t)] C_{is}(t) - k_{-2} DR_2(t) \quad (5)$$

where  $k_{vi} = CL_{vi} / V_{vas}$ ,  $k_{iv} = CL_{vi} / V_{app, is}$  and  $C_{is}(t) = D_{is}(t) / V_{app, is}$  denotes the unbound digoxin concentration in the interstitial space.

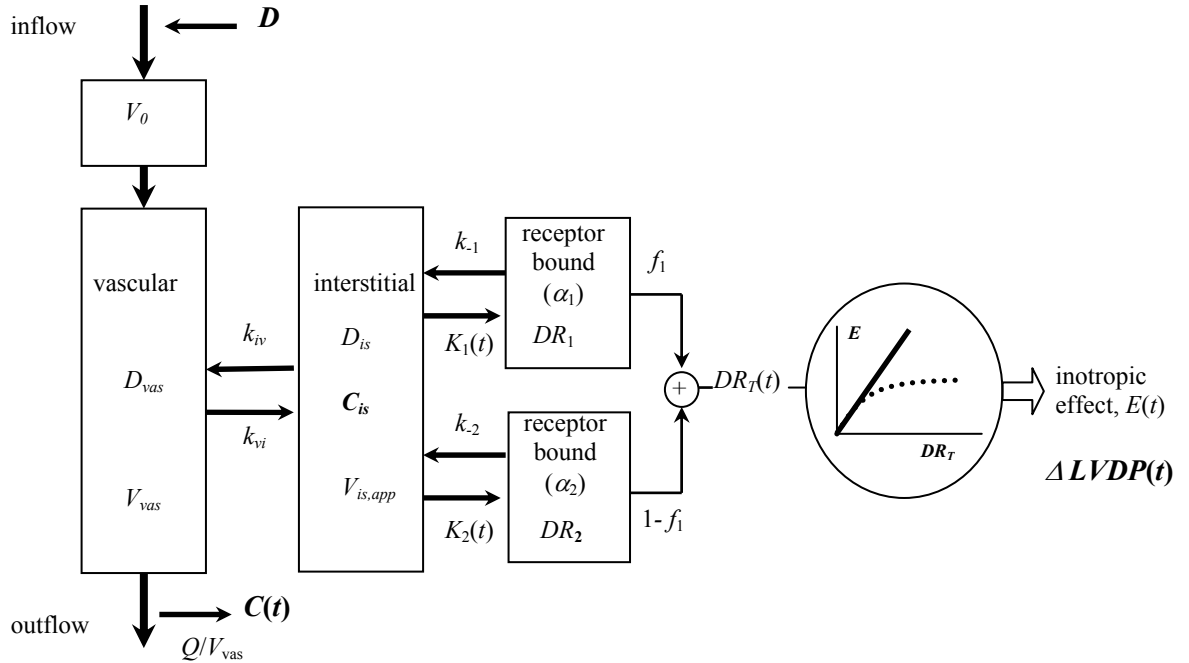


**Figure 9.** Comprehensive kinetic model of cardiac kinetics and inotropic response of digoxin. First order rate constants of transcapillary transport are denoted by  $k_{vi}$  and  $k_{iv}$ . The fractional rate for saturable receptor binding  $K_i(t) = k_i [R_{tot,i} - DR_i(t)]$  is governed by the unbound interstitial digoxin concentration  $C_{is}(t) = D_{is}(t)/V_{app,is}$ . The association and dissociation constants are denoted by  $k_i$  and  $k_{-i}$ , respectively. The chain of postreceptor events determines the effect as a function of receptor occupations  $DR_i$ . The index  $i = 1,2$  denotes the receptor population  $\alpha_i$ .

As shown in the compartmental model, perfusate flow ( $Q$ ) and drug outflow occur in the vascular space (distribution volume  $V_{vas}$ ), transcapillary transport of the unbound drug between vascular and interstitial space is described by rate constants  $k_{vi}$  and  $k_{iv}$ , respectively, and the apparent permeability surface-area or permeation clearance  $CL_{vi} = k_{vi}V_{vas}$  (net clearance of digoxin from the vasculature) is determined by  $k_{vi}$  and  $V_{vas}$ . Assuming passive transport processes,  $k_{vi}V_{vas} = k_{iv} V_{app,is}$  where  $V_{app,is}$  denotes the apparent volume that governs initial distribution of digoxin in the interstitial space; i.e., exceeding the distribution space  $V_{is}$  due to quasi-instantaneous nonspecific tissue binding,  $V_{app,is}$  is given by  $V_{app,is} = V_{is} (1 + K_{eq})$  where the equilibrium partition coefficient  $K_{eq} = k_{on}/k_{off}$  characterizes unspecific tissue binding (Weiss, 1999). From the experiments with the vascular marker, Evans blue, a lag time  $t_0$  and an additional compartment with volume  $V_0$  were introduced to account for the delay drug appearance and mixing in nonexchanging elements of the system, respectively. Since the short delay  $t_0$  and mixing volume  $V_0$ , needed to fit the initial appearance of outflow concentration (due to the perfusion system and large vessels) had little influence on the estimation of the other parameters, they were set to fixed values,  $t_0 = 0.03$  min and  $V_0 = 0.33$  ml in the final Bayesian model identification.

#### 3.1.2. Kinetics of receptor binding and cellular effectuation

Assuming a reversible interaction between digoxin and two receptor classes  $R_1$  and  $R_2$  on the sodium pump ( $[^3H]$ -digoxin binding sites)



the binding probability of digoxin in the interstitial space (unbound amount  $D_{is,u}$ ) to two saturable binding sites ( $i=1,2$ ) is dependent on the association rate constants  $k_i$  and free membrane receptors which is equal to  $(R_{tot,i} - DR_i)$  where  $R_{tot,i}$  is the unknown amount of available receptor sites and  $DR_i$  denotes the digoxin - receptor complexes (i.e., amount of bound digoxin), the resulting fractional binding rate  $K_i = k_i [R_{tot,i} - DR_i(t)]$  is time-dependent (Eqs.4 and 5). The rate constants for the dissociation of the bound ligand were denoted by  $k_{-i}$  (in units of 1/min);  $K_{D,i} = k_{-i}/k_i$  and  $K_{A,i} = 1/K_{D,i}$  represent the

### 3. Model development and data analysis

---

equilibrium dissociation and affinity constants, respectively, of the two receptor systems. Note that due to quasi-instantaneous nonspecific tissue binding the free concentration in the interstitial space is reduced and given by  $C_{is}(t) = D_{is}/V_{app,is}$ , instead of  $D_{is}/V_{is}$  (Weiss, 1999); since free digoxin concentration governs receptor binding (Eqs. 2 to 5),  $k_i$  is defined in terms of  $C_{is}$  (in units of 1/min/nmol/ml).

The binding of digoxin to receptors (sodium pumps) initiates a series of dynamic events that ultimately leads to an increase in the force of contraction. Since a mechanistic model of these postreceptor events as indicated in Fig. 9 (higher  $Ca^{2+}$  availability due to activation of  $Ca^{2+}$  influx via NCX after small increase in  $[Na^+]_i$ ) would be necessarily overparameterized, a minimal transduction model, i.e., an *ad hoc* equation, was selected to mimic the observed behavior (Kenakin, 1993; Mager and Jusko, 2001a). Considering initiation of physiological activity upon binding to the heterogeneous receptor system, the pharmacological response  $E(t)$  is a function of the number of receptors occupied by drug, i.e., ligand-receptor complexes,  $DR_1(t)$  and  $DR_2(t)$ . For the heterogeneous receptor system, the pharmacological response  $E(t)$  induced by the mixture of occupied receptors is a function of the weighted sum of both isoforms

$$DR_T(t) = f_1 DR_1(t) + (1 - f_1) DR_2(t) \quad (7)$$

where  $f_1$  is the fraction of  $R_1$ -occupancy contribution. Thus,  $DR_T(t)$  is the total functional receptor occupation (stimulus) leading to a response  $E(t) = \Psi [DR_T(t)]$ , where the function  $\Psi$  refers to the cascade of cellular processes which convert the stimulus into response. Using a Michaelis-Menten-like hyperbolic function and a delayed response (Kenakin, 1993; Mager and Jusko, 2001a)

$$E(t) = \frac{\phi_{max} DR_T(t)}{K_{DR} + DR_T(t)} * \left( \frac{1}{\tau} e^{-t/\tau} \right) \quad (8)$$

the stimulus-effect relationship, is characterized by parameters  $\phi_{max}$  and  $K_{DR}$  ( $DR_T$  producing 50% of  $\phi_{max}$ ), and \* denotes the convolution operation which accounts for the transduction delay with time constant  $\tau$  (Eq. 8). The corresponding differential equation is Eq. 9 ;

$$dE(t)/dt = \frac{1}{\tau} \left[ \frac{\phi_{\max} DR_T(t)}{K_{DR} + DR_T(t)} - E(t) \right] \quad (9)$$

The effectuation model greatly simplifies when pump inhibition (rate of receptor occupation) is the rate limiting step [the effect is in phase with  $DR_T(t)$ ] and no saturation occurs, i.e., the effect is proportional to  $DR_T(t)$  and Eq. 3 collapses to a linear combination of receptor occupations  $DR_1(t)$  and  $DR_2(t)$

$$E(t) = e_T [f_1 DR_1(t) + (1 - f_1) DR_2(t)] \quad (10)$$

where  $e_T$  denotes the total transduction efficiency (or stimulus amplification) with contributions of  $f_1$  and  $f_2 = 1 - f_1$  of  $R_1$  and  $R_2$  receptors, respectively. Note that in the present paper the low affinity/high capacity and high affinity/low capacity [ $^3\text{H}$ ]-digoxin binding sites  $R_1$  and  $R_2$ , are assumed to be identical with the  $\alpha_1$ - and  $\alpha_2$ -subunit isoforms of the  $\text{Na}^+, \text{K}^+$ -ATPase, respectively (Sweadner, 1993; Mathias et al., 2000).

### 3.2. Data Analysis

The digoxin outflow data,  $C_{out}(t)$ , were first analyzed to obtain estimates of the transport and binding parameters. Those values were then fixed in fitting the  $\Delta LVDP(t)$  data obtained from the same experiments. The latter was used as a measure of inotropic response, i.e., the increase in  $LVDP$  with respect to the baseline (pre-drug) value  $LVDP_0$ ,

$$E(t) = \frac{LVDP(t) - LVDP_0(t)}{LVDP_0(t)} \quad (11)$$

To get a quantitative estimate of the positive inotropic effect that is independent of the model we calculated the time integral (over 7 min) of the developed effect using trapezoidal rule.

$$AUEC = \int_0^7 [E(t) - E_0] \quad (12)$$

The terminology “effect”,  $E(t)$ , will be used throughout for the fractional change of  $LVDP$ . As noted above, in Bayesian estimation we made use of a priori knowledge on the ratios of the receptor affinities ( $K_{A,2}/K_{A,1}$ ) and capacities ( $R_{tot,1}/R_{tot,2}$ ). Since data obtained for digoxin using rat ventricle microsomal preparations (Noel and Godfraind, 1984) alone may not provide reliable information (Lopez et al., 2002), we used more recent binding data (Ver et al., 1997) and, additionally, receptor affinities estimated in rat cardiac myocytes by measuring the  $\text{Na}^+$  pump current (Ishizuka et al., 1996). Thus, we based our analysis on *a priori* values of the affinity and capacity ratios,  $K_{A,2}/K_{A,1} = 45$  and  $R_{tot,1}/R_{tot,2} = 3$ , respectively. We selected a fractional standard deviation of 20 % to ensure that the estimates will be both data and *a priori* knowledge driven. The volume of the vascular compartment was fixed for a literature value ( $V_{vas} = 0.06$  ml/g) taken from anatomic data (Dobson and Cieslar, 1997). Thus, the primary parameters estimated directly were the pharmacokinetic parameters,  $CL_{vi}$ ,  $V_{app, is}$ ,  $R_{tot,1}$ ,  $k_1$ ,  $k_{-1}$ ,  $R_{tot,2}$ ,  $k_2$ ,  $k_{-2}$  and the pharmacodynamic parameters  $e_T$ ,  $f_1$  or  $\Phi_{max}$ ,  $K_{DR}$  under control condition or in the presence of KBR, respectively. One set of parameter starting values was used for all of the data sets. Identifiability was verified by showing convergence to the same solution with alternative sets of parameter starting values. Any model showing a noninvertible Fisher's information matrix was discarded as non-identifiable. The assessment of numerical identifiability was guided by the asymptotic fractional standard deviations ( $CV$ ) provided by the fitting procedure, which represent the uncertainty in parameter estimates resulting from the fit, and correlation coefficients. Model selection in fitting the  $C_{out}(t)$  and  $E(t)$  data was based on the generalized information criterion (GEN-IC) for MAP estimation and the AIC criterion, respectively.

To limit the number of parameters to be adjusted, only model structures reasonably consistent with the physiological knowledge of digoxin uptake and action were investigated. For our nonlinear model, we are still faced with the question of its identifiability. Since the information content of the outflow data is inadequate to support such a model with a relative rich parameterization, we take advantage of the fact that *a priori* information on some of the unknown model parameters is available in the literature. The Bayesian approach to model identification [e.g., maximum a posteriori (*MAP*) estimation] is a theoretically sound method to incorporate such knowledge in probabilistic terms. The system of differential equations was solved numerically and

### 3. Model development and data analysis

---

MAP Bayesian parameter estimation was performed with the ADAPT II software (D'Argenio and Schumitzky, 1997). For all pharmacokinetic and pharmacodynamic fits, an additive plus proportional intraindividual error model was used.

The associated concentration of drug at time  $t$ , denoted  $y(t)$ , is given by the following output equation, model equation for parameter estimation.

$$y(t) = x(t) / V_{vas} \quad (13)$$

It is necessary to specify a model for the variance of the additive error of the measured data (i.e., variance model). Measurements are generally collected at discrete times,  $t_i$ , and include additive error as follows:

$$z(t_i) = y(t_i) + v(t_i) \quad i = 1, \dots, m \quad (14)$$

where  $z_i(t_i)$  represents the measured value of the model output  $y(t_i)$  at time  $t_i$ , and  $v(t_i)$  is the associated error. A portion of  $v(t_i)$  is generally attributed to errors in the measurement process.  $v(t)$  is assumed to be normally distributed, an error variance model relates the variance of  $v(t)$  [ $\text{var}(v(t))$ ] to the model output  $y(t)$  as follows:

$$\text{var}\{v(t)\} = (\sigma_{inter} + \sigma_{slope} y(t))^2 \quad (15)$$

where  $\sigma_{inter}$  and  $\sigma_{slope}$  are referred to as the variance model parameters (D'Argenio and Schumitzky, 1997).

There are two types of model parameters for parameter estimation: system parameter  $\alpha$ :  $\alpha$  constant, either known or unknown;  $\alpha$  random vector with density function  $p(\alpha)$ . The density function for  $\alpha$  can be defined as  $p(\alpha) = N(\mu, \Omega)$ ,  $LN(\mu, \Omega)$  for multivariate and normal or lognormal distribution output, where  $\mu$  and  $\Omega$  represent the prior mean vector and covariance matrix, respectively, of the model parameter  $\alpha$ . The variance parameter vector  $\beta$  represents additional parameters that are unique to the error variance model. Bayesian estimation which can be calculated in a computationally straightforward manner (given certain distributional assumptions) is the mode of the posterior parameter



### 3. Model development and data analysis

---

density (i.e. the maximum a posteriori probability (*MAP*) estimation). For normally distributed output error and with  $\alpha \sim N(\mu, \Omega)$ , the *MAP* estimates the system and variance parameters, assuming a non-informative prior for the latter, is obtained by minimizing the following objective function:

$$O_{MAP} = \sum_{i=1}^l \sum_{j=1}^m \left[ \frac{(z_i(t_j) - y_i(\alpha, t_n))^2}{g_i(\alpha, t_j, \beta)} + \ln g_i(\alpha, t_j, \beta) \right] + [\alpha - \mu]^T \Omega^{-1} [\alpha - \mu] \quad (16)$$

where the superscript T means transpose and if  $\alpha$  is partitioned into informative and non-informative parts, then  $\alpha_1$ ,  $\mu_1$  and  $\Omega_1$  replace  $\alpha$ ,  $\mu$  and  $\Omega$  in *Eqs. 16*.

For the case when  $\alpha \sim LN(\mu, \Omega)$ , the objective function becomes:

$$O_{MAP} = \sum_{i=1}^l \sum_{j=1}^m \left[ \frac{(z_i(t_j) - y_i(\alpha, t_n))^2}{g_i(\alpha, t_j, \beta)} + \ln g_i(\alpha, t_j, \beta) \right] + [\alpha - \mu]^T \Omega^{-1} [\alpha - \mu] \\ + [\ln \alpha - \nu]^T \Phi^{-1} [\ln \alpha - \nu] + 2 \sum_{i=1}^p \ln \alpha_i \quad (17)$$

where the mean vector,  $\nu = \{\nu_i\}$ ,  $i = 1, \dots, p$  and covariance matrix  $\Phi = \{\phi_{ij}\}$ ,  $i, j = 1, \dots, p$ . The elements of  $\nu$  and  $\Phi$  are defined in terms of the elements of  $\mu$  and  $\Omega$  as follows:

$$\nu_i = \ln \mu_i - \phi_{ij}/2, \quad i = 1, \dots, p \quad (18)$$

$$\phi_{ij} = \ln \left( \frac{w_{ij}}{\mu_i \mu_j} + 1 \right), \quad i, j = 1, \dots, p \quad (19)$$

The approximate standard deviations of the estimated parameters are obtained from the covariance matrix and the corresponding coefficient of variation are calculated as  $CV\alpha_i = \sigma_i / \alpha_i$ .

For the *MAP* estimator, the generalized information criterion is calculated as follows,

$$GEN - IC = O_{MAP} + \frac{2(p+q)}{l \cdot m} \quad (20)$$

in this equation, the *MAP* objective function given in *Eqs.* 16, 17 is evaluated at the *MAP* estimates both system and variance model parameters,  $\hat{\alpha}$  and  $\hat{\beta}$ .

### 3.3. Statistics

Descriptive data are expressed as mean  $\pm$  S.D. To get a quantitative estimate of the positive inotropic effect that is independent of the model, we calculated the time integral of developed effect using a trapezoidal rule. The responses in the experimental groups were compared using two-way ANOVA with repeated measures performed on the three-dose levels followed by a Student-Newman-Keuls post hoc test for multiple comparisons. Differences in parameter estimates between control and treatment groups were assessed by Student's *t*-test. For all analyses, a two-tailed *P* value of  $<0.05$  was used to indicate statistical significance.

## 4. Results and Discussion

### 4.1 Cardiac uptake of digoxin

Wistar rats weighing 280-320 g were used, and spontaneous beating heart rate was about  $270 \pm 20$  beats/min. After an equilibration period of 30 min, baseline physiological parameters were checked; left ventricular developed pressure ( $LVDP_0$ ) was  $75 \pm 8.54$  mmHg, left ventricular end-diastolic pressure ( $LVEDP$ ) was  $6.39 \pm 3.21$  mmHg and coronary vascular resistance ( $CVR$ ) was  $4.31 \pm 0.58$  mmHg·min/ml (mean  $\pm$  S.D.,  $n=15$ ).

The averaged outflow concentration-time curves after 1-min infusion of three doses of digoxin is shown Fig. 10. The curves reach a plateau level within about 30seconds and the rapid decay upon cessation of infusion is followed by a slower terminal phase.

The recoveries of digoxin in the outflow perfusate up to 7 min were  $96.7 \pm 3.2$ ,  $98.4 \pm 4.3$  and  $98.2 \pm 5.3$  % for doses of 15, 30 and 45  $\mu$ g, respectively.

The myocardial uptake of digoxin was barrier limited due to the relatively low transcapillary permeation clearance of digoxin compared with perfusion flow, 9.5 ml/min. If entry into the heart is by passive diffusion through interendothelial clefts, one would expect a  $CL_{vi}$  value  $\sim 0.7$  folds less than that for sucrose (the square root of the ratio of molecular weights of sucrose and digoxin, 0.7, accounts for the different diffusion coefficients). The estimated  $CL_{vi}$  was  $3.13 \pm 0.80$  ml/min for sucrose in isolated perfused rat heart, whereas  $CL_{vi}$  for digoxin was  $7.25 \pm 2.5$  ml/min. With a reduced model consisting only of a vascular and interstitial compartment, the apparent interstitial distribution volume of sucrose ( $V_{app, is\_suc.}$ ) was also estimated  $0.64 \pm 0.06$  ml/g. This suggests that transcapillary exchange of digoxin is primarily via diffusion through gaps between the endothelial cells. Assuming passive transport process,  $k_{vi} V_{vas} = k_{iv} V_{app, is}$ .  $V_{app, is}$  is given by  $V_{app, is} = V_{is}(1+K_{eq})$ , where the equilibrium partition coefficient  $K_{eq} = k_{on}/k_{off}$  characterizes nonspecific tissue binding (Weiss, 1999). The apparent interstitial distribution volume of digoxin,  $V_{app, is}$  was  $0.771 \pm 0.24$  ml/g, and the equilibrium partition coefficient  $K_{eq}$  was  $0.3 \pm 0.2$  for a volume of the interstitial space  $V_{is} = 0.64$  ml/g, according to the previously shown data from sucrose.

## 4.2 Receptor binding kinetics of digoxin

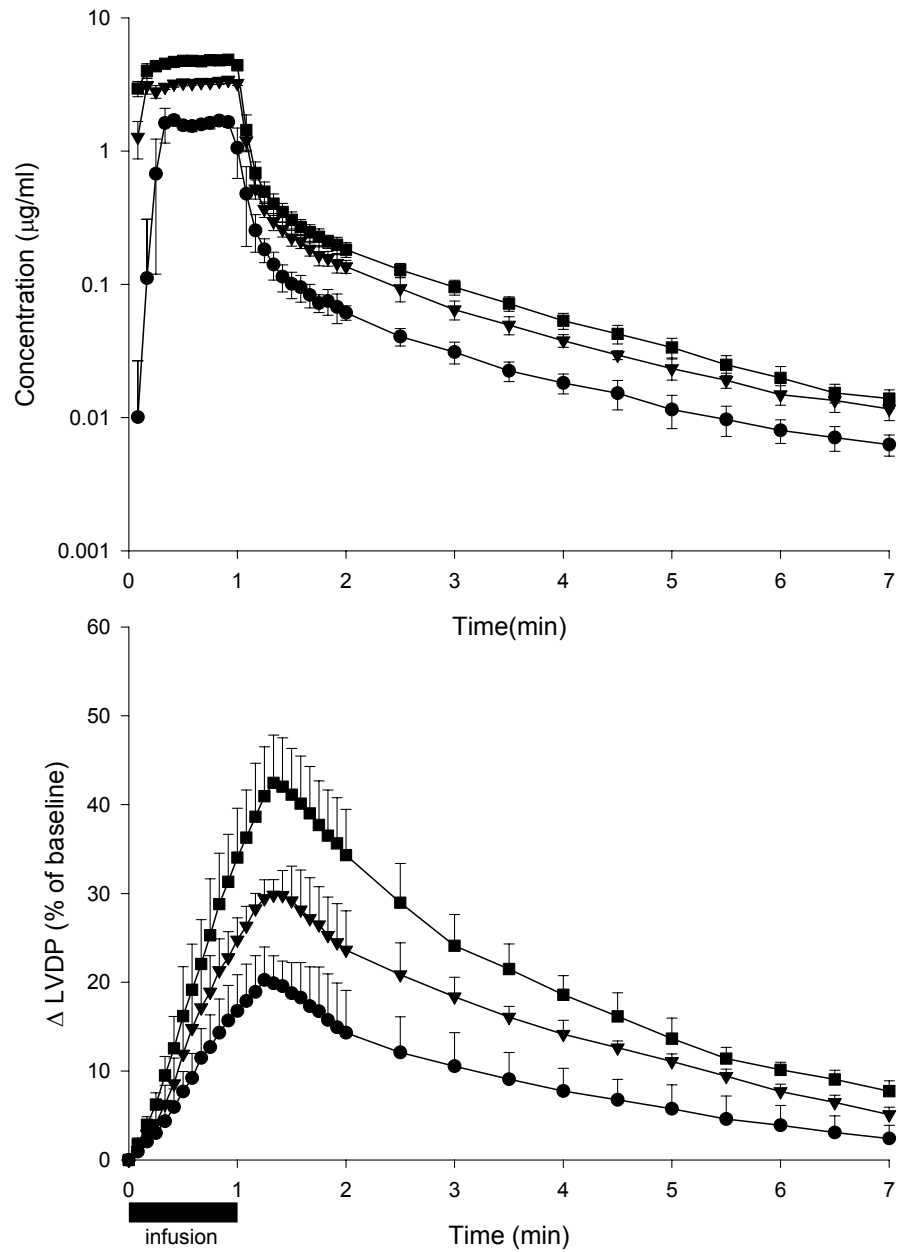
Figure 10 shows also the average inotropic response curve-time profiles as a percentage of the difference to the vehicle effect (% increase of *LVDP*) corresponding to the outflow curve. Treatment with digoxin results in an increase in *LVDP* at 1 min, the time of end of infusion, to  $20.25 \pm 3.74$ ,  $29.81 \pm 1.73$  and  $42.45 \pm 5.38$  % of the vehicle level for each three doses, and recovered within 10 min.

Figure 11 shows a representative set of outflow and response data (three consecutive doses in one heart) together with the line obtained by a simultaneous model fit. It is apparent that the *PK/PD* model well fitted the data; the pharmacodynamics predictions are concordant with the observed time course of positive inotropy. The model was conditional identifiable, and parameter estimates (mean  $\pm$  S.D.,  $n = 15$ ), obtained with ADAPT II, are reported in Table 1, together with the precision of the estimates.

**Table 1.** Model parameter estimates for the *PK/PD* of 1-min infusion of three consecutive doses of digoxin (15, 30, and 45  $\mu\text{g}$ ) in isolated rat heart with external calcium concentration of 1.5mM (mean  $\pm$  S.D.,  $n = 15$ ).

Parameters	Estimated values
<i>Cardiac Uptake</i>	
$CL_{vi}$ (ml/min/g)	$7.245 \pm 2.48$ ( $21 \pm 10$ ) <sup>a</sup>
$V_{app, is}$ (ml/g)	$0.771 \pm 0.24$ ( $28 \pm 17$ )
<i>Receptor Binding</i>	
$R_{tot,1}$ (nmol/g)	$31.99 \pm 8.95$ ( $37 \pm 17$ )
$k_1$ (1/min/nmol/ml)	$0.027 \pm 0.03$ ( $26 \pm 14$ )
$k_{-1}$ (1/min)	$2.579 \pm 0.86$ ( $29 \pm 12$ )
$R_{tot,2}$ (nmol/g)	$9.914 \pm 2.54$ ( $35 \pm 17$ )
$k_2$ (1/min/nmol/ml)	$0.229 \pm 0.07$ ( $55 \pm 26$ )
$k_{-2}$ (1/min)	$0.729 \pm 0.13$ ( $16 \pm 6$ )
$K_{D,1}$ (nmol/ml)	$158.6 \pm 63.5$
$K_{D,2}$ (nmol/ml)	$3.516 \pm 1.41$
$K_{A,2}/K_{A,1}$	$45.18 \pm 1.17$ ( $2 \pm 1$ )
$R_{tot,1}/R_{tot,2}$	$3.337 \pm 0.73$ ( $12 \pm 3$ )
<i>Cellular Effectuation</i>	
$e_T$ (%/nmol)	$21.48 \pm 6.21$ ( $47 \pm 31$ )
$f_1$	$0.484 \pm 0.07$ ( $56 \pm 21$ )

<sup>a</sup>Values in parentheses are the asymptotic coefficients of variation (CV) of parameter estimates (mean  $\pm$  S.D.) obtained from individual fits.



**Figure 10.** Average outflow concentration (upper panel) and percent increase in developed left ventricular pressure (lower panel) for 1-min infusion of three doses of 15( $\bullet$ ), 30( $\blacktriangledown$ ), and 45( $\blacksquare$ )  $\mu\text{g}$  of digoxin in the isolated heart. (mean  $\pm$  S.D.,  $n = 15$ ).

## 4. Results and discussion

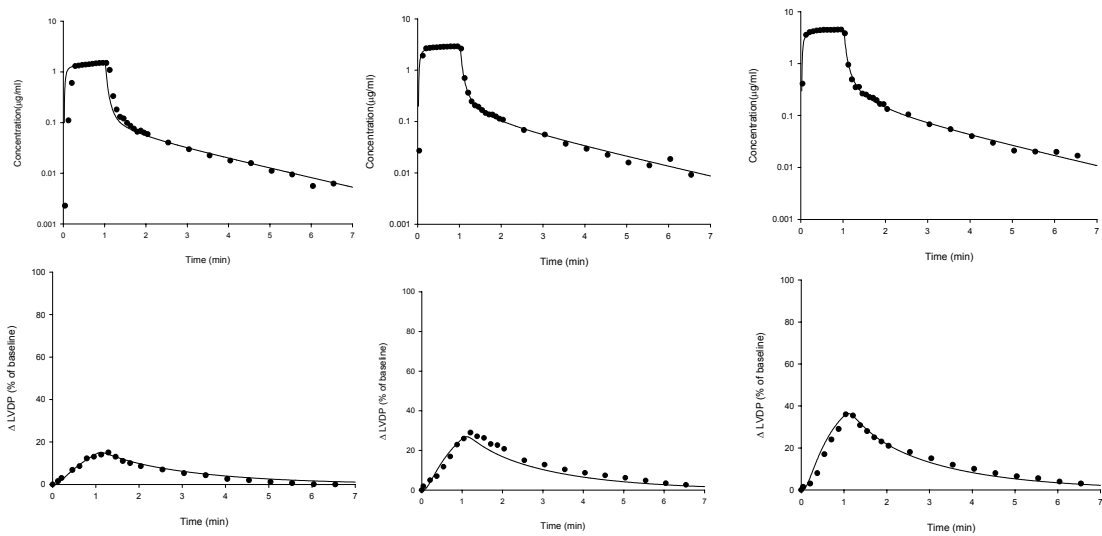


**Figure 11.** Representative simultaneous fits of the model (smooth curves) to experimental data (symbols): Digoxin outflow concentration (upper panel) and percentage increase in developed left ventricular pressure (lower panel) for three doses (15, 30, and 45  $\mu\text{g}$ ).

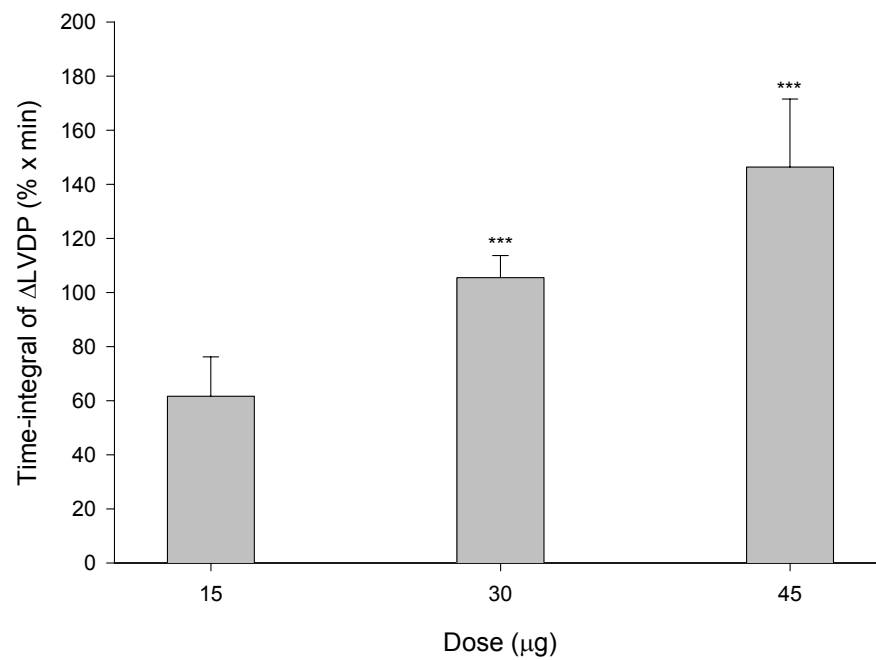


**Figure 12.** Time integral of effect profiles of digoxin (mean  $\pm$  S.D.,  $n = 15$ , \*\*\*  $P < 0.001$ ).

Cardiac kinetics of digoxin was characterized by transport across the capillary barrier and specific binding to two distinct extracellular sites,  $R_1$  and  $R_2$ . Cellular uptake of digoxin was not detectable under the present experimental conditions. Cardiac metabolism of digoxin in the heart was also negligible according to the result of correlated HPLC with liquid scintillation counter (LSC) determination of radio labelled compound analysis of digoxin in the perfusate. When the digoxin concentration in perfusate was analyzed with HPLC, there was no peak which was suspiciously metabolite and the concentration was not different from that of LSC results as expected. The transcapillary permeation clearance of digoxin ( $CL_{vi}$ ) was  $7.245 \pm 2.48$  ml/min/g. In our model, the cellular uptake of digoxin was ignored since it did not have any effect on the fitting of data.  $V_{vas, is}$ , the apparent volume of distribution which governs initial distribution of digoxin in the interstitial space, was  $0.771 \pm 0.24$  ml/g.

The binding kinetics was determined by a mixture of two receptor subtypes, a low affinity/high capacity binding site ( $\alpha_1$ ) and high affinity/low capacity binding site ( $\alpha_2$ ). The capacity ratio  $R_{tot,1}/R_{tot,2}$  was  $3.337 \pm 0.73$  and each estimated capacity were  $31.99 \pm 8.95$ ,  $9.914 \pm 2.54$  nmol/g, respectively.

The distribution kinetics in interstitium was determined by binding to a low-affinity receptor with high capacity ( $R_1, K_{D,1} = 158.6 \pm 63.5$  nmol/ml) and a dissociation time constant,  $1/k_{-1} = 0.027 \pm 0.03$  min<sup>-1</sup>, as well as binding to a high affinity receptor with low capacity ( $R_2, K_{D,2} = 3.516 \pm 1.41$  nmol/ml) and a “fast” dissociation process (time constant,  $1/k_{-2} = 0.73 \pm 0.13$  min<sup>-1</sup>).

### 4.3 Generation of cellular response to digoxin

The time integral of percentage increase in  $LVDP(t)$ , positive inotropism, was significantly increased with increasing dose of digoxin (Fig. 12). The time course of inotropic action of digoxin  $\Delta LVDP$  was successfully described as the weighted sum of drug-receptor complexes  $R_{D,1}$ , and  $R_{D,2}$ , whereby the parameters  $e_T$  can be regarded as the efficacy, i.e., the inotropic response per amount of stimulus  $DR_T(t)$ . The stimulus amplification  $e_T$  was  $21.48 \pm 6.21$  %/nmol, and the contribution of  $R_1, f_1$  was 0.484; in other words, each subtype contribution was 50 % to the total stimulus.

To quantify the pharmacokinetics and pharmacodynamics of digoxin in the present work, a mathematical model of transcapillary exchange, receptor interaction, and effectuation of digoxin in the intact rat heart was built. Although it was necessary to postulate two sarcolemmal binding sites to explain the PK data, the identification of the ratio of high- to low- affinity binding sites was only possible by simultaneous fitting of both *PK* and *PD* modeling, in which drug-receptor interaction does not influence pharmacokinetics (i.e., mass balance) (Breimer and Danhof, 1997; Mager and Jusko, 2001a). Specific binding was an important determinant of digoxin distribution kinetics in the rat heart. To obtain reliable parameter estimates, *a priori* information was utilized on digoxin receptor binding determined in vitro (Ishizuka et al., 1996). Incorporating the ratios of binding parameters,  $K_{A,2}/K_{A,1} = 45$  and  $R_{tot,1}/R_{tot,2} = 3$ , the results of Bayesian modeling were satisfactory both in terms of the capability of the model to describe the data and in terms of parameter estimation (Table 1). The results of this study suggest that the kinetics and inotropic response of digoxin in the normal rat heart are mediated by a mixture of two receptor subtypes, a low-affinity/high-capacity binding site ( $R_1$ ) and a high-affinity/low-capacity binding site ( $R_2$ ), which account for  $89.4 \pm 0.4$  and  $10.6 \pm 0.4\%$  of the total number of receptors ( $R_{tot,1} + R_{tot,2}$ ), respectively (Kang and Weiss, 2002). The fact that the myocardium of the adult rat heart contains two sodium pump subunits exhibiting low ( $\alpha_1$ ) and high ( $\alpha_2$ ) affinity for glycosides, whereby  $\alpha_2$  comprises only 10 to 25% of the sodium pump (Lucchesi and Sweadner, 1991; Askew et al., 1994; Blanco and Mercer., 1998), indicates that  $R_1$  and  $R_2$  are identical to the  $\alpha_1$  and  $\alpha_2$ -isozymes, respectively. According to the results, the term “receptor” as used here is mainly based on the ability of the model to predict the time course of the inotropic effect. The proportionality between effect and receptor occupation suggests that the time dependence of signal transduction (Mager and Jusko, 2001a) was negligible. Finally, it is important to note that our model explains the pharmacodynamics of digoxin without postulating action via an intracellular receptor, i.e., an alternative or additional mechanism to sodium pump inhibition (Sagawa et al., 2002). Although such an effect cannot be excluded, a significant contribution appears unlikely in view of the negligible cellular digoxin uptake during the 1-min infusion period. The vehicle ethanol does also not influence cardiac function in this dose range (Kojima et al., 1993).

No quantitative information could be extracted from the data on the trans-sarcolemmal transport process of digoxin. The nearly complete recovery of injected dose and



sensitivity analysis indicate that the cellular accumulation of digoxin in the 1-min infusion experiment was too small to be detectable with this method. Such a low uptake rate appears consistent with receptor-mediated endocytosis as a possible uptake mechanism (Nunez-Duran et al., 1988; Eisner and Smith, 1992).

The *PK/PD* model was selected according to the principle of parsimony as a minimal mechanistic model, which is in accordance with the information content of the outflow and effect data. The mathematical model, although greatly simplified as a description of a complex process, offers a means to pose hypotheses concerning cardiac pharmacokinetics and pharmacodynamics of digoxin. Although a satisfactory fit to the experimental data is not proof of its correctness, the predictive power of the model is encouraging in view of the ability to accurately predict the time course of inotropic response from receptor occupancy and the principal consistency with previous results on receptor binding obtained in vitro.

### 4.4 Model validity

The results suggest that intracellular uptake of digoxin was negligible; i.e., since this model analysis did not account for a contribution of cellular uptake, digoxin was apparently not able to cross the sarcolemma in significant amounts within the 10-min infusion time. Although the result does not exclude that cardiac glycosides may additionally act at other intracellular sites of action than the  $\text{Na}^+$  pump (Ruch et al., 2003; Sagawa et al., 2002), it was not necessary to postulate such a mode of action in order to explain the inotropic effect of digoxin in experiments. This is in accordance with the evidence that the ouabain-induced increase in contractility in mice is solely mediated by the  $\text{Na}^+, \text{K}^+$ -ATPase (Dostanic et al., 2003). This holds also for a possible activation of signal pathways that may contribute to the effect development at longer timescales (Xie and Askari, 2002).

To check whether the model developed for single dose 1-min infusion of digoxin is also valid for long term infusion, additional experiments were performed whether 1-min infusion was followed by a 10-min infusion. The estimated parameters were not significantly different (Table 2) from those obtained after three consecutive 1-min

#### 4. Results and discussion

infusions (Table 1). Fig. 13 shows that the model was capable to fit the 10-min infusion data as good as the 1-min infusion data.

**Table 2.** Model parameter estimates for the *PK/PD* of 1-min and 10-min consecutive infusion of digoxin (30 and 300  $\mu\text{g}$ ) in isolated rat heart (mean  $\pm$  S.D.,  $n = 5$ ).

Parameters	Estimated values
<i>Cardiac Uptake</i>	
$CL_{vi}$ (ml/min/g)	$8.258 \pm 1.91$ (12 $\pm$ 5) <sup>a</sup>
$V_{app, is}$ (ml/g)	$0.653 \pm 0.24$ (12 $\pm$ 9)
<i>Receptor Binding</i>	
$R_{tot,1}$ (nmol/g)	$28.43 \pm 7.57$ (10 $\pm$ 3)
$k_1$ (1/min/nmol/ml)	$0.032 \pm 0.01$ (18 $\pm$ 9)
$k_{-1}$ (1/min)	$4.440 \pm 2.12$ (23 $\pm$ 15)
$R_{tot,2}$ (nmol/g)	$8.614 \pm 2.55$ (17 $\pm$ 4)
$k_2$ (1/min/nmol/ml)	$0.394 \pm 0.25$ (15 $\pm$ 6)
$k_{-2}$ (1/min)	$0.740 \pm 0.19$ (16 $\pm$ 3)
$K_{D,1}$ (nmol/ml)	$141.9 \pm 75.5$
$K_{D,2}$ (nmol/ml)	$2.469 \pm 1.32$
$K_{A,2}/K_{A,1}$	$44.93 \pm 0.22$ (2 $\pm$ 1)
$R_{tot,1}/R_{tot,2}$	$3.330 \pm 0.50$ (8 $\pm$ 3)
<i>Cellular Effectuation</i>	
$e_T$ (%/nmol)	$15.97 \pm 2.23$ (18 $\pm$ 3)
$f_1$	$0.580 \pm 0.16$ (18 $\pm$ 6)

<sup>a</sup>Values in parentheses are the asymptotic coefficients of variation (CV) of parameter estimates (mean  $\pm$  S.D.) obtained from individual fits.

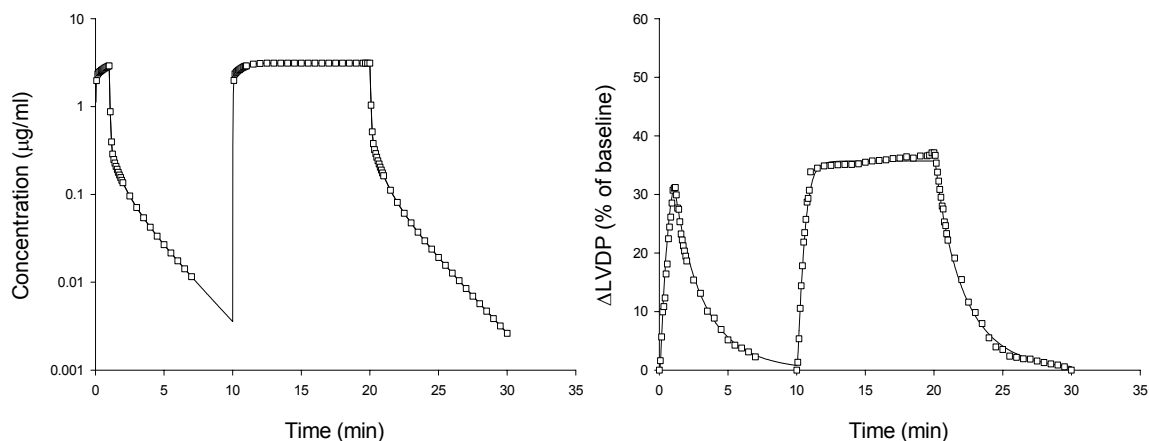


**Figure 13.** Representative fit of the model (smooth curve) to experimental data (open squares). Digoxin outflow concentration (upper panel) and percentage increase in left ventricular developed pressure (LVDP) for digoxin infusion. Doses were 30 and 300 µg for each infusion.

The major advantage of this approach is that the study of the interplay between binding kinetics to a heterogeneous receptor population and effectuation processes at the cellular level is possible in the intact heart. Thus, the present results underline the heuristic potential of kinetic modeling for providing quantitative insight into the mechanisms underlying system response (Kitano, 2002). However, there are a number of limitations to this approach. Like any model, our model is a great simplification of reality and the results are dependent on model selection and the quality of parameter estimation. Reliability of parameter estimation was improved by using data obtained at three dose levels. Although we have incorporated only those steps in our model known to be essential for modeling of digoxin kinetics and action in the rat heart, the model contains more parameters than can be estimated from the data. Despite these limitations, kinetic modeling approach combined with specifically designed experiments offers a quantitative understanding of the effects of inotropic response to a 1-min infusion and 10-min infusion of digoxin in the isolated rat heart. It allows differentiation between effects elicited at the receptor and postreceptor level and provides parameters characterizing the functional heterogeneity of the sodium pump. This systems analysis of transient response kinetics provides new insight into the effects of sodium pump inhibition in the rat heart that cannot be obtained by the classical steady-state approach of measuring dose-response curves.

#### 4.5 Effect of external $\text{Ca}^{2+}$ and NCX inhibition

##### 4.5.1 Measurement of outflow concentration and cardiac performance

Figure 14 shows a typical recording of the left ventricular pressure response to three consecutive digoxin doses (15, 30, and 45  $\mu\text{g}$ ) measured in hearts with calcium concentrations of 0.5 and 1.5 mM, respectively, in perfusate under control conditions and in the presence of KBR. The average digoxin outflow concentration and inotropic response data ( $n = 5$  in each group) are depicted in Figure 15. Percentage increase in *LVDP* caused by digoxin was significantly enhanced in the 0.5 versus 1.5 mM  $[\text{Ca}^{2+}]_o$  group ( $P < 0.05$ ).

At digoxin doses of 30 and 45  $\mu\text{g}$ , the presence of KBR (0.1  $\mu\text{M}$ ) in perfusate induced a significant decrease in pressure developed (Fig. 15) and its time integral (Fig. 17).

An increase in  $[\text{Ca}^{2+}]_o$  from 0.5 to 1.5 mM led to a ~3-fold increase ( $P < 0.001$ ) in baseline contractility (*LVDP*<sub>0</sub>) and a small decrease ( $P < 0.05$ ) in coronary vascular resistance (*CVR*). No significant change in left ventricular end-diastolic pressure (*LVEDP*) was observed and KBR in perfusate did not affect baseline function of the heart (Table 3). The 1-min infusions of digoxin did not affect coronary vascular resistance and left ventricular end-diastolic pressure.

**Table 3.** Effects of calcium and KB-R7943 on baseline values of left ventricular developed pressure (*LVDP*<sub>0</sub>), left ventricular developed end-diastolic pressure (*LVEDP*) and coronary vascular resistance (*CVR*) prior to digoxin administration.

	0.5 mM $[\text{Ca}^{2+}]_o$		1.5 mM $[\text{Ca}^{2+}]_o$	
	Control	KB-R7943	Control	KB-R7943
<i>LVDP</i> <sub>0</sub> (mmHg)	27.6 ± 8.03	26.6 ± 5.29	75.8 ± 8.55***	72.8 ± 8.59***
<i>LVEDP</i> (mmHg)	6.42 ± 0.56	6.66 ± 4.94	6.74 ± 3.37	6.88 ± 3.13
<i>CVR</i> (mmHg × min/ml)	5.22 ± 0.26	5.34 ± 0.27	4.49 ± 0.44*	4.68 ± 0.40*

\* $P < 0.05$  and \*\*\*  $P < 0.001$  for 1.5 vs. 0.5 mM  $[\text{Ca}^{2+}]_o$  group.

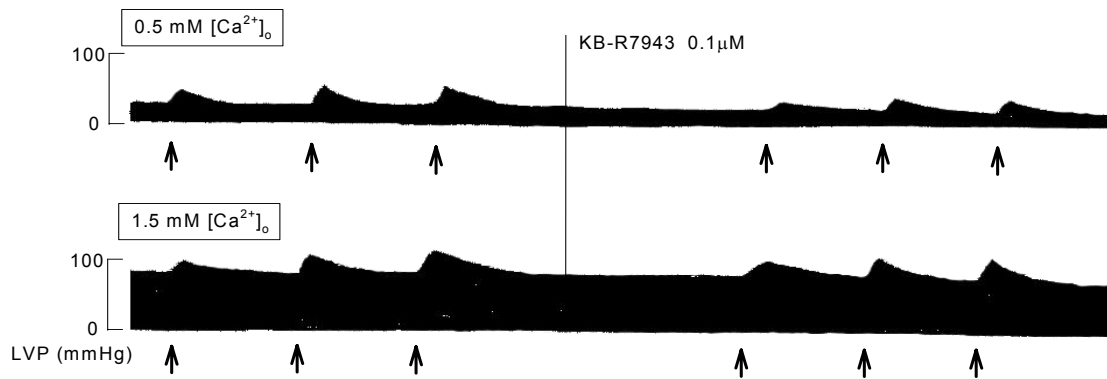


**Figure 14.** Original recording of the left ventricular pressure after three consecutive digoxin doses (15, 30, and 45  $\mu\text{g}$ ) under control conditions and in the presence of KB-R7943 for experiments with external calcium concentrations of 0.5 and 1.5 mM.

## 4. Results and discussion

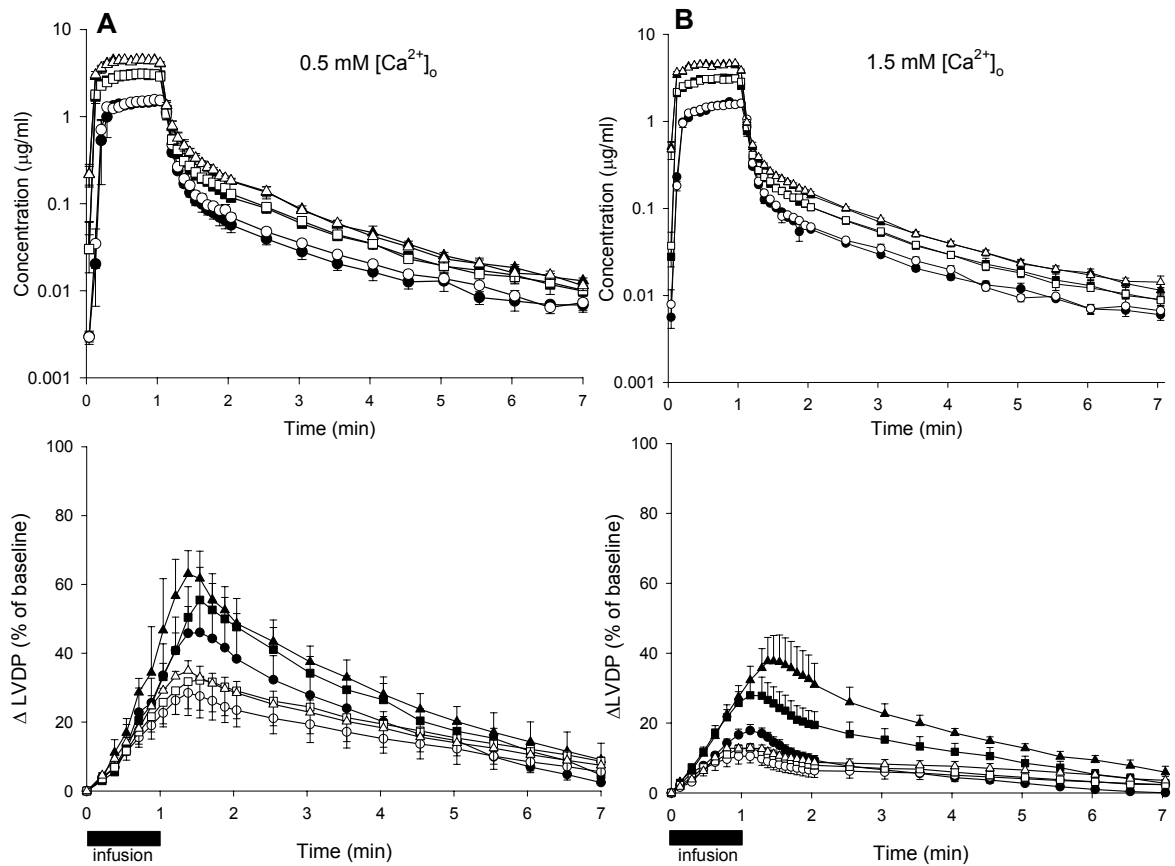


**Figure 15.** Average digoxin outflow concentration (upper panel) and percent increase in developed left ventricular pressure (lower panel) for three digoxin doses of 15 (●), 30 (■) and 45 (▲) µg under control conditions and in the presence of KB-R7943 (0.1 µM) (open symbols) as observed in experiments with external calcium concentrations of 0.5 (A) and 1.5 mM (B), respectively.

## 4. Results and discussion

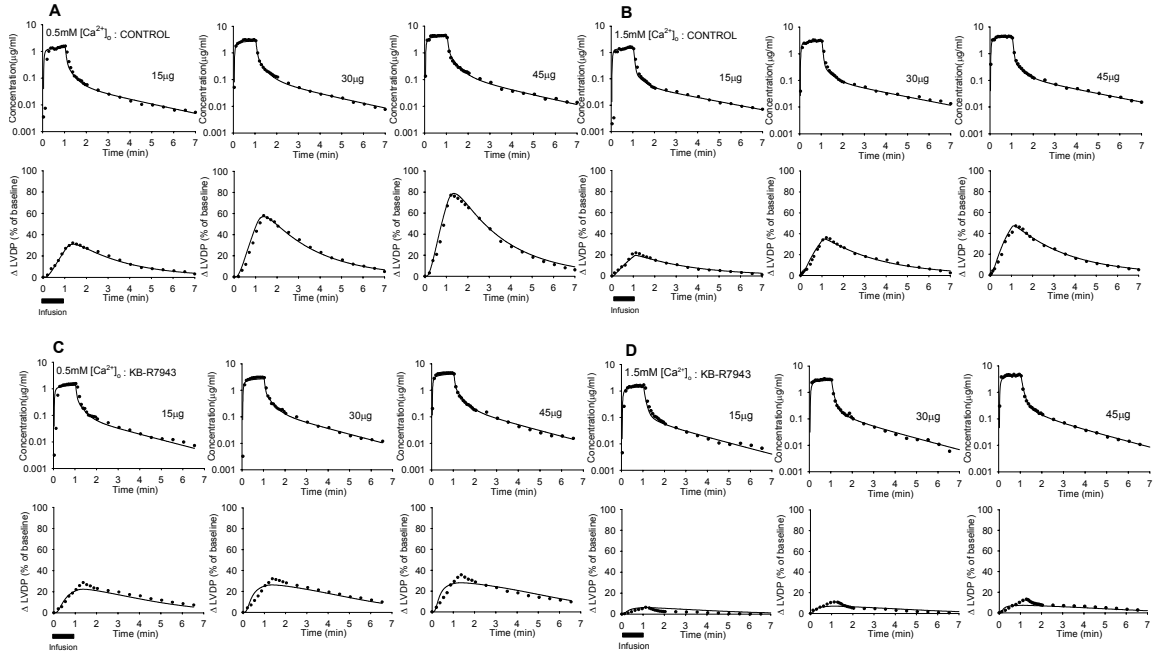


**Figure 16.** Representative simultaneous fits of the model (smooth curves) to experimental data (symbols): Digoxin outflow concentration (upper panels) and percent increase in developed left ventricular pressure (lower panels) for three digoxin doses (15, 30, and 45  $\mu\text{g}$ ) before (A and B) and after KB-R7943 (0.1  $\mu\text{M}$ ) (C and D) as observed in experiments with external calcium concentrations of 0.5 (A and C) and 1.5 mM (B and D), respectively.

### 4.5.2 PK/PD Parameter estimation

Representative simultaneous fits of the model to data obtained for three consecutive digoxin doses (15, 30, and 45  $\mu\text{g}$ ) and external calcium concentrations of 0.5 and 1.5 mM are depicted in Fig. 16. In all control experiments (i.e., without NCX inhibition), the simplest effectuation model (Eq. 10) that assumes additivity of responses mediated by both isoforms (Gao et al., 1995; Sweadner, 1993) was sufficient to describe the data (Kang and Weiss, 2002). The model was conditionally identifiable and parameters were estimated with reasonable precision. The averaged model parameters and estimation errors, as a percentage of related parameter estimates, are listed in Table 4. Notably, the increase in digitalis sensitivity with decreasing external calcium concentration is due to

#### 4. Results and discussion

a significantly increased efficiency of response generation (the slope of the occupancy-response relationship,  $e_T$ , increases from 17.7 to 25.6 %  $\Delta LVDP/nmol$ ,  $P<0.05$ ) and this effect is mediated by both isoforms. The fractional contributions  $f_1$  and  $f_2$  ( $= 1-f_1$ ) of  $\alpha_1$ - and  $\alpha_2$ - isoforms, respectively, to stimulus amplification  $e_T$  were not significantly different. However,  $f_1$  decreased (and  $f_2$  increased) significantly by 20 % when  $[Ca^{2+}]_o$  was reduced from 1.5 and to 0.5 mM ( $P<0.01$ ). Furthermore, a decrease in  $[Ca^{2+}]_o$  from 1.5 to 0.5 mM was accompanied by a significant ( $P<0.01$ ) increase in apparent interstitial distribution volume of digoxin,  $V_{app, is}$ , in the control group, corresponding to an increase in equilibrium partition coefficient  $K_{eq}$  from  $0.3 \pm 0.2$  to  $0.5 \pm 0.3$  (for a volume of the interstitial space of  $V_{is}=0.64$  ml/g ).

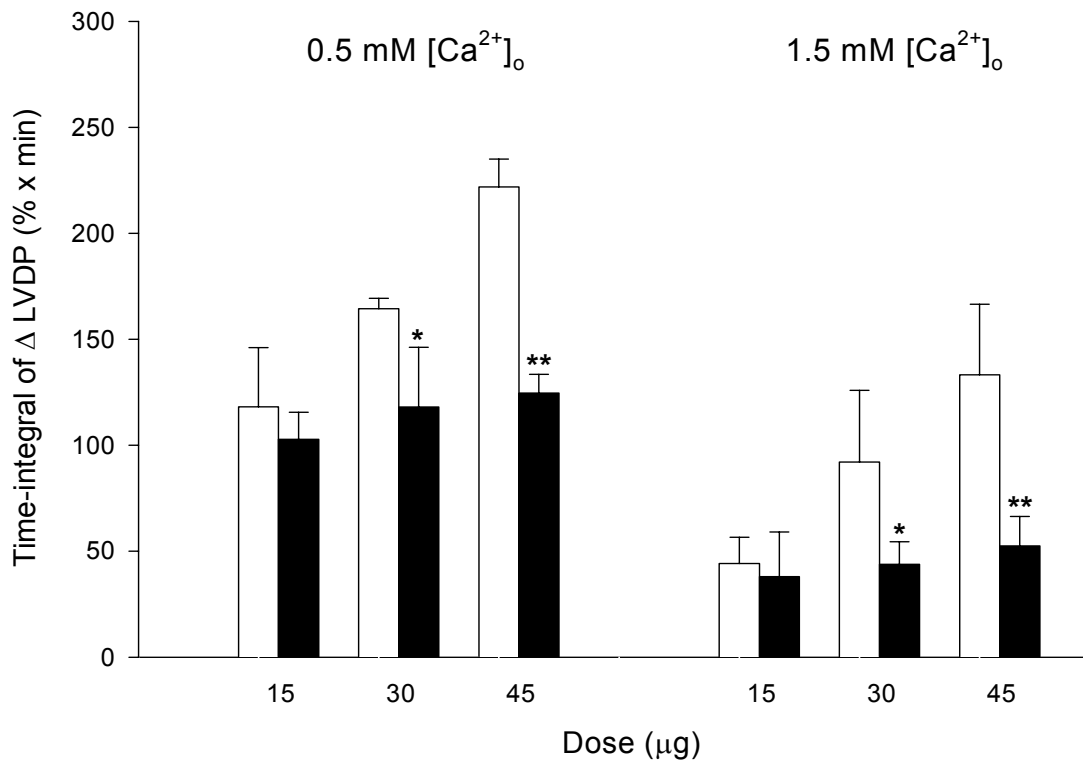


**Figure 17.** Effect of external calcium ( $[Ca^{2+}]_o$ ) and NCX inhibition by KB-R7943 (0.1  $\mu M$ ) on the time integral of effect. Data are means  $\pm$  S.D. from 5 experiments in each of the 0.5 and 1.5 mM  $[Ca^{2+}]_o$  groups. \* $P<0.05$  and \*\* $P<0.01$  compared with the value before exposure to KB-R7943.



#### 4. Results and discussion

**Table 4.** Parameters estimated by simultaneous fitting of outflow and inotropic response data after 1-min infusions of 15, 30, and 45 µg digoxin in isolated rat hearts with external calcium concentration of 0.5 and 1.5 mM (mean ± S.D.,  $n = 5$  in each group).

	0.5 mM[Ca <sup>2+</sup> ] <sub>o</sub>	
	Control	KB-R7943
<i>Cardiac Uptake</i>		
$CL_{vi}$ (ml/min/g)	7.959 ± 1.84(24 ± 9) <sup>a</sup>	9.321 ± 1.61(27 ± 6)
$V_{app, is}$ (ml/g)	0.930 ± 0.19(19 ± 10)	0.741 ± 0.19(21 ± 11)
<i>Receptor Binding</i>		
$R_{tot,1}$ (nmol/g)	30.87 ± 7.46(41 ± 15)	28.03 ± 8.33(32 ± 21)
$k_1$ (1/min/nmol/ml)	0.021 ± 0.01(54 ± 33)	0.020 ± 0.01(49 ± 12)
$k_{-1}$ (1/min)	2.957 ± 0.98(83 ± 13)	2.470 ± 1.19(77 ± 26)
$R_{tot,2}$ (nmol/g)	9.857 ± 3.59(40 ± 14)	9.407 ± 2.57(31 ± 21)
$k_2$ (1/min/nmol/ml)	0.215 ± 0.06(60 ± 29)	0.310 ± 0.17(46 ± 25)
$k_{-2}$ (1/min)	0.674 ± 0.05(9 ± 2)	0.770 ± 0.10(9 ± 2)
$K_{D,1}$ (nmol/ml)	154.8 ± 61.4	135.2 ± 60.6
$K_{D,2}$ (nmol/ml)	3.439 ± 1.36	3.011 ± 1.35
$K_{A,2}/K_{A,1}$	45.04 ± 0.68(2 ± 1)	44.87 ± 0.07(2 ± 1)
$R_{tot,1}/R_{tot,2}$	3.244 ± 0.42(11 ± 1)	2.962 ± 0.25(10 ± 1)
<i>Cellular Effectuation</i>		
$e_T$ (%/nmol)	25.59 ± 5.11(33 ± 27)	
$f_1$	0.380 ± 0.04(29 ± 25)	
$\Phi_{max}$ (%)		26.11 ± 5.50(8 ± 2)
$K_{DR}$ (nmol)		0.256 ± 0.09(18 ± 2)
$\Phi_{max}/e_T$ (nmol)		0.997 ± 0.19
$\tau$ (min)		0.138 ± 0.09(39 ± 13)

<sup>a</sup>Values in parentheses are the asymptotic coefficients of variation (CV) of parameter estimates (mean ± S.D.) obtained from individual fits.

\* $P < 0.05$ , \*\* $P < 0.01$  and \*\*\* $P < 0.001$  vs. corresponding value in 0.5 mM [Ca<sup>2+</sup>]<sub>o</sub> group. Changes in response to KB-R7943 in each group did not achieve statistical significance.

#### 4. Results and discussion

**Table 4.** Continued

	1.5 mM[Ca <sup>2+</sup> ] <sub>o</sub>			
	Control		KB-R7943	
<i>Cardiac Uptake</i>				
$CL_{vi}$ (ml/min/g)	6.627 ± 1.24	(30 ± 4)	9.649 ± 2.00	(27 ± 4)
$V_{app, is}$ (ml/g)	0.614 ± 0.09	(28 ± 19)	0.650 ± 0.29	(17 ± 5)
<i>Receptor Binding</i>				
$R_{tot,1}$ (nmol/g)	29.39 ± 11.6	(30 ± 17)	27.61 ± 10.2	(47 ± 17)
$k_1$ (1/min/nmol/ml)	0.020 ± 0.01	(50 ± 9)	0.020 ± 0.01	(55 ± 40)
$k_{-1}$ (1/min)	2.591 ± 0.46	(85 ± 24)	2.584 ± 0.77	(65 ± 17)
$R_{tot,2}$ (nmol/g)	9.451 ± 3.86	(57 ± 36)	9.203 ± 3.20	(46 ± 17)
$k_2$ (1/min/nmol/ml)	0.227 ± 0.10	(65 ± 43)	0.242 ± 0.07	(64 ± 25)
$k_{-2}$ (1/min)	0.657 ± 0.06	(9 ± 2)	0.659 ± 0.09	(10 ± 7)
$K_{D,1}$ (nmol/ml)	162.7 ± 106		142.6 ± 84.4	
$K_{D,2}$ (nmol/ml)	3.638 ± 2.37		3.176 ± 1.88	
$K_{A,2}/K_{A,1}$	44.94 ± 0.92	(2 ± 1)	44.91 ± 0.06	(2 ± 1)
$R_{tot,1}/R_{tot,2}$	3.123 ± 0.21	(10 ± 1)	3.101 ± 0.07	(10 ± 1)
<i>Cellular Effectuation</i>				
$e_T$ (%/nmol)	17.66 ± 6.92*	(59 ± 20)		
$f_1$	0.479 ± 0.05**	(80 ± 34)		
$\Phi_{max}$ (%)			10.06 ± 1.50***	(7 ± 1)
$K_{DR}$ (nmol)			0.281 ± 0.04	(15 ± 1)
$\Phi_{max}/e_T$ (nmol)			0.667 ± 0.41	
$\tau$ (min)			0.010 ± 0.01*	(39 ± 4)

The simple transduction model used under control conditions (Eq. 10) failed to describe the effect-time data in the presence of the NCX-inhibitor KBR. A reasonable fit was obtained with the nonlinear stimulus-response model (Eq. 8) indicating a decrease in digoxin effect for receptor-occupancies  $DR_T$  above  $\approx 0.5$ -1  $\mu\text{g}$  (Fig. 18). Since the contribution to total amplification mediated by low affinity receptor  $\alpha_l$  (parameter  $f_1$ ) could not be estimated with sufficient reliability in the presence of KBR, this parameter was fixed to the estimate obtained under control conditions. Although this model well captured the major features of the data, it failed to fit the peak of the curve in the case of the 0.5 mM [Ca<sup>2+</sup>]<sub>o</sub> experiments (Fig. 16). The decrease in [Ca<sup>2+</sup>]<sub>o</sub> led also under KBR to higher sensitivity to inotropic stimulation here characterized by significant (2.6-fold) increase of  $\phi_{max}$  ( $P < 0.001$ ). In addition, the delay in response generation was

significantly increased (Table 4). Although there was some tendency for a higher reduction of stimulus amplification by KBR at 1.5 mM versus 0.5 mM  $[Ca^{2+}]_o$  (Fig. 18 and  $\phi_{max}/e_T$  in Table 4), this difference was not statistically significant.

### 4.5.3 Simulated response characteristics

The model analysis indicated that positive inotropic digoxin effect was predominantly mediated by the high affinity pumps ( $\alpha_2$ ). This was illustrated by Fig. 20 where the contributions of both  $\alpha$ -isoforms to inotropic response for 1.5 mM  $[Ca^{2+}]_o$  were calculated on the basis of the mean parameter estimates. In the transient case of our 1-min infusion as well as in the simulation for a 10-min infusion, the inhibition of the  $\alpha_2$ -isoform by digoxin was clearly dominating (more than 80 % of the effect is  $\alpha_2$ -mediated). An increase in  $\alpha_2$ -contribution with decreasing digoxin dose was only suggested by the simulated response to the 10-min infusion where the response at 5 min corresponds to the steady state situation.

The occupancy-response relationships predicted from the mean parameter estimates under control conditions (Eq.10) and in the presence of KBR (Eq. 8) visualized the effect of reverse NCX inhibition on digoxin response generation (Fig. 18). Due to the saturation characteristics (governed by parameters  $K_{DR}$  and  $\phi_{max}$ ) KBR reduced the efficiency of the cellular transduction process with increasing receptor occupancy. In accordance with the results shown in Fig. 17, this reduction in inotropy disappeared (or became very small) for  $DR_T < 0.5 - 1 \mu g$ . (According to Fig. 18, the 15  $\mu g$  dose led to maximum receptor occupancies,  $DR_T$ , of about 1 and 0.7  $\mu g$  for 0.5 and 1.5 mM  $[Ca^{2+}]_o$ , respectively.)

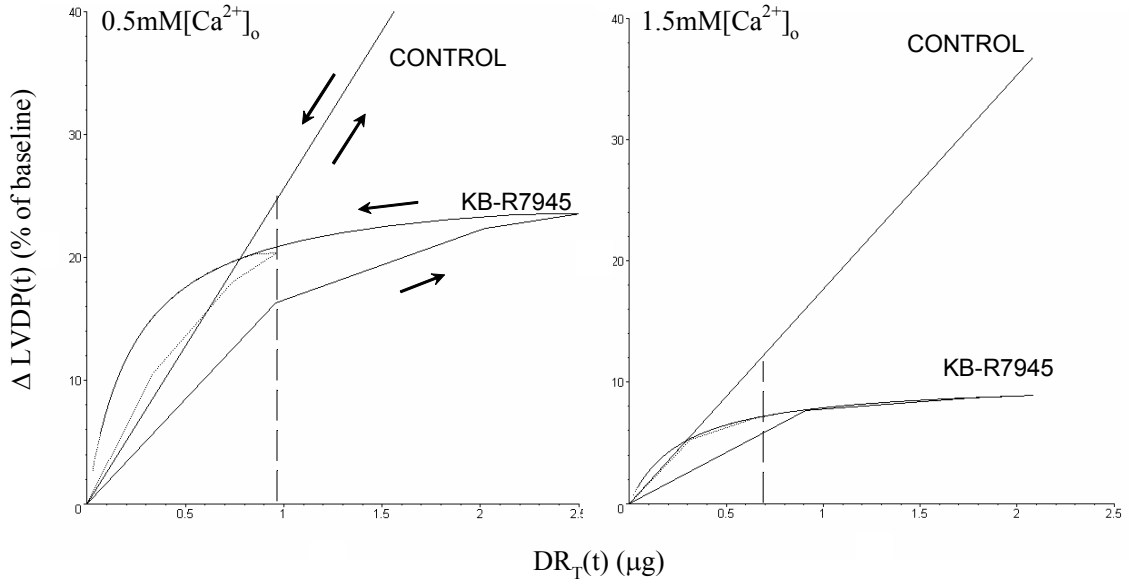


**Figure 18.** Model simulations of the relationship between total receptor occupancy  $[\text{DR}_T(t)]$  and inotropic response (phase-plane plot) under control conditions and after NCX inhibition by KBR ( $0.1\ \mu\text{M}$ ) for the  $45\ \mu\text{g}$  and  $15\ \mu\text{g}$  dose of digoxin, computed with average parameters estimated for  $0.5$  and  $1.5\ \text{mM}\ [\text{Ca}^{2+}]_o$ , respectively (Table 4). The dashed lines indicate maximum receptor occupancy for the  $15\ \mu\text{g}$  dose and arrows the temporal evolution of response.

To explain the linear relationship between receptor occupation and response (*Eq. 10*) in terms of the underlying effectuation process, the equation for the sodium pump mediated  $\text{Na}^+$  efflux rate,  $V_{\text{Na}}$  was used (Verdonck et al., 2003).

$$V_{\text{Na}} = \frac{V_{\text{Na},\alpha 1,\text{max}} [\text{Na}^+]_i^n}{[\text{Na}^+]_i^n + K_{\text{Na},\alpha 1}} + \frac{V_{\text{Na},\alpha 2,\text{max}} [\text{Na}^+]_i^n}{[\text{Na}^+]_i^n + K_{\text{Na},\alpha 2}} \quad (21)$$

where  $[\text{Na}^+]_i$  is the intracellular sodium concentration and  $K_{\text{Na},\alpha 1}$  ( $K_{\text{Na},\alpha 2}$ ) denotes the apparent affinities for  $\text{Na}^+$  of the  $\alpha_1$ - ( $\alpha_2$ ) isoform. For a certain pump activity, one can calculate the increase in  $[\text{Na}^+]_i$  with increasing pump inhibition (receptor occupation  $\text{DR}_i$ ) by solving *Eq.21* for  $[\text{Na}^+]_i$ . While no direct information is available on the relationship between extracellular calcium concentration  $[\text{Ca}^{2+}]_o$  and  $\text{Na}^+$  pump activity,

#### 4. Results and discussion

---

Simor et al. (1997) have evaluated the dependence of  $[\text{Na}^+]_i$  from  $[\text{Ca}^{2+}]_o$  in isolated perfused rat hearts using nuclear magnetic resonance and could describe it by

$$[\text{Na}^+]_i = 11.33 \exp(-[\text{Ca}^{2+}]_o/3.65) \quad (22)$$

Thus, for a decrease of  $[\text{Ca}^{2+}]_o$  from 1.5 to 0.5 mM an increase of  $[\text{Na}^+]_i$  from 7.5 to 9.9 mM is predicted. Substituting these values into Eq. 21 (using  $K_{Na,1} = 12.4$  mM,  $K_{Na,2} = 22$  mM and  $n = 2.5$  (Verdonck et al., 2003)), pump activities of 28 and 48 % of the maximum activity for  $[\text{Ca}^{2+}]_o = 0.5$  and 1.5 mM were obtained, respectively. As mentioned above, these values were used to simulate the  $[\text{Na}^+]_i$ - $DR_2$  relationships shown in Fig. 19. The intracellular  $\text{Na}^+$  concentration increases with increasing pump inhibition ( $\alpha_2$ -receptor occupancy  $DR_2$ ) and the slope of the curve decreases with increasing external calcium concentration  $[\text{Ca}^{2+}]_o$ . (For the sake of simplicity, the influence of  $\alpha_1$ -receptor occupation has been neglected in this simulation study.)

Evaluation of the kinetics of digoxin disposition and action in the isolated perfused heart preparation is a useful method to examine the respective roles of myocardial uptake, drug-receptor interaction and cellular effectuation process in the whole organ using dynamic systems analysis.

The results can be summarized as follows: first, the digoxin-induced positive inotropic effect is mainly (> 80 %) mediated through the  $\alpha_2$ -isoform of the  $\text{Na}^+, \text{K}^+$ -ATPase; second, a decrease in  $[\text{Ca}^{2+}]_o$  from 1.5 to 0.5 mM increases the stimulus amplification (slope of the receptor occupancy-response curve) probably due to a steeper relation between  $[\text{Na}^+]_i$  and contractility and third, KBR decreases the digoxin action with increasing receptor occupancy to a limiting maximum value indicating an inhibition of  $\text{Ca}^{2+}$  influx via NCX.

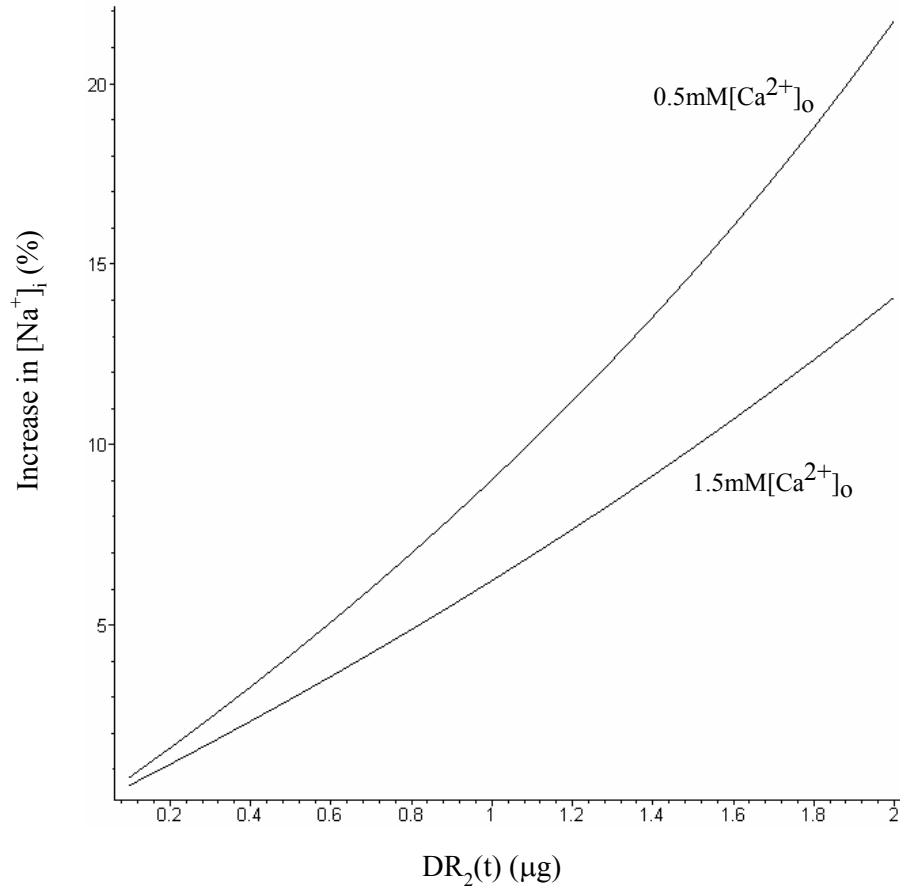


**Figure 19.** Influence of external calcium concentration on the relationship between increase  $[\text{Na}^+]_i$  and sodium pump inhibition [ $\alpha_2$ -receptor occupation,  $DR_2(t)$ ] as predicted by Eqs.21 and 22.

#### 4.5.4 Functional receptor heterogeneity

The results obtained here regarding the correlation of physiological response to  $\alpha_1$ - and  $\alpha_2$ - isoform inhibition are in general agreement with these findings if one takes into account that more refined *a priori* information on  $K_{A,2}/K_{A,1}$  and  $R_{tot,1}/R_{tot,2}$  ratios were used in this study. This result that the inotropic response to digoxin was more than 80 % mediated by the  $\alpha_2$ -isoform (Fig. 20) was in accordance with recent results obtained for ouabain in the mouse heart (Dostanic et al., 2003). The simulation of a steady-state situation (response to a 10-min infusion) gave nearly the same result, except that  $\alpha_2$ -contribution further increased (to about 90 %) for the 15  $\mu\text{g}$  dose (Fig. 20). That

similarly the  $\alpha_2$ -contribution also slightly increased when  $[\text{Ca}^{2+}]_o$  was decreased from 1.5 to 0.5 mM can be explained by the increase in  $\alpha_2$ -efficacy ( $f_2 = 1 - f_1$ ).

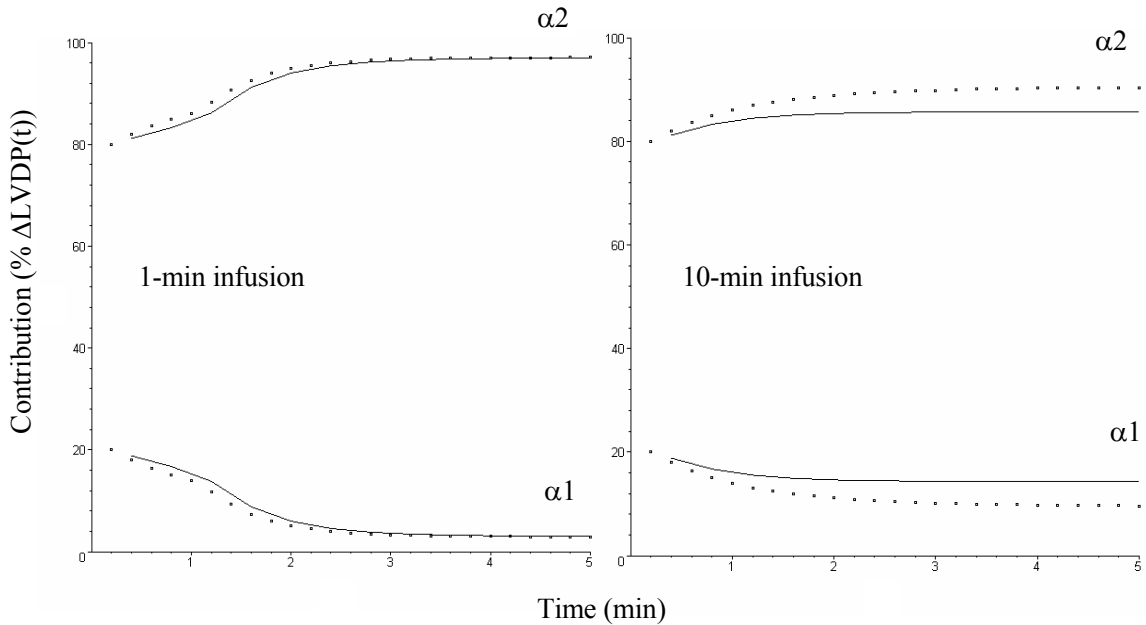


**Figure 20.** Model-predicted percent contribution of low affinity/high capacity ( $\alpha_1$ ) and high affinity/low capacity ( $\alpha_2$ ) receptors to inotropic response following a 1-min infusion (left) and a 10-min infusion (right) of 45  $\mu\text{g}$  (line) and 15  $\mu\text{g}$  (points) digoxin, computed with average parameters estimated for 1.5 mM  $[\text{Ca}^{2+}]_o$  (Table 4).

#### 4.5.5 Receptor occupancy-response relationship

The linear model of the receptor occupancy-response relationship (Eq. 10) used in this study to describe postreceptor events is in principal accordance with the simulated quasi-linear  $[\text{Na}^+]_i\text{-DR}_2$  relationship (Fig. 20) and the proportionality of digitalis-induced inotropic response and increase in  $[\text{Na}^+]_i$  observed in rat (Harrison et al., 1992) and cat (Vila Petroff et al., 2003) ventricular myocytes. This indicates that under control conditions, the process of receptor binding appears to be the rate-limiting step in response generation (i.e., the effect was in phase with receptor occupancy). The nearly equal fractional contributions  $f_1$  and  $f_2$  ( $= 1 - f_1$ ) of  $\alpha_1$ - and  $\alpha_2$ - isoforms, respectively, to

stimulus amplification  $e_T$  (slope of the relationship between total receptor occupancy  $DR_T$  and effect), is consistent with the predicted effect of receptor occupation on the increase in  $[\text{Na}^+]_i$  (Eq. 21). It is currently under debate whether the  $\text{Na}^+$  pump  $\alpha$ -isoforms have specific functional roles (Bers, 2001; Bers et al., 2001; James et al., 1999; Verdonck et al., 2003). Since only for the low calcium concentration slightly higher stimulus amplification was found for the  $\text{Na}^+$  pump  $\alpha_2$ -isoform, our findings can hardly be explained by a preferentially  $\alpha_2$ -mediated response due to a possible colocalization with the NCX in the sarcolemma at sites of restricted diffusion (Blaustein and Lederer, 1999; Golovina et al., 2003; James et al., 1999). The dominating role of the  $\alpha_2$ -isoform under our experimental conditions (Fig. 19) was solely due to its higher affinity.

### 4.5.6 Effect of external calcium concentration

In all groups, an increase in  $[\text{Ca}^{2+}]_o$  from 0.5 to 1.5 mM resulted in an increase in baseline contractility; the 2.7-fold increase in  $LVDP_0$  is comparable with the value observed by Gaszner et al. (2001) and in accordance with the positive correlation between inotropy and external calcium concentration in rats (Forester and Mainwood, 1974). Note that external calcium concentration of 1.5 mM corresponds to the physiological level of unionized calcium in rats (Chambers et al., 1991).

There are no reports in the literature that give a quantitative mechanistic explanation of the increasing sensitivity to digitalis-induced cardiac inotropy with decreasing  $[\text{Ca}^{2+}]_o$  observed in rat (Hickerson et al., 1988) and mouse (Schwartz and Petrashevskaya et al., 2001) hearts. The result of this study suggests that a change in  $[\text{Ca}^{2+}]_o$  affects solely the cellular effectuation process. The observed 50% increase in the slope of the occupancy-response relationship (i.e., stimulus amplification) after decreasing  $[\text{Ca}^{2+}]_o$  from 1.5 to 0.5 mM (Fig. 18) could be attributed to the increase in the slope of the  $[\text{Na}^+]_i$  -occupancy relationship predicted by Eqs. 21 and 22 (Fig. 20). Due to the uncertainty in the underlying  $K_{Na, \alpha i}$  values (Bers et al., 2003) and the assumption of an unchanged  $\Delta[\text{Na}^+]_i$  -inotropic response relation, this simulation is only a very rough approximation to illustrate the role of  $[\text{Ca}^{2+}]_o$ . Nevertheless, the results are qualitatively consistent with our experimental data. This finding obtained here by a model analysis of the transient inotropic response to a 1-min infusion of digoxin is in accordance with the biphasic



dose-response curves of ouabain measured for low  $[Ca^{2+}]_o$  in mouse (Schwartz and Peteshevskaya et al., 2001) and rat heart (Hickerson et al., 1988). A further reduction in stimulus amplification  $e_T$  to a value of about 10 % of the value estimated at 1.5 mM  $[Ca^{2+}]_o$  was found in experiments with 2.5 mM  $[Ca^{2+}]_o$ , where the digoxin doses were 5-fold higher (Kang and Weiss, 2002).

Taken together, the increasing sensitivity to inotropic stimulation with decreasing external calcium concentrations can be clearly attributed to the cellular effectuation process (parameter  $e_T$ ) since no influence of  $[Ca^{2+}]_o$  on receptor binding (dissociation constants  $K_{D,i}$ ,  $i = 1,2$ ) was observed. It should be noted that the terminology of “sensitivity to inotropic stimulation” adopted in this paper differs from “cardiac glycoside sensitivity” which usually refers to receptor affinity alone (e.g., Bers et al., 2003; Levi et al., 1994; McDonough et al., 1995).

The transcapillary exchange clearance of digoxin ( $CL_{vi} = 6.6 \pm 1.2$  ml/min/g at  $[Ca^{2+}]_o = 1.5$  mM) was not significantly different to the value of  $3.0 \pm 1.0$  ml/min/g measured for sucrose in isolated perfused rat heart, the data from Caldwell et al. (1998) was consistent with this result ( $5.1 \pm 1.4$  ml/min/g). This is indicating barrier-limited uptake by passive transport through interendothelial gaps. Since reduction in  $[Ca^{2+}]_o$  was suggested to increase endothelial permeability and the vascular surface area available for albumin exchange (Donahue et al., 1998), the 34% increase in the apparent interstitial distribution volume  $V_{app, is}$  of digoxin observed for the decrease of  $[Ca^{2+}]_o$  from 1.5 to 0.5 mM, could be attributed to fluid and albumin accumulation in the interstitium. The slight but significant decrease in basal  $CVR$  with increasing  $[Ca^{2+}]_o$  (Table 3) may reflect an autoregulatory response to the increased heart work and oxygen consumption.

### 4.5.7 Effect of NCX inhibition by KB-R7943

The  $Na^+/Ca^{2+}$  exchange inhibitor KBR (0.1  $\mu$ M) markedly attenuated the rise in  $LVDP$  induced by digoxin doses of 30 and 45  $\mu$ g (Fig. 15 and 17) but did not influence cardiac performance at basal conditions and the lowest digoxin dose (15  $\mu$ g). That co-administration of KBR only influences the chain of postreceptor events (it did not affect receptor binding) is in accordance with the well-established central role of NCX in

inotropic response generation. In terms of our empirical model, this has the following consequences: First, the apparent linear effectuation process (Eq. 8) becomes saturated (Eq. 10) resulting in a decrease in the effect per unit digoxin-receptor occupancy, as shown by the simulated phase portrait of the time course of stimulus-response curves (Fig. 18). The decreasing deviation of the hyperbolic from the linear curves with decreasing total receptor occupancy explains the lack of KBR effect at the lowest dose level of 15  $\mu\text{g}$  (Fig. 17), which corresponds to a receptor occupation of  $\approx 1 \mu\text{g}$ . Second, NCX inhibition by KBR leads to a response  $E(t)$  that lags behind the time course of occupancy,  $DR_T(t)$ , as reflected by the counterclockwise hysteresis loop after NCX inhibition (Fig. 18). Thus, it is reasonable to assume that the generation of the response becomes the rate-limiting step. Together with the lack of effect of KBR on basal contractility, these findings suggest that the concentration of KBR used in the present experiments in perfused rat heart (0.1  $\mu\text{M}$ ) was able to selectively block the  $\text{Ca}^{2+}$  influx mode of the NCX. In this case, the lack of an inhibitory KBR effect on digoxin induced inotropy for low receptor occupancy ( $< DR_T \approx 0.5 \mu\text{g}$ , Fig. 18; or doses  $< 15 \mu\text{g}$ , Fig. 17) may be explained by the fact that in this situation (small increase in  $[\text{Na}^+]_i$ ) no net  $\text{Ca}^{2+}$  influx via NCX is necessary to increase contractility (Sato et al., 2003). The inotropic response to increasing digoxin doses would then be effectively limited under KBR to the contribution that is independent of net  $\text{Ca}^{2+}$  influx via NCX. The  $[\text{Ca}^{2+}]_i$ -dependency of  $\phi_{\text{max}}$  can be due to the different slopes of the  $[\text{Na}^+]_i$  - $DR_T$  curves (Fig. 20) (analogously to the  $[\text{Ca}^{2+}]_i$ -dependency of  $e_T$ ). This is consistent with previous results showing that KBR preferentially blocks the  $\text{Ca}^{2+}$  influx (reverse) mode of the cardiac NCX rather than the extrusion (forward) mode (Billman, 2001; Elias et al., 2001; Ladilov et al., 1999; Shigekawa and Iwamoto, 2001; Vila Petroff et al., 2003), and that KBR inhibits  $\text{Ca}^{2+}$  influx through NCX under  $\text{Na}^+$ -loaded conditions in rat myocardium (Inserte et al., 2002; Seki et al., 2002; Su et al., 2001; Yamamura et al., 2001). Furthermore, it has been shown that calcium influx (via reversal of NCX) is essential for digitalis-induced potentiation of cardiac basal energy expenditure (Guild et al., 2003). Note also that the selective inhibition of the reverse mode of NCX is especially pronounced at low concentrations of KBR (Billman, 2001; Shigekawa and Iwamoto, 2001; Yamamura et al., 2001) and characterized by an  $\text{IC}_{50}$  of 0.15  $\mu\text{M}$  in isolated cardiomyocytes (Inserte et al., 2002). Thus, the result of this study suggest that the differences in the inhibitory effect of KBR among investigators (Sato et al., 2000) can

be explained, in part, by the differences in digitalis dose (apart from the rat strain (Yamamura et al., 2001) and the experimental condition (Seki et al., 2002)).

#### 4.6 Effect of left ventricular hypertrophy on uptake, receptor binding and inotropic response of digoxin

##### 4.6.1 Baseline cardiac function in vehicle- and ISO-pretreated rats

There was a significant increase in total, left ventricle (LV), and atrial weight in animals subjected to continuous isoprenaline (ISO) infusion over 4 days but no significant elevation in right ventricular weight (Fig. 21). The body weights of vehicle- and ISO-pretreated rats were  $315.6 \pm 9.48$  and  $299.0 \pm 13.7$  g, respectively. In the ISO group, baseline contractility ( $LVDP_0$ ) was reduced to 70 % of vehicle group values ( $P < 0.001$ ). No significant changes in left ventricular end-diastolic pressure ( $LVEDP$ ) and in coronary vascular resistance ( $CVR$ ) were observed. KBR in perfusate did not affect baseline function of the heart (Table 5).

**Table 5.** Effects of hypertrophy on baseline values of left ventricular developed pressure ( $LVDP_0$ ), left ventricular developed enddiastolic pressure ( $LVEDP$ ) and coronary vascular resistance ( $CVR$ ) prior to digoxin administration.

	Vehicle-pretreated		ISO-pretreated	
	Control	KB-R7943	Control	KB-R7943
$LVDP_0$ (mmHg)	$74.3 \pm 4.74$	$77.5 \pm 5.39$	$51.9 \pm 8.42^{***}$	$56.7 \pm 7.72^{***}$
$LVEDP$ (mmHg)	$6.02 \pm 3.41$	$7.31 \pm 4.15$	$4.42 \pm 2.61$	$5.23 \pm 3.21$
$CVR$ (mmHg x min/ml)	$4.11 \pm 0.79$	$4.87 \pm 1.02$	$3.33 \pm 0.79$	$4.03 \pm .95$

\*\*\* $P < 0.001$  for vehicle- vs. ISO-pretreated group.

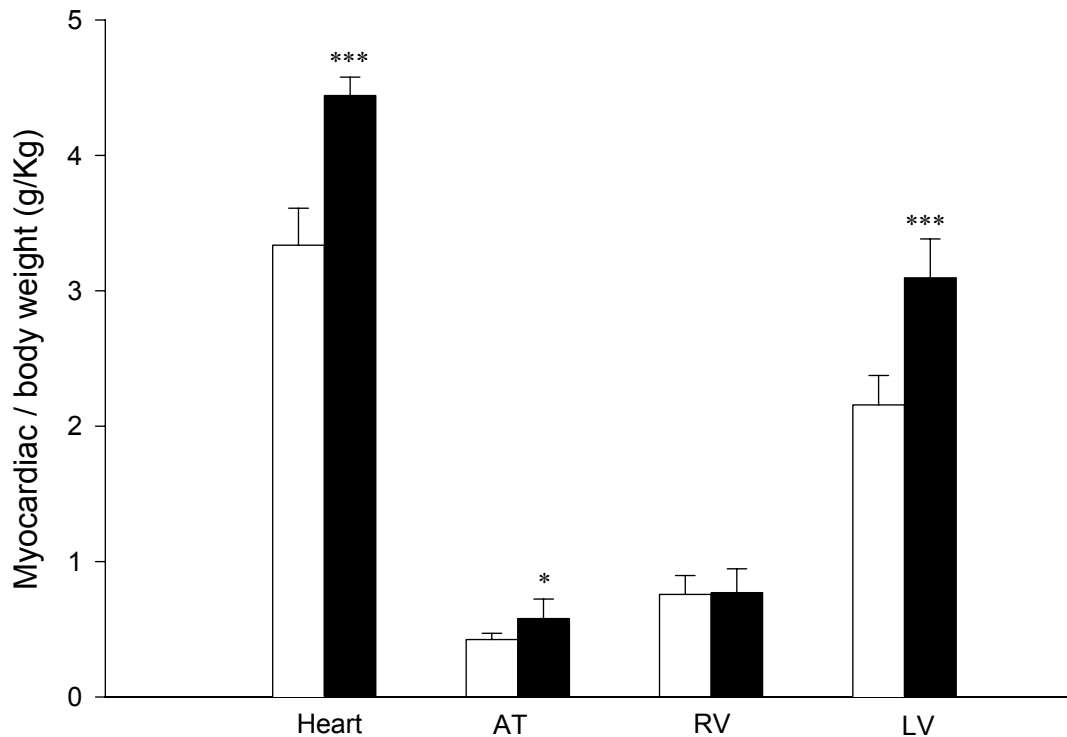


**Figure 21.** Isoprenaline induced increase in myocardial wet weight.

#### 4.6.2 Outflow concentration and inotropic response to digoxin

Figure 22 shows representative time profile of digoxin outflow concentration,  $C(t)$ , and inotropic effect,  $E(t)$ , profiles after three consecutive digoxin doses (15, 30, and 45  $\mu\text{g}$ ) measured in hearts of vehicle- and ISO-pretreated rats, respectively, in the absence and

presence of KBR. The time-integral  $\int_0^7 E(t)dt$  of percentage increase in  $LVDP(t)$  caused

by digoxin doses of 30 and 45  $\mu\text{g}$  was significantly reduced in hypertrophied versus normal hearts ( $P < 0.05$ ). At digoxin doses greater than 15  $\mu\text{g}$ , the presence of KBR (0.1  $\mu\text{M}$ ) in perfusate induced a significant decrease in positive inotropism (time-integrals of  $E(t)$ ) both in normal and hypertrophied hearts (Fig. 23).

## 4.6.3 Model Analysis

Figure 24 also shows typical fits of the model to the data obtained for three consecutive digoxin doses (15, 30, and 45  $\mu\text{g}$ ) in normal and hypertrophied hearts. The model was conditionally identifiable and parameters were estimated with reasonable precision as suggested by the approximate coefficients of variations obtained in individual fits. The averaged model parameters and averaged estimation errors, as a percentage of related parameter estimates, are listed in Table 6.

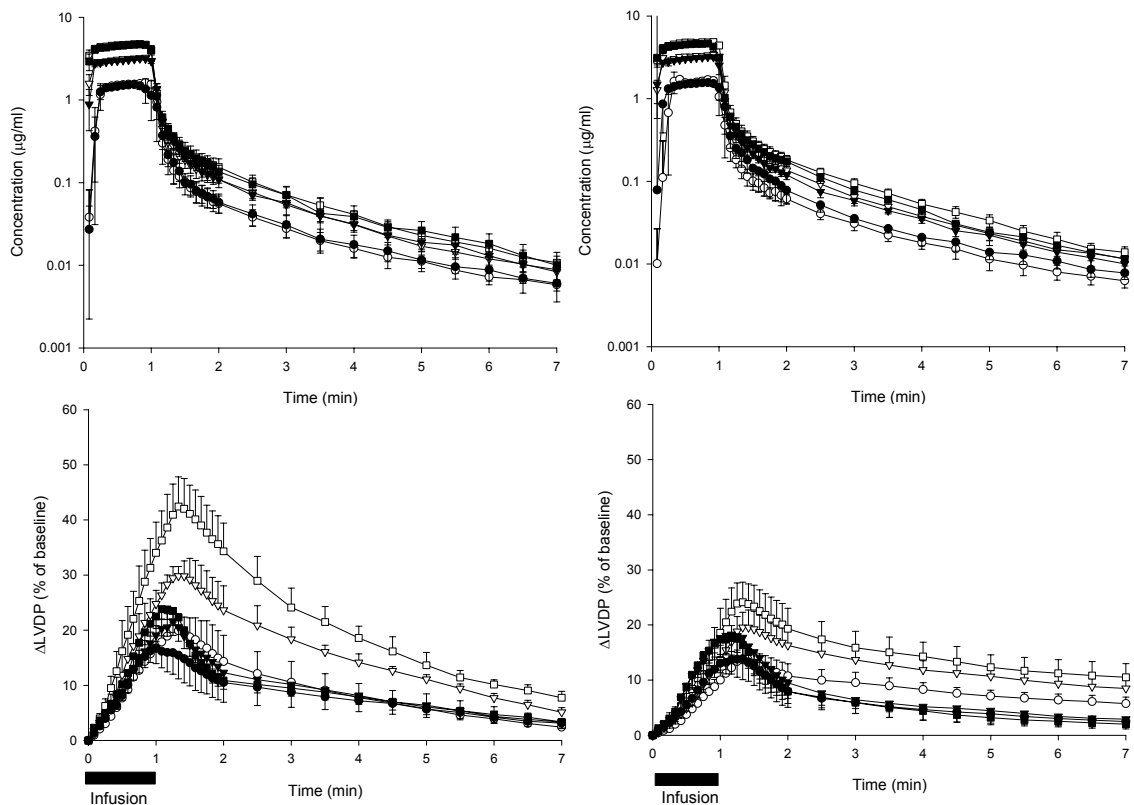


**Figure 22.** Representative digoxin outflow concentration (upper panel) and percent increase in developed left ventricular pressure (lower panel) after three digoxin doses (15, 30, and 45  $\mu\text{g}$ ) in normal and hypertrophied hearts as observed under control conditions and in the presence of KB-R7943 (0.1  $\mu\text{M}$ ) (closed symbols), respectively; together with simultaneous fits of the model (smooth curves) to experimental data (symbols).

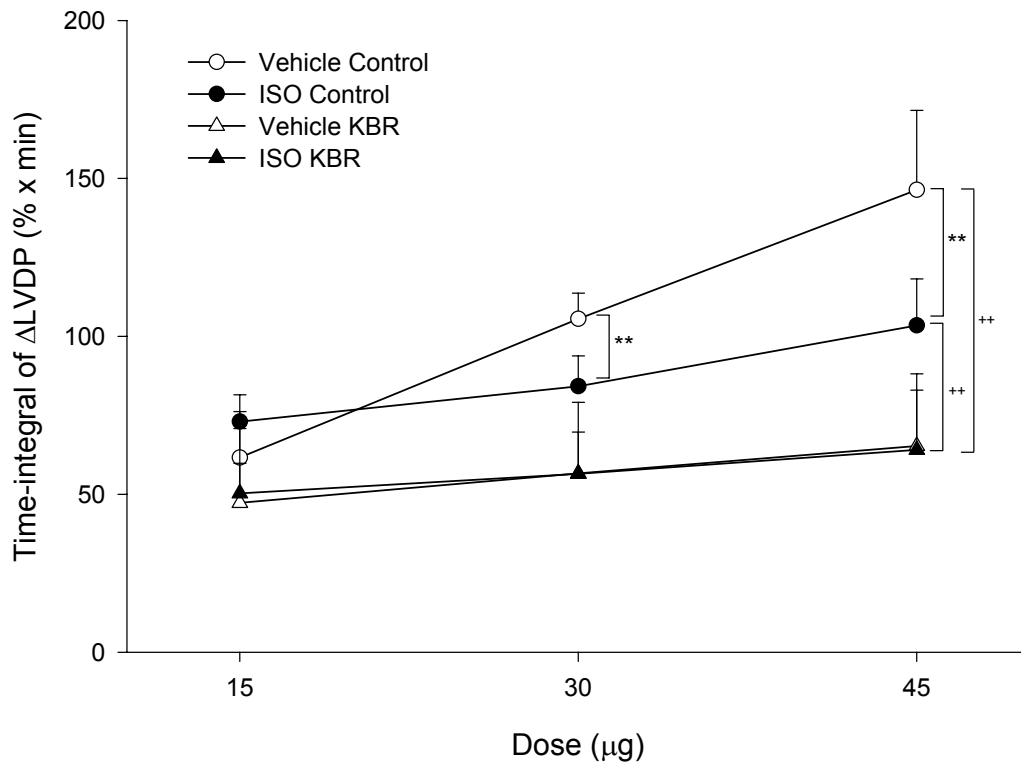


**Figure 23.** Dose-response curves of normal and hypertrophied hearts in the absence and presence of reverse NCX blocker KB-R7943 (0.1 μM), where response is the time-integral of digoxin effect. \*\* $P < 0.01$  and ++ $P < 0.01$  compared with the value of vehicle-pretreated rat heart and before exposure to KB-R7943, respectively.

$$\text{Time integral of digoxin effect} = \int_0^7 E(t) dt$$

#### 4. Results and discussion

**Table 6.** Parameters estimated by simultaneous fitting of outflow and inotropic response data after 1-min infusions of 15, 30, and 45  $\mu\text{g}$  digoxin in isolated hearts of vehicle- and ISO-pretreated rats in the absence and presence of reverse NCX blocker KB-R7943 (0.1  $\mu\text{M}$ ) (mean  $\pm$  S.D.,  $n = 5$  in each group).

	Vehicle pretreated			
	Control		KB-R7943	
<i>Cardiac Uptake</i>				
$CL_{vi}$ (ml/min)	7.354 $\pm$ 1.22	(15 $\pm$ 5) <sup>a</sup>	7.466 $\pm$ 0.68	(26 $\pm$ 8)
$V_{app, is}$ (ml)	0.820 $\pm$ 0.15	(13 $\pm$ 4)	0.864 $\pm$ 0.06	(22 $\pm$ 12)
<i>Receptor Binding</i>				
$R_{tot,1}$ (nmol)	33.87 $\pm$ 5.98	(37 $\pm$ 21)	29.50 $\pm$ 4.73	(40 $\pm$ 24)
$k_1$ (1/min/nmol/ml)	0.016 $\pm$ 0.01	(36 $\pm$ 19)	0.010 $\pm$ 0.01	(58 $\pm$ 33)
$k_{-1}$ (1/min)	2.277 $\pm$ 0.57	(61 $\pm$ 10)	1.568 $\pm$ 0.58	(63 $\pm$ 26)
$R_{tot,2}$ (nmol)	10.87 $\pm$ 1.91	(32 $\pm$ 22)	9.368 $\pm$ 1.74	(37 $\pm$ 24)
$k_2$ (1/min/nmol/ml)	0.193 $\pm$ 0.06	(40 $\pm$ 23)	0.182 $\pm$ 0.02	(47 $\pm$ 27)
$k_{-2}$ (1/min)	0.657 $\pm$ 0.06	(5 $\pm$ 1)	0.439 $\pm$ 0.10	(6 $\pm$ 2)
$K_{D,1}$ (nmol/ml)	162.6 $\pm$ 43.3		144.0 $\pm$ 35.0	
$K_{D,2}$ (nmol/ml)	3.628 $\pm$ 1.01		2.468 $\pm$ 0.74	
$K_{A,2}/K_{A,1}$	44.94 $\pm$ 0.92	(2 $\pm$ 1)	45.18 $\pm$ 0.43	(2 $\pm$ 1)
$R_{tot,1}/R_{tot,2}$	3.123 $\pm$ 0.21	(10 $\pm$ 2)	3.086 $\pm$ 0.79	(10 $\pm$ 1)
<i>Cellular Effectuation</i>				
$e_T$ (%/nmol)	21.69 $\pm$ 4.29	(9 $\pm$ 1)		
$f_1$	0.458 $\pm$ 0.09	(12 $\pm$ 3)		
$\Phi_{max}$ (%)			12.50 $\pm$ 3.19	(7 $\pm$ 1)
$K_{DR}$ (nmol)			0.234 $\pm$ 0.09	(15 $\pm$ 2)
$\tau$ (min)			0.016 $\pm$ 0.01	(36 $\pm$ 2)

<sup>a</sup>Values in parentheses are the asymptotic coefficients of variation of parameter estimates (mean  $\pm$  S.D.) obtained from individual fits. \* $P < 0.05$ , \*\* $P < 0.01$  and \*\*\* $P < 0.001$  for vehicle- vs. ISO-pretreated group. Changes in response to KB-R7943 in each group did not achieve statistical significance.

#### 4. Results and discussion

**Table 6.** Continued..

	Control		ISO-pretreated	
				KB-R7943
<i>Cardiac Uptake</i>				
$CL_{vi}$ (ml/min)	8.613 ± 1.79	(14 ± 8)	8.570 ± 1.76	(16 ± 2)
$V_{app, is}$ (ml)	1.056 ± 0.30	(22 ± 8)	1.176 ± 0.08***	(23 ± 9)
<i>Receptor Binding</i>				
$R_{tot,1}$ (nmol)	31.05 ± 0.92	(3 ± 1)	30.28 ± 1.80	(3 ± 1)
$k_1$ (1/min/nmol/ml)	0.013 ± 0.01*	(10 ± 2)	0.010 ± 0.01*	(11 ± 2)
$k_{-1}$ (1/min)	0.185 ± 0.03***	(6 ± 1)	0.124 ± 0.07**	(9 ± 3)
$R_{tot,2}$ (nmol)	5.194 ± 0.24**	(2 ± 1)	5.106 ± 0.48**	(8 ± 3)
$k_2$ (1/min/nmol/ml)	0.444 ± 0.08	(7 ± 4)	0.329 ± 0.11	(39 ± 22)
$k_{-2}$ (1/min)	0.136 ± 0.01***	(13 ± 4)	0.093 ± 0.05***	(46 ± 21)
$K_{D,1}$ (nmol/ml)	13.86 ± 1.43**		12.61 ± 2.13***	
$K_{D,2}$ (nmol/ml)	0.308 ± 0.03**		0.288 ± 0.11***	
$K_{A,2}/K_{A,1}$	44.94 ± 0.05	(2 ± 1)	44.99 ± 0.20	(2 ± 1)
$R_{tot,1}/R_{tot,2}$	5.983 ± 0.13***	(4 ± 1)	5.948 ± 0.27***	(9 ± 3)
<i>Cellular Effectuation</i>				
$e_T$ (%/nmol)	8.325 ± 1.79***	(5 ± 1)		
$f_1$	0.467 ± 0.15	(9 ± 4)		
$\Phi_{max}$ (%)			11.34 ± 2.55	(6 ± 1)
$K_{DR}$ (nmol)			0.323 ± 0.14	(17 ± 3)
$\tau$ (min)			0.010 ± 0.01	(35 ± 1)



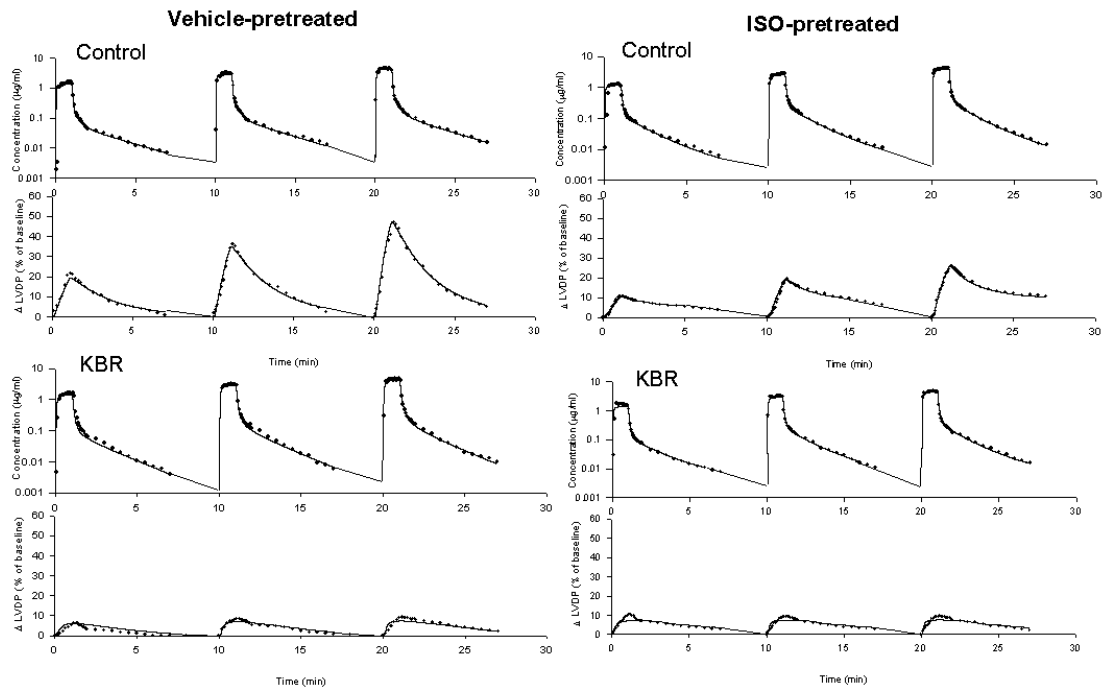


**Figure 24.** Representative simultaneous fits of the model (smooth curve) to experimental data (symbols): digoxin outflow concentration (top) and percent increase in developed left ventricular pressure (bottom) for three digoxin doses (15, 30, and 45  $\mu\text{g}$ ) before and after KB-R7943 0.1 mM as observed in experiments with both group of vehicle pre-treated and Isoprenaline pre-treated.

#### 4.6.4 Capacity and affinity of digoxin binding sites

Binding kinetics was determined by a mixture of two receptor subtypes, a low affinity/high capacity binding site ( $\alpha_1$ ) and a high affinity/low capacity binding site ( $\alpha_2$ ) (Table 6). The capacity ratios  $R_{\text{tot},1}/R_{\text{tot},2} = 3.12$  and 5.98 estimated in control and hypertrophied hearts are not much different from the respective *a priori* values used in the Bayesian estimation procedure, which stem from the literature or were obtained from the mRNA levels of  $\alpha_1$  and  $\alpha_2$  isoforms, respectively.

In hypertrophied hearts, the  $\alpha_2$  isoform ( $R_2$ ) was markedly downregulated to 52 % of the level in the vehicle group, whereas the  $\alpha_1$  level remained unchanged. The dissociation rate constants of  $\alpha_1$  and  $\alpha_2$  receptors ( $k_{-1}$  and  $k_{-2}$ ) decreased to 8 and 21 %, respectively,

of those in the control hearts. Together with a 2-fold increase in the fractional  $\alpha_2$  binding rate ( $k_2$ ), this leads to a 12-fold increase in digoxin receptor binding affinities. In accordance with the *a priori* value, no differences in the resulting affinity ratios  $K_{A,2}/K_{A,1}$  of about 45 were observed among the groups. The consequences of these alterations in receptor properties are illustrated by the time course of receptor occupancy simulated on the basis of the mean parameter estimates (Fig. 25). While maximum occupancy is not changed in hypertrophied hearts, the washout occurs much slower.

### 4.6.5 Occupancy-response relationship

At the postreceptor level, ISO pretreatment reduced the inotropic potency of digoxin, i.e., the slope of the receptor occupancy-response relationship ( $e_T$ ) to 38 % of control hearts (Table 6 and Fig. 26). This linear occupancy-response relationship became nonlinear in the presence of the NCX-inhibitor KBR; i.e., a hyperbolic occupancy-response function had to be used to fit the response data as previous results. Under reverse NCX inhibition, hypertrophy did not affect the parameters  $\phi_{\max}$  and  $K_{DR}$ , characterizing the cellular effectuation process (Table 6), as also illustrated by the average receptor occupancy-response relationships (Fig. 26).

Modeling of digoxin receptor binding and response kinetics in ISO-induced hypertrophied rat heart confirmed the downregulation of Na<sup>+</sup> pump  $\alpha_2$  isoform and revealed the functional consequences regarding the action of cardiac glycosides: 1) decrease in dissociation rate constants of  $\alpha_1$  and  $\alpha_2$  receptors together with increase in fractional  $\alpha_2$  binding rate led to a marked increase in digoxin receptor binding affinities, 2) at the cellular level, hypertrophy substantially reduced the inotropic potency of digoxin (slope of the receptor occupancy-response relationship), 3) the impaired inotropic response after reverse NCX inhibition was not further diminished by hypertrophy.

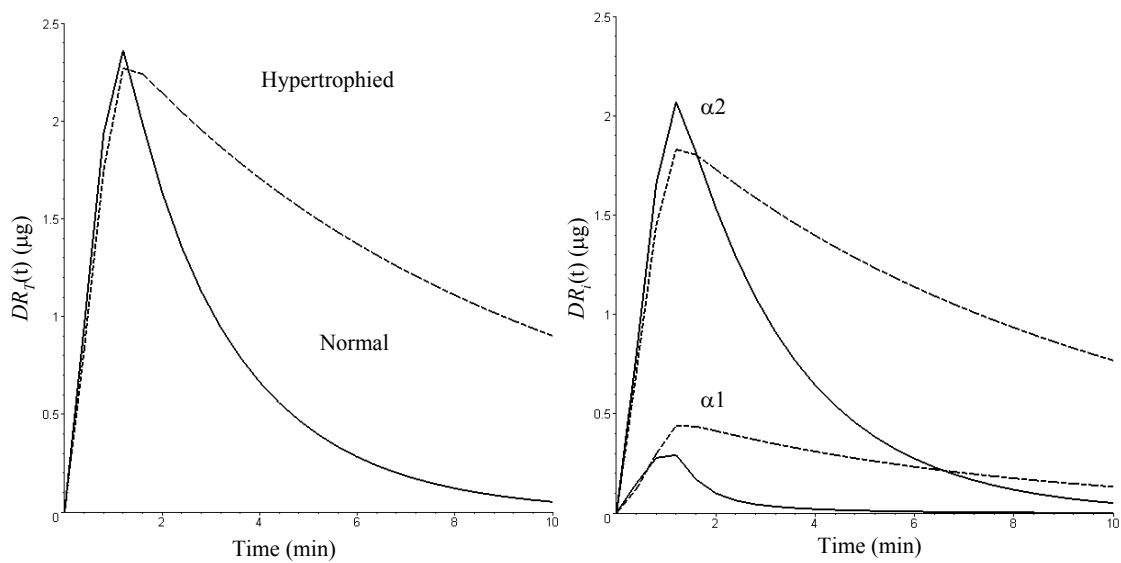


**Figure 25.** Model simulations of the time course of total receptor occupancy  $[DR_T(t)]$  (left) as well as underlying occupancies of  $\alpha_1$  and  $\alpha_2$  receptors  $[DR_f(t)]$  (right) in normal and hypertrophied hearts for the 45  $\mu\text{g}$  dose of digoxin, computed with average parameters (Table 6).

The hypertrophy development was comparable to that reported by Boluyt et al. (1995) where after ISO infusion (same dosing) the heart weight-to-body weight ratio and the alterations in gene expression peaked after about 4 days of treatment. The reduced baseline  $LVDP_0$  in the ISO-pretreated group (Table 5) points to a decompensated left ventricular ( $LV$ ) hypertrophy (Badenhorst et al., 2003). Although recent results in pressure overload hypertrophied hearts (Minakawa et al., 2003) suggest that this contractile failure could be also explained by the decrease in the relative level of sarcoplasmic reticulum  $\text{Ca}^{2+}$ -ATPase (SERCA mRNA) (Boluyt et al., 1995), this question is still under dispute (Badenhorst et al., 2003; Ward et al., 2003; Houser and Margulies, 2003; Sun and Ng, 1998) (vide infra). The lack of right ventricular ( $RV$ ) hypertrophy (Fig. 21) is in accordance with the response observed after continuous infusion of noradrenaline in rats (Laycock et al., 1995; Irlbeck et al., 1996; Sun and Ng, 1998). Note that gene expression observed in ISO-induced cardiac hypertrophy is similar to that caused by pressure overload (Boluyt et al., 1995).

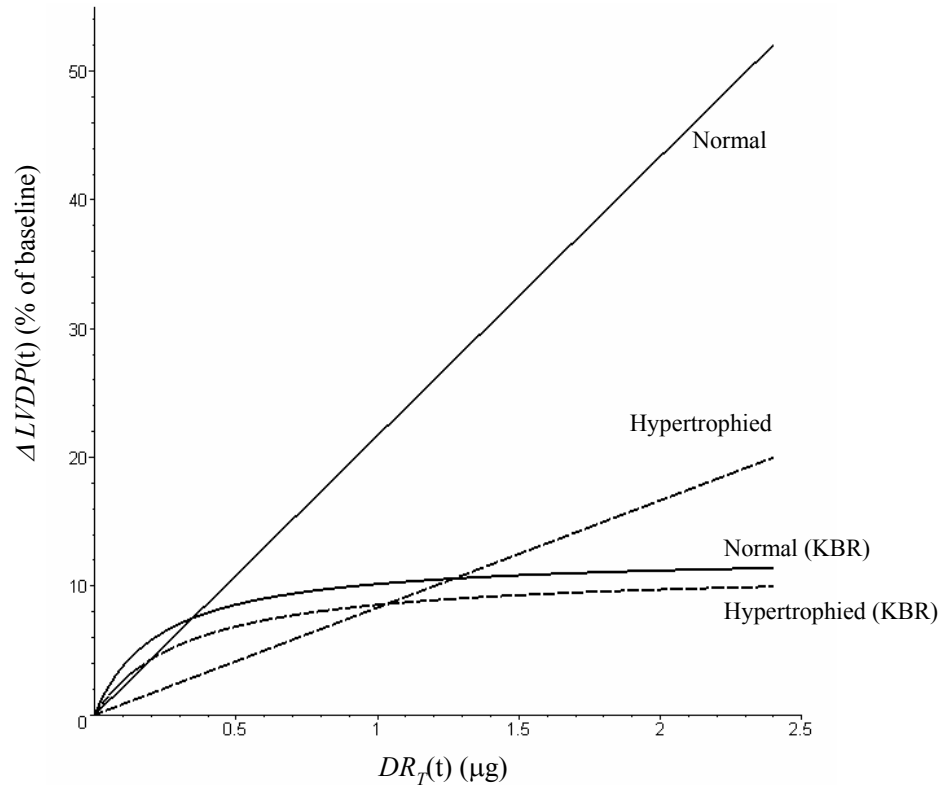


**Figure 26.** Stimulus-response relationships as predicted by the model for normal and hypertrophied hearts in the absence and presence of reverse NCX blocker KB-R7943 ( $0.1 \mu\text{M}$ ).

Our finding obtained by modeling of digoxin receptor binding kinetics that isoprenaline-induced *LV* hypertrophy is accompanied by the specific downregulation of  $\text{Na}^+$  pump  $\alpha_2$  isoform, parallels the alterations of mRNA and/or protein levels observed in different rat pressure-overload models (Sweadner et al., 1994; Sahin-Erdemli et al., 1995; Charlemagne et al., 1994; Book et al., 1994; Magyar et al., 1995; Liu and Songu-Mize, 1997) as well as in a post-infarction rat model of hypertrophy and cardiac failure (Semb et al., 1998) where  $\alpha_2$  isoform protein was reduced to a similar degree ( $\sim 50\%$ ) (Verdonck et al., 2003). In salt sensitive rats, the decrease of the  $\alpha_2$  level to about 65 and 40 % of control observed with the development of *LV* hypertrophy and failure, respectively, was accompanied by an increase and decrease, respectively of the  $\alpha_1$  level (Fedorova et al., 2004). The ability to confirm the shift in  $\text{Na}^+, \text{K}^+$ -ATPase isoforms gene expression by receptor binding kinetics in the intact heart appears of importance in

view of quantitative uncertainties of the biochemical methods (e.g., Larsen et al., 1997; Pogwizd et al., 2003).

Based on a more rigorous approach, results on altered functional properties of the  $\text{Na}^+, \text{K}^+$ -ATPase in hypertrophied myocardium shed new light on the slower decline of inotropic response to ouabain during washout in hypertrophied rat hearts and the reduced dissociation rate constants measured on isolated vesicles (Lelievre et al., 1986; Berrebi-Bertrand et al., 1990). The 12-fold increase in digoxin binding affinities of both  $\alpha_1$  and  $\alpha_2$  receptors was the result of a decrease in dissociation rate constants of  $\alpha_1$  and  $\alpha_2$  receptors (to 8 and 21 %, respectively) and a 2-fold increase in the fractional  $\alpha_2$  binding rate ( $k_2$ ) (Table 6). Note that Fedorova et al. (2004) observed a 11- and 2.4- fold increase in ouabain binding affinity of  $\alpha_2$  and  $\alpha_1$  receptors, respectively, in cardiac hypertrophy with transition to heart failure.

It was suggested that the downregulation of  $\text{Na}^+$  pump  $\alpha_2$  isoform alone could decrease the sensitivity of hypertrophied myocardium to cardiac glycosides (Book et al., 1994), explaining why in rat hypertrophy ouabain is less toxic than normal (Chevalier et al., 1989; Charlemagne and Swynghedauw, 1995). This conclusion is not supported by results because the reduced inotropic responsiveness could be explained fully by a decrease in coupling efficiency, i.e., effects occurring at postreceptor level. Fig. 25 demonstrates for the 45  $\mu\text{g}$  digoxin dose that the time course of functional receptor occupation in hypertrophied *LV* differs from the normal only by the slower washout; however, the slope of the stimulus-response curve (Fig. 26) is reduced indicating that the depressed inotropic response of the *LV* can be solely attributed to alteration in cellular effectuation process.

This is also illustrated by the steady-state concentration-response curves simulated using Eq. 23 with the mean parameter estimates (Fig. 27).

$$DR_{T,ss} = \frac{f_1 R_{tot,1} C_{ss}}{K_{D,1} + C_{ss}} + \frac{(1-f_1) R_{tot,2} C_{ss}}{K_{D,2} + C_{ss}} \quad (23)$$

The steady state response behavior can be predicted, at steady-state, the total receptor occupancy is obtained from the function of concentration,  $C_{ss}$ , and steady-state effect  $E_{ss}$  vs.  $C_{ss}$  curves in the absence and presence of KBR can be predicted by substitution of Eq. 23 into following equations.

$$E(t) = e_T DR_T(t) \quad (24)$$

$$E(t) = \frac{\phi_{\max} DR_T(t)}{K_{DR} + DR_T(t)} \quad (25)$$

Only in the low concentration range ( $< 1$  ng/ml), increased receptor affinity in hypertrophied *LV* could compensate for reduced cellular response generation. This is also reflected by the time integral of developed pressure (Fig. 23) where no significant influence of hypertrophy could be detected at the lowest dose level (15  $\mu$ g). Furthermore, Fig. 27 is in general accordance with dose-response curves to ouabain measured in rat hearts pressure-hypertrophied and sham-operated rat hearts (Berrebi-Bertrand et al., 1990). A reduced positive inotropic effect of ouabain was also previously observed in ISO-induced cardiac hypertrophy by Szabo et al. (1989).

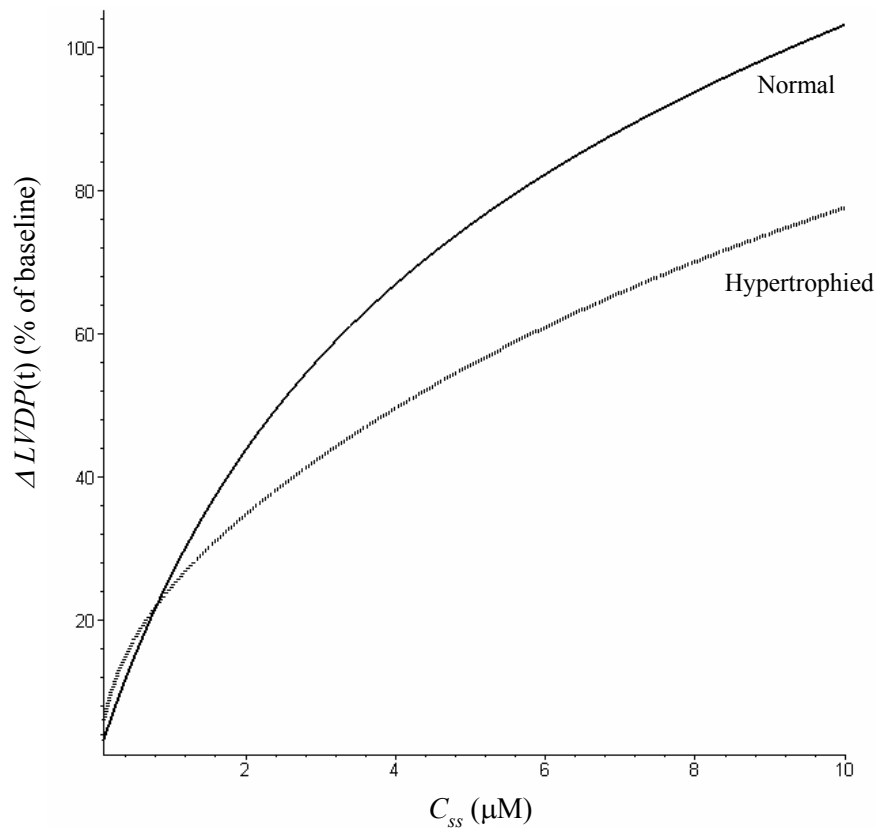


**Figure 27.** Model simulations of concentration-response curve at steady state in normal and hypertrophied hearts.

The mechanism behind this contractile dysfunction, i.e., the reduced inotropic response to digoxin per occupied receptor (inhibited  $\text{Na}^+$  pump) is not clarified; possible explanations include: 1) chamber dilatation and changes in the extracellular matrix (Briest et al., 2001; Badenhorst et al., 2003; Ward et al., 2003), 2) reduced SERCA 2a activity (Charlemagne et al., 1994; Boluyt et al., 1995; Minakawa et al., 2003; Muller-Ehmsen et al., 2003; Schultz et al., 2004), 3) NCX overexpression (Muller-Ehmsen et al., 2003; Bölck et al., 2004), or a combination of these processes. Previous studies indicate that ISO-induced hypertrophy is accompanied by an increase in NCX expression (Golden et al., 2001; Chorvatova et al., 2004), and that NCX and  $\text{Na}^+, \text{K}^+$ -ATPase (mainly  $\alpha_2$  isoform) are inversely regulated (Magyar et al., 1995). The fact that at the relatively high intracellular  $\text{Na}^+$  concentration in the rat heart  $\text{Na}^+$  pump inhibition favors  $\text{Ca}^{2+}$  influx, since the NCX predominantly acts in reverse mode (Bers et al., 2003; Bers, 2002; Verdonck et al., 2003), makes it difficult to explain how NCX upregulation could influence the inotropic action of cardiac glycosides (Muller-Ehmsen et al., 2003; Bölck et al., 2004). An inhibition of  $\text{Ca}^{2+}$  influx by the reverse mode NCX blocker KBR limits the inotropic response to increasing digoxin doses to that of the low dose range (Figs. 23 and 26); this is in accordance with previous results, where it was hypothesized that for a small increase in  $[\text{Na}^+]_i$  at low receptor occupancy the inotropic effect may be independent of net  $\text{Ca}^{2+}$  influx, while  $\text{Ca}^{2+}$  entry via NCX can increase greatly when  $[\text{Na}^+]_i$  rises. In other words, the linear relationship between receptor stimulus and inotropic response becomes hyperbolic because the selective inhibition of net  $\text{Ca}^{2+}$  influx by KBR affects response for doses higher than about  $15 \mu\text{g}$  (Fig. 23) corresponding to receptor occupancies  $> DR_T \approx 0.5 \mu\text{g}$  (Fig. 26). That inhibition of response generation by KBR leads to practically the same stimulus-response curves in normal and hypertrophied LV (Fig. 26) may suggest that processes connected with digoxin induced  $\text{Ca}^{2+}$  influx are responsible for the reduced (hyperbolic) coupling of stimulus with inotropic response in hypertrophied hearts. This conclusion is compatible with the NCX overexpression hypothesis but also with that of a reduced SERCA activity (that may be still sufficient for a small increase in  $[\text{Ca}^{2+}]_i$ ). The stimulus-response curves are also consistent with the suggestion that NCX normally does not work near to saturation (Chorvatova et al., 2004). That KBR inhibits the digoxin induced inotropy solely under conditions that favor net  $\text{Ca}^{2+}$  influx via NCX may also

explain the difference between our results and earlier findings in rat ventricular myocytes (Sato et al., 2000).

The capacity and affinity of the two populations of functional receptors in the vehicle group are in agreement with previous results showing that normal rat hearts express two functionally distinct  $\text{Na}^+$ -pumps: one with a high affinity for inhibition digoxin and the other with a low affinity. That positive inotropism is nearly completely mediated through  $\alpha_2$  receptors (Fig. 25) is consistent with data in mice (Dostanic et al., 2003). This simulation also demonstrates that at the time of maximum effect, downregulation of  $\alpha_2$  isoform in the ISO group increases the occupancy of  $\alpha_1$  receptors from 10 to 20 %. Finally, it should be noted that no significant influence of hypertrophy on the kinetics of digoxin uptake into the myocardium, i.e., transcapillary permeation clearance  $CL_{vi}$  and apparent interstitial distribution volume  $V_{app, is}$ , could be detected (Table 6). Thus, it appears unlikely that changes in onset and offset of inotropic effect are due to changes in myocardial transport processes as previously suggested for ouabain (Berrebi-Bertrand et al., 1990).

Although a reduced concentration of myocardial  $\text{Na}^+, \text{K}^+$ -ATPase concentration was also observed in patients with aortic valve disease (Larsen et al., 1997), its functional relevance remains controversial (Schwinger et al., 2003; McDonough et al., 2002). Note that digoxin receptor affinity is much higher but association and dissociation processes are much slower in human than in rat heart (Weiss and Kang, 2004; McDonough et al., 1995; Lelievre et al., 2001).

The Bayesian approach allowed the estimation of all parameters of our relatively complex model, but on the cost of using *a priori* information on the  $\alpha_1$  to  $\alpha_2$  -ratios of receptor capacities and affinities. For the normal heart, the values  $K_{A,2}/K_{A,1} = 45$  and  $R_{tot,1}/R_{tot,2} = 3$  taken from independent studies appear reasonable. However, while the change of capacity ratio in the hypertrophied hearts was based on our mRNA measurements, the affinity ratio was assumed unchanged since there are no empirical or theoretical evidence which suggests that hypertrophy development influences this ratio (Verdonck et al., 2003). However, this remains to be confirmed in further investigations. Our inferences are, of course, only as good as the validity of the assumptions underlying the model. Moreover, in hypertrophied hearts, the estimation of association and dissociation rate constants was based on a simultaneous fit of both concentration and



effect data since prolonged receptor binding in the terminal phase was too low to be detected in outflow concentration. However, under normal conditions (vehicle group) the receptor binding parameters can be estimated solely on the basis of  $C(t)$  data (Weiss and Kang, 2002). That digoxin binding to receptors is a determinant of outflow  $C(t)$  data in perfused heart experiments is analogous to the concept of “target-mediated drug disposition” (Mager and Jusko, 2001a); for digoxin this property gets lost, however, at the whole body level since the amount bound to myocardial receptors does not significantly influence plasma concentration (Weiss and Kang, 2004).

In summary, we attempted to clarify the complex experimental results on hypertrophy-induced changes in inotropic response to cardiac glycosides using a mathematical modeling approach that allows differentiation between effects elicited at the receptor and postreceptor level. The results of this study indicate that ISO-induced cardiac hypertrophy reduces the development of inotropic effect per inhibited sodium pump. It is confirmed that the reduction in  $\alpha_2$  isoform and showed that this downregulation is accompanied by an increase in receptor affinity.

### **4.7 Receptor binding kinetics and inotropic action of digoxin in endotoxin-treated rat hearts.**

#### **4.7.1 Baseline cardiac function in sham and sepsis rats**

With Lipopolysaccharides (LPS) injection (4 mg/kg), body temperature was significantly increased and the movement of LPS pre-treated rat was markedly weakened (Fig. 28).

Following 4 hrs exposure to LPS (4 mg/kg), the isolated hearts demonstrated significantly lower left ventricular developed pressures. As shown in Table 7 and Fig. 28, hearts subjected to LPS exhibited a significant impairment of LVDP ( $65.1 \pm 13.6 \%$ ,  $P < 0.001$ ), when compared with the sham treated group and the reduced contractility was in agreement with that of previous report (Chaoshu et al., 1998; Harold et al., 2002). There was no significant change in left ventricular end-diastolic pressure and coronary vascular resistance (Table 7). Under the NCX inhibitor, KB-R7943, baseline cardiac function was not different to the control group, as previous results.

#### 4. Results and discussion

**Table 7.** Effect of sepsis on baseline values of left ventricular developed pressure at ( $LVDP_0$ ), left ventricular developed end-diastolic pressure ( $LVEDP$ ) and coronary vascular resistance ( $CVR$ ) prior to digoxin administration.

	Sham		Sepsis	
	Control	KB-R7943	Control	KB-R7943
$LVDP_0$ (mmHg)	$76.4 \pm 9.9$	$76.9 \pm 10.3$	$49.3 \pm 7.0^{***}$	$50.2 \pm 6.9^{***}$
$LVEDP$ (mmHg)	$6.37 \pm 1.2$	$6.50 \pm 1.1$	$6.03 \pm 1.7$	$6.18 \pm 1.8$
$CVR$ (mmHg min/ml)	$5.0 \pm 1.4$	$5.0 \pm 1.5$	$4.1 \pm 0.6$	$4.2 \pm 0.8$
Body temperature	$37.0 \pm 0.19$		$38.5 \pm 0.49^{***}$	

\*\*\* $P < 0.001$  for Sham vs. Sepsis group

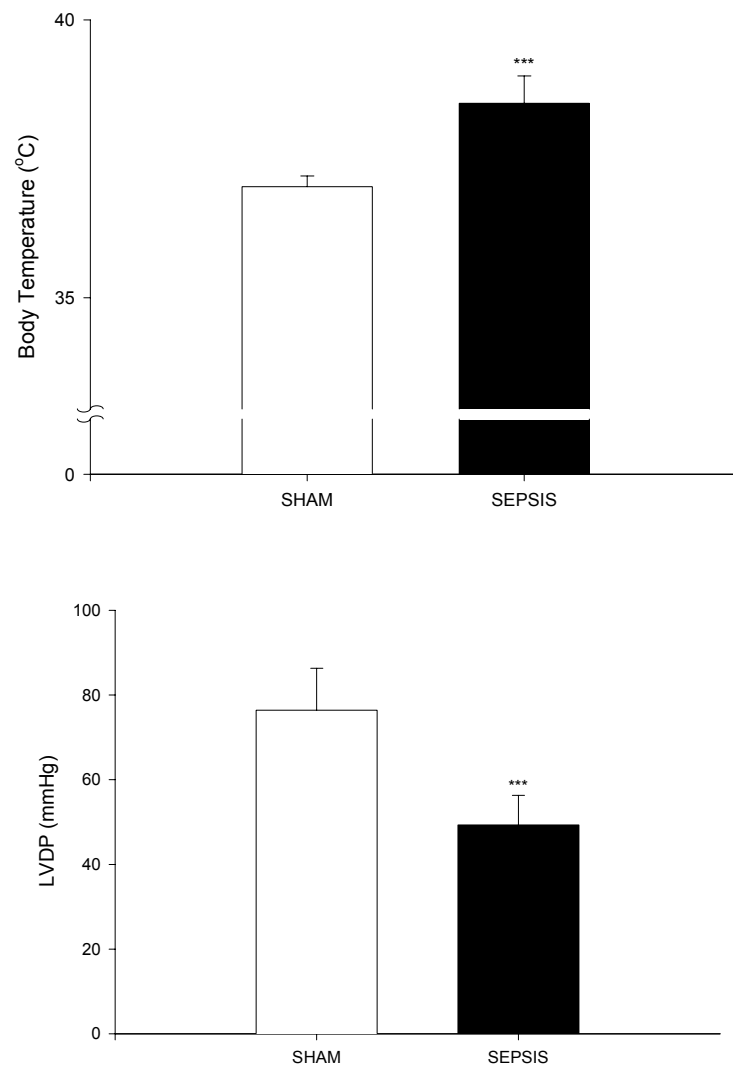


**Figure 28.** Body temperature and baseline contractility in sepsis (\*\*\* $P < 0.001$ )

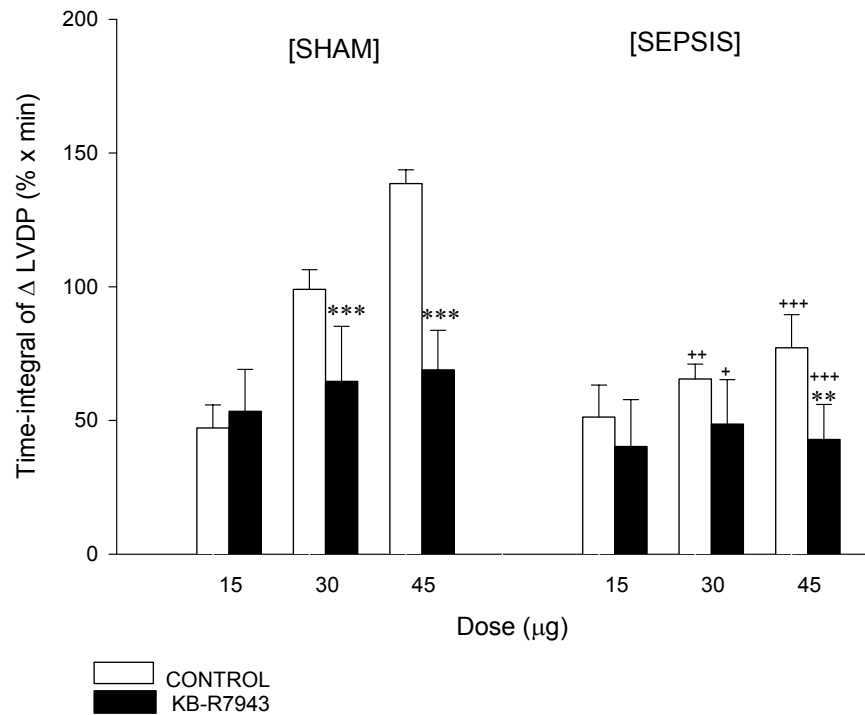


**Figure 29.** Effect of sepsis and NCX inhibition by KB-R7943 (0.1 $\mu M$ ) on the time-integral of effect. Data are means  $\pm$  S.D. from 5 experiments in each of sham and sepsis groups.  $^+P < 0.05$ ,  $^{++}P < 0.01$  and  $^{+++}P < 0.001$ , compared with the value of sham group,  $^{**}P < 0.01$  and  $^{***}P < 0.001$  compared with the value before exposure to KB-R7943.

#### 4.7.2 Outflow concentrations and inotropic response to digoxin

Figure 30 shows an average digoxin outflow concentration,  $C(t)$ , and percent increase in developed left ventricular pressure,  $\Delta LVDP$  (% of baseline), profiles after three consecutive digoxin doses (15, 30, and 45  $\mu g$ ) measured in hearts of saline injected (sham operated) and LPS-injected (sepsis) rats, respectively, and in the absence and presence of KBR. The digoxin induced increase in time integral of developed pressure ( $\Delta LVDP$ ) was significantly reduced for the 30 and 45  $\mu g$  doses,  $66 \pm 22$  % for 30  $\mu g$  and  $50 \pm 11$  % for 45  $\mu g$  ( $P < 0.01$ ) (Fig. 29).

Figure 31 shows typical fits of the model to the data obtained for three consecutive digoxin doses (15, 30, and 45  $\mu g$ ) in sham and sepsis group. The model was

conditionally identifiable and parameters were estimated with reasonable precision as suggested by the approximate coefficients of variations obtained in individual fits. The average model parameters and averaged estimation errors, as a percentage of related parameter estimates, are listed in Table 8.

### 4.7.3 Capacity and affinity of digoxin

There was no significant change in cardiac uptake of digoxin into the interstitial space ( $CL_{vi}$  and  $V_{app, is}$ ).

Receptor binding affinity ( $1/K_{Di}$ ,  $i = 1, 2$ ) was significantly increased ( $P < 0.01$ ) with sepsis. The cellular generation of digoxin response (slope of the receptor occupancy-response curve,  $e_T$ ) was significantly reduced to  $66 \pm 20\%$  (Fig. 32).

Both the myocardial contractility and the inotropic response to digoxin were impaired in the septic heart. Sepsis increased digoxin receptor binding and significantly reduced cellular response generation (occupancy-response relationship). The latter is in accordance with the suggestion that sepsis impairs systolic force generation by reducing calcium release from the sarcoplasmic reticulum (Stamm et al., 2001).

The NCX inhibitor KB-R7943 markedly attenuated the digoxin induced positive inotropic effect, probably due to the inhibition of calcium inflow.

The model analysis allowed, for the first time, to elaborate the effects of sepsis on the positive inotropic response to digoxin with regard to receptor binding kinetics and on postreceptor events (cellular effectuation process).

## 4. Results and discussion

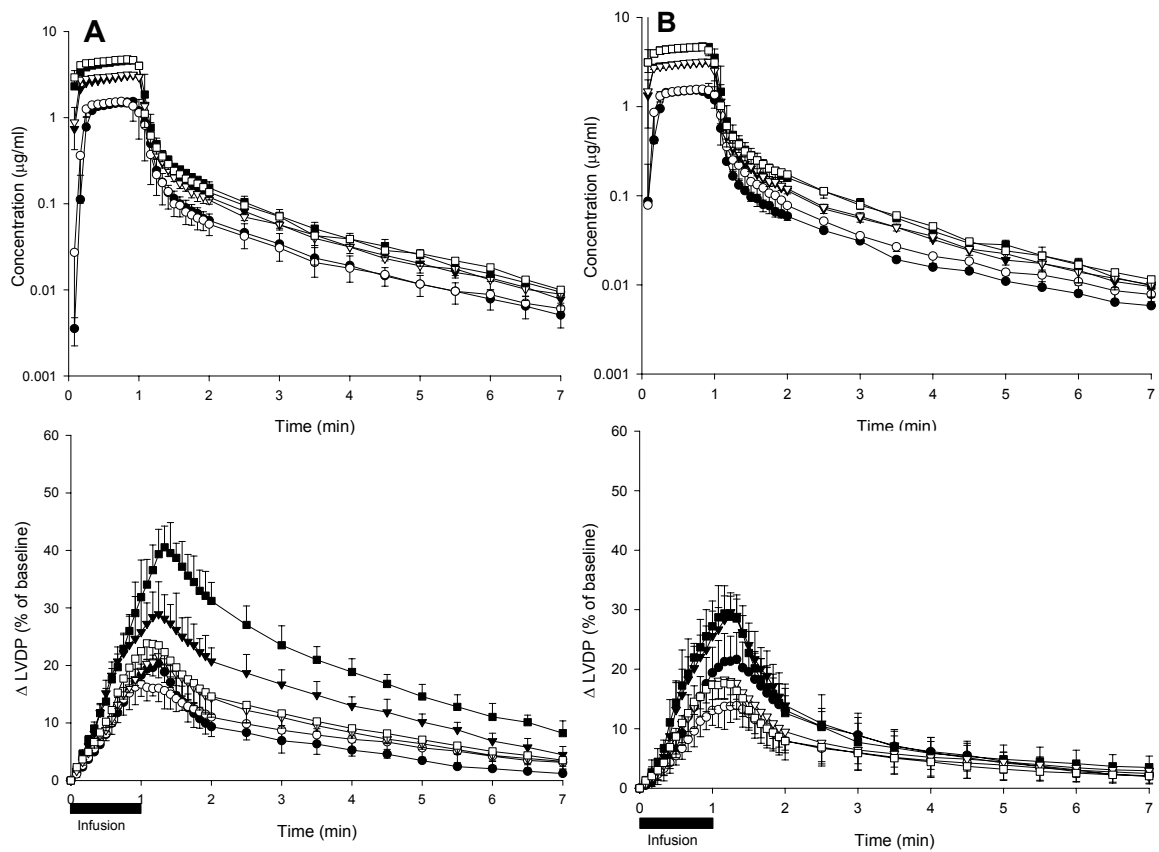


**Figure 30.** Average digoxin outflow concentration (upper panel) and percent increase in developed left ventricular pressure (lower panel) for three digoxin doses of 15 (●), 30 (▼) and 45 (■) µg under control conditions and in the presence of KB-R7943 (0.1 µM) (open symbols) as observed in experiments of sham (A) and sepsis (B), respectively.

## 4. Results and discussion

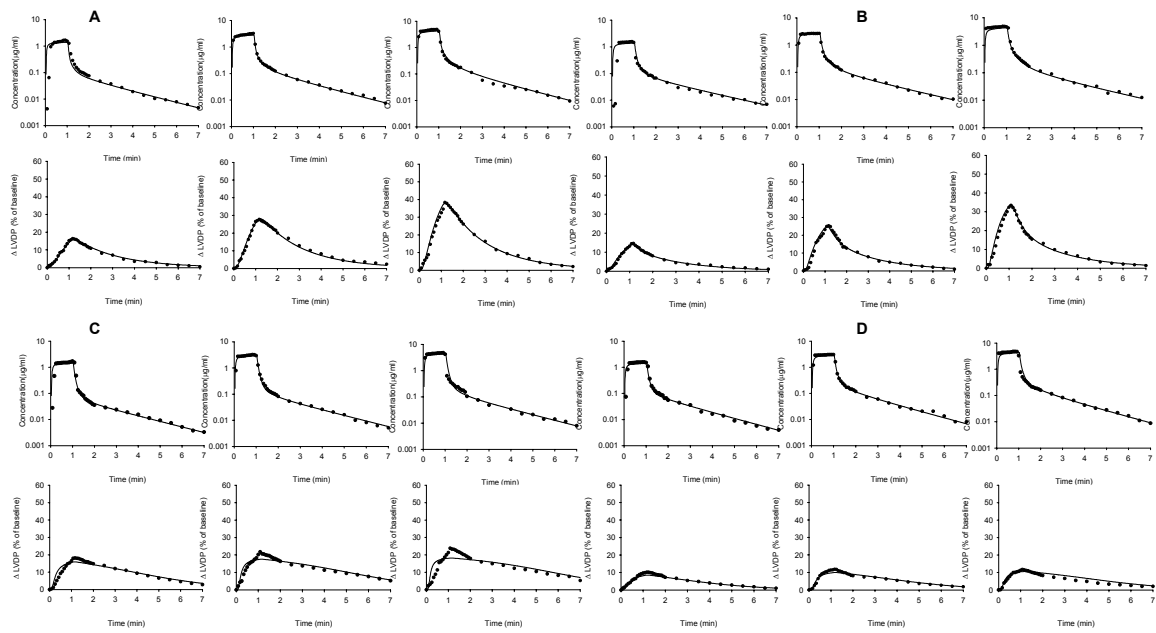


**Figure 31.** Representative simultaneous fits of the model (smooth curves) to experimental data (symbols): Digoxin outflow concentration (upper panels) and percent increase in developed left ventricular pressure (lower panels) for three digoxin doses (15, 30, and 45  $\mu\text{g}$ ) before (A and B) and after KB-R7943 (0.1  $\mu\text{M}$ ) (C and D) as observed in experiments with sham group (A and C) and sepsis group (B and D), respectively.

#### 4. Results and discussion

**Table 8.** Parameters estimated by simultaneous fitting of outflow and inotropic response data after 1-min infusions of 15, 30, and 45  $\mu\text{g}$  digoxin in isolated rat hearts in sham and sepsis group. (mean  $\pm$  S.D.,  $n = 5$  in each group).

	Sham			
	Control		KB-R7943	
<i>Cardiac Uptake</i>				
$CL_{vi}$ (ml/min/g)	7.755 $\pm$ 4.21	(21 $\pm$ 10) <sup>a</sup>	8.385 $\pm$ 1.55	(28 $\pm$ 17)
$V_{app,is}$ (ml/g)	0.877 $\pm$ 0.36	(28 $\pm$ 17)	0.819 $\pm$ 0.15	(15 $\pm$ 2)
<i>Receptor Binding</i>				
$R_{tot,1}$ (nmol/g)	32.70 $\pm$ 9.81	(37 $\pm$ 17)	29.57 $\pm$ 4.30	(37 $\pm$ 4)
$k_1$ (1/min/nmol/ml)	0.021 $\pm$ 0.01	(26 $\pm$ 14)	0.020 $\pm$ 0.01	(54 $\pm$ 14)
$k_{-1}$ (1/min)	2.870 $\pm$ 1.35	(29 $\pm$ 12)	2.820 $\pm$ 1.46	(51 $\pm$ 12)
$R_{tot,2}$ (nmol/g)	9.423 $\pm$ 1.53	(35 $\pm$ 17)	6.387 $\pm$ 1.11	(33 $\pm$ 4)
$k_2$ (1/min/nmol/ml)	0.269 $\pm$ 0.03	(55 $\pm$ 26)	0.282 $\pm$ 0.23	(45 $\pm$ 6)
$k_{-2}$ (1/min)	0.872 $\pm$ 0.10	(16 $\pm$ 6)	0.627 $\pm$ 0.10	(7 $\pm$ 1)
$K_{D,1}$ (nmol/ml)	150.6 $\pm$ 28.6		131.9 $\pm$ 54.2	
$K_{D,2}$ (nmol/ml)	3.289 $\pm$ 0.55		2.906 $\pm$ 1.14	
$K_{A,2}/K_{A,1}$	45.66 $\pm$ 1.63	(2 $\pm$ 1)	45.12 $\pm$ 1.53	(2 $\pm$ 1)
$R_{tot,1}/R_{tot,2}$	3.761 $\pm$ 1.19	(12 $\pm$ 3)	3.648 $\pm$ 0.42	(11 $\pm$ 1)
<i>Cellular Effectuation</i>				
$e_T$ (%/nmol)	19.76 $\pm$ 4.14	(47 $\pm$ 31)		
$f_1$	0.516 $\pm$ 0.07	(56 $\pm$ 21)		
$\Phi_{max}$ (%)			15.87 $\pm$ 1.06	(5 $\pm$ 1)
$K_{DR}$ (nmol)			0.195 $\pm$ 0.06	(12 $\pm$ 1)
$\tau$ (min)			0.010 $\pm$ 0.01	(33 $\pm$ 1)

<sup>a</sup>Values in parentheses are the asymptotic coefficients of variation of parameter estimates (mean  $\pm$  S.D.) obtained from individual fits. \* $P < 0.05$ , \*\* $P < 0.01$  compared with the corresponding value in sham group.

**Table 8.** Continue

	Sepsis			
	Control		KB-R7943	
<i>Cardiac Uptake</i>				
$CL_{vi}$ (ml/min/g)	6.927 ± 1.47	(20 ± 5)	8.174 ± 1.78	(23 ± 3)
$V_{app, is}$ (ml/g)	0.849 ± 0.21	(22 ± 13)	0.804 ± 0.28	(19 ± 7)
<i>Receptor Binding</i>				
$R_{tot,1}$ (nmol/g)	26.70 ± 12.7	(23 ± 9)	25.87 ± 4.10	(28 ± 16)
$k_1$ (1/min/nmol/ml)	0.018 ± 0.01	(66 ± 12)	0.022 ± 0.01	(58 ± 15)
$k_{-1}$ (1/min)	2.228 ± 1.10	(83 ± 65)	2.118 ± 0.79	(73 ± 34)
$R_{tot,2}$ (nmol/g)	8.964 ± 4.10	(22 ± 8)	7.084 ± 1.31	(26 ± 16)
$k_2$ (1/min/nmol/ml)	0.310 ± 0.17	(39 ± 17)	0.341 ± 0.05	(46 ± 26)
$k_{-2}$ (1/min)	0.760 ± 0.13	(14 ± 9)	0.720 ± 0.12	(14 ± 6)
$K_{D,1}$ (nmol/ml)	102.3 ± 47.7		77.49 ± 14.8	
$K_{D,2}$ (nmol/ml)	2.273 ± 1.06		1.669 ± 0.34*	
$K_{A,2}/K_{A,1}$	45.05 ± 0.11	(2 ± 1)	46.54 ± 1.23	(2 ± 1)
$R_{tot,1}/R_{tot,2}$	2.950 ± 0.07	(10 ± 1)	3.708 ± 0.67	(11 ± 1)
<i>Cellular Effectuation</i>				
$e_T$ (%/nmol)	11.61 ± 2.13**	(20 ± 8)		
$f_1$	0.659 ± 0.17	(25 ± 11)		
$\Phi_{max}$ (%)			15.07 ± 3.73	(6 ± 1)
$K_{DR}$ (nmol)			0.284 ± 0.18	(13 ± 1)
$\tau$ (min)			0.010 ± 0.01	(33 ± 1)

#### 4.7.4 Occupancy-response relationship

The observed degree of left ventricular (LV) dysfunction is in accordance with previous reports of impaired contractility of isolated perfused hearts from LPS-treated rats (Spiers et al., 2000; Grandel et al., 2000; Khadour et al., 2002; Fauvel et al., 2002). However, at present, no information is available in septic shock about the inotropic effect of digoxin. At doses greater than 15  $\mu\text{g}$ , inotropic responsiveness to digoxin (time integral of inotropic effect) was reduced by about 50 %. This study provides the first evaluation of the diminished inotropic response to digoxin in septic hearts. The results of the pharmacokinetic/pharmacodynamic modeling approach suggest that this response attenuation is due to a reduced slope  $e_T$  of the linear stimulus-response relationship (i.e., postreceptor events); sepsis reduced this coupling ration to  $66 \pm 20$  % of the value



estimated in the sham group. Especially in the low concentration range the increase in receptor affinity could partly offset this decreased responsiveness at the postreceptor level. Although the cellular mechanism underlying this impairment of inotropic response to digoxin remains unclear, some of the explanations discussed for the diminished baseline contractility in LPS-treated rats could be taken into account; as, for example, inhibition of  $\text{Ca}^{2+}$  transport across the sarcoplasmic reticulum (Stamm et al., 2001; Wu et al., 2002) or reduced myofibrillar  $\text{Ca}^{2+}$  sensitivity (Yasuda and Lew, 1997; Tavernier et al., 2001).

The data demonstrated that both the increase in receptor binding affinity and the decrease in inotropic potency of digoxin were significantly correlated with the LPS-induced rise in temperature (Fig. 34). One may speculate that this correlation was caused by a common mediator behind the LPS-induced changes in digoxin action and body temperature (e.g., levels of circulating proinflammatory cytokines). Obviously, the resulting response variability in the sepsis group prevented a significant difference with regard to an  $K_{A,i}$  increase. The differences in inotropic responsiveness between septic and normal hearts disappeared after NCX inhibition by KB-R7943 where digoxin response was reduced to the same limiting behavior (Fig. 33) characterized by practically identical (hyperbolic) stimulus-response curves. Taken together, these results are similar to those observed previous results of isoprenaline-induced LV hypertrophy, where the stimulus-response ratio  $e_T$  was reduced to 38 % of control values and the parameters  $\phi_{\max}$  and  $K_{DR}$  characterizing the nonlinear stimulus-effect relationship in the presence of KB-R7943 remained unchanged. Interestingly, Takeuchi et al. (2000) suggested that contractile dysfunction in septic and hypertrophic hearts may be caused by similar abnormalities of calcium handling. On the other hand, the previous results on the effect of KB-R7943 on inotropic response to digoxin showed that endotoxin induced NCX inhibition (Liu and Xuan, 1986; Wang et al., 2000) could be involved in the reduced digoxin action during septic shock. The capacity and affinity of the two populations of functional receptors in the vehicle group were in agreement with previous results showing that normal rat hearts express two functionally distinct  $\text{Na}^+$  pumps: one with a high affinity for inhibition digoxin and the other with a low affinity.

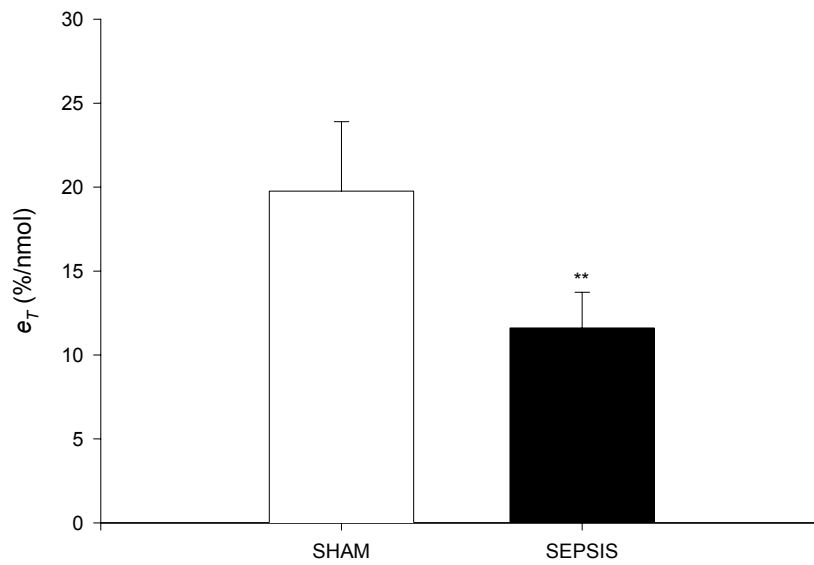


**Figure 32.** Effect of sepsis on stimulus amplification, slope of the receptor occupancy response relationship (\*\* $P < 0.01$ ).

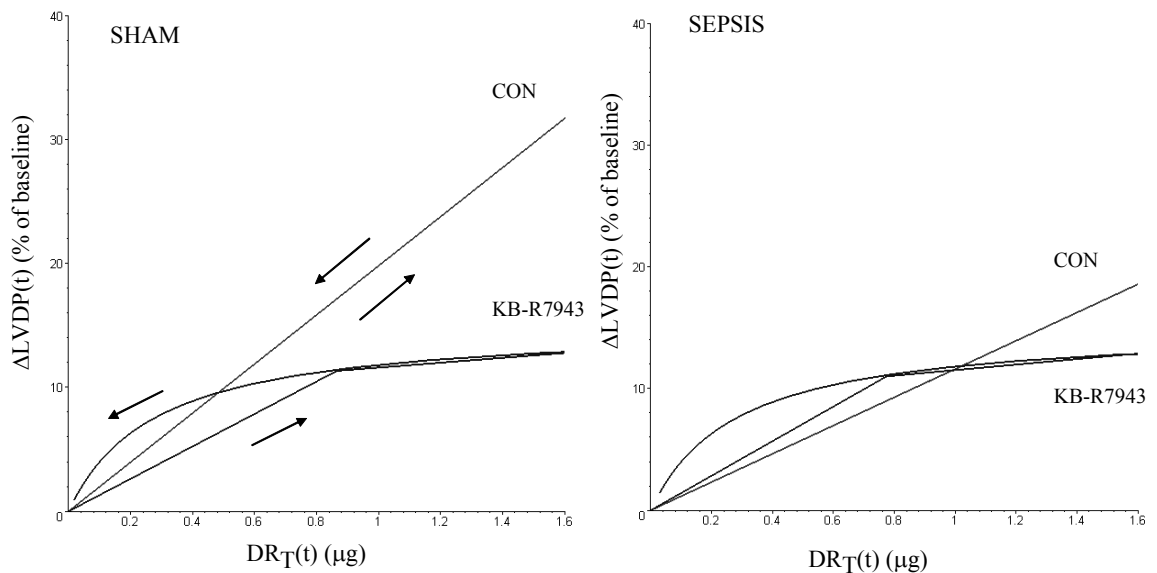


**Figure 33.** Model simulations of the relationship between total receptor and occupancy [ $DR_T(t)$ ] and inotropic response (phase-plane plot) under control conditions and after NCX inhibition by KB-R7943 for digoxin.

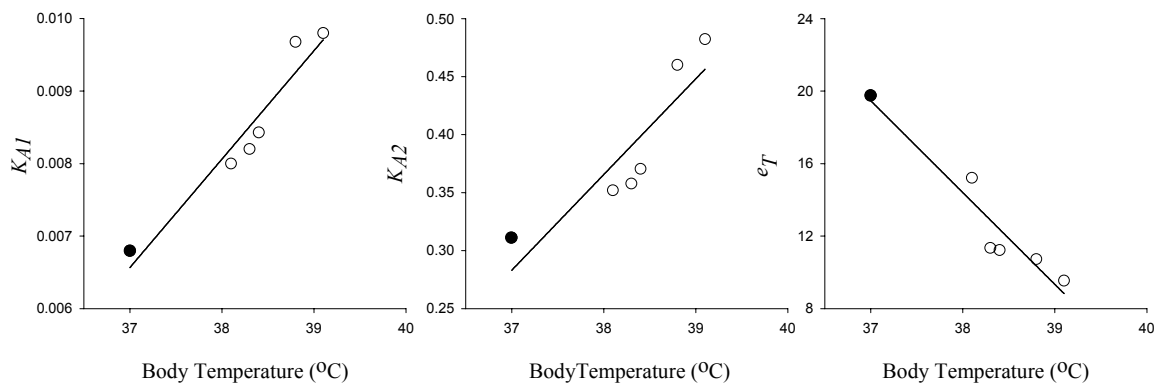


**Figure 34.** The correlation between parameters of digoxin action and LPS-induced rise in body temperature: (A) affinity of  $\alpha_1$  receptors ( $r^2 = 0.93$ ,  $P < 0.01$ ), (B) affinity of  $\alpha_2$  receptors and ( $r^2 = 0.91$ ,  $P < 0.01$ ) and (C) stimulus-response ratio ( $r^2 = 0.92$ ,  $P < 0.01$ ). The filled circles are the means of the vehicle group and the solid curves are the linear regression lines (all slopes different from zero,  $P < 0.01$ ).

Also the effects of sepsis on  $\text{Na}^+, \text{K}^+$ -ATPase remain unclear, despite numerous investigations. That endotoxemia slightly increased the affinity of  $\text{Na}^+, \text{K}^+$ -ATPases to digoxin could be interpreted as the consequence of an increased pump activity (e.g., Clausen, 2003). This would be in accordance with the effect of sepsis on skeletal muscle  $\text{Na}^+, \text{K}^+$ -ATPase activity (O'Brien et al., 1996; Bundgaard et al., 1996), but in contrast to the finding by Schornack et al. (1997) of a reduced transport activity of the  $\text{Na}^+$  pump in septic rat hearts (where, however, sepsis was not accompanied by a decrease in contractility).

A limitation of this approach is that due to the underlying identifiability problem the parameter estimation procedure had to be based on *a priori* values of the receptor affinity and capacity ratios,  $K_{A,2}/K_{A,1}$  and  $R_{tot,1}/R_{tot,2}$ . Since relevant information was lacking for the septic heart, we left these ratios unchanged. Although this assumption led to a satisfactory fit of the data from the LPS-group, this only means that the resulting set of parameter estimates is in accordance with the measurements, i.e., this analysis does theoretically not provide not unique answer. In other words, our inferences are only as good as the validity of the assumptions underlying the model.

### 5. Summary

This study investigates cardiac uptake, receptor binding kinetics and the positive inotropic effect of digoxin in normal, hypertrophic and septic rat hearts using a mathematical modeling approach.

Pharmacokinetic/Pharmacodynamic modeling provides information about the mechanisms of drug action, which is unavailable from equilibrium studies. This methodology for the nondestructive measurement of membrane transport and receptor binding kinetics in intact hearts provides, for the first time, an integrated description of cardiac kinetics and dynamics of digitalis drugs. It is possible that the results may resolve some of the controversy regarding the functional role of Na<sup>+</sup>,K<sup>+</sup>-ATPase isoforms. Passive transcapillary uptake followed by binding to two distinct sarcolemmal receptor populations determines cardiac kinetics and, in accordance with the pump inhibition hypothesis, also the inotropic effect of digoxin. The time course of inotropic response was linked to receptor occupation, i.e., consecutive inhibition of first the  $\alpha_2$ - and then the  $\alpha_1$ - isoform of Na<sup>+</sup>,K<sup>+</sup>-ATPase mediates the positive inotropic effect of digoxin with increasing dosage.

Digoxin sensitivity increased with decreasing external Ca<sup>2+</sup> concentration due to higher stimulus amplification. Na<sup>+</sup>/Ca<sup>2+</sup> exchanger inhibition with KB-R7943 significantly reduced the positive inotropic effect of digoxin at higher doses, 30 and 45  $\mu$ g and led to a saturated and delayed receptor occupancy-response relationship in the cellular effectuation model. The results provide further evidence for the functional heterogeneity of the Na<sup>+</sup>,K<sup>+</sup>-ATPase and suggest that in the presence of KB-R7943 a reduction of the Ca<sup>2+</sup> influx rate via the reverse mode Na<sup>+</sup>/Ca<sup>2+</sup> exchanger might become the limiting factor in digoxin response generation.

This study was also designed to clarify the complex experimental results on cardiac hypertrophy induced changes in inotropic response to cardiac glycosides. The results of this study indicated that isoprenaline induced cardiac hypertrophy reduces the development of inotropic effect per inhibited sodium pump. In the hypertrophied rat heart, the amount of  $\alpha_2$  receptors was significantly reduced and digoxin binding affinity was increased due to a decrease in dissociation rate constants of both receptor

## 5. Summary

---

subtypes. The inotropic responsiveness to digoxin was attenuated on the stimulus-response level. Coadministration of KB-R7943 significantly reduced cellular response generation at higher digoxin doses to the same limiting stimulus-response relationship in both groups. In lipopolysaccharide (endotoxin) induced sepsis, baseline contractility and inotropic response to digoxin were attenuated. The decrease in the stimulus-response ratio and the increase in receptor affinity were correlated with rise in body temperature (fever).

The modeling approach combined with specifically designed experiments offers a quantitative understanding of effects of decreasing external  $\text{Ca}^{2+}$  concentration and  $\text{Na}^+/\text{Ca}^{2+}$  exchanger inhibition on inotropic response of digoxin in normal and diseased rat hearts. It allows differentiation between the effects elicited at the receptor and postreceptor level and provides parameters characterizing the functional heterogeneity of the  $\text{Na}^+,\text{K}^+$ -ATPase. The model analysis also allowed, for the first time, to elaborate the effects of cardiac hypertrophy and sepsis on the positive inotropic response to digoxin.

These results may provide a better understanding of cardiac pharmacokinetics and pharmacodynamics of digoxin in normal and diseased hearts.

## 6. Zusammenfassung und Ausblick

Diese Arbeit untersucht den kardialen Transport, die Rezeptor-Bindungskinetik und den positiv-inotropen Effekt von Digoxin in normalen, hypertrophierten und septischen Rattenherzen unter Anwendung eines mathematischen Modells.

Die Methode der Pharmakokinetik/Pharmakodynamik-Modellierung liefert Informationen über den Mechanismus der Arzneimittelwirkung, die mit Hilfe von Steady-state-Experimenten nicht gewonnen werden können. Diese Methode der nicht-destruktiven Messungen des Membrantransports und der Rezeptor-Bindungskinetik am intakten Herzen liefert erstmalig eine integrierte Beschreibung der kardialen Kinetik und Dynamik von Herzglykosiden. Es ist möglich, dass die Ergebnisse der Arbeit offene Fragen bezüglich der funktionellen Rolle der  $\text{Na}^+, \text{K}^+$ -ATPase- Isoformen, die gegenwärtig noch kontrovers diskutiert werden, erklären können. Passiver transkapillärer Transport, gefolgt von der Bindung an zwei verschiedene sarkolemmale Rezeptorpopulationen, bestimmt die kardiale Kinetik und, in Übereinstimmung mit der Pumpenhemmungs-Hypothese, auch den inotropen Effekt von Digoxin. Der Zeitverlauf des inotropen Effektes war der funktionellen Rezeptor-Besetzung (Stimulus) proportional, d.h. die konsekutive Hemmung der  $\alpha_2$ - und dann der  $\alpha_1$ -Isoformen der  $\text{Na}^+, \text{K}^+$ -ATPase vermittelt den positiv-inotropen Effekt von Digoxin bei Dosissteigerung.

Die Digoxin-Empfindlichkeit wird mit abnehmender externer Kalzium-Konzentration in Folge einer gesteigerten Stimulusverstärkung erhöht. Eine Hemmung des Na/Ca-Austauschers durch KB-R7943 verminderte den Digoxin induzierten positiv-inotropen Effekt besonders bei höheren Dosen (30 und 45  $\mu\text{g}$ ) (wahrscheinlich in Folge einer Hemmung des Kalzium-Einstroms) und führte zu einer gesättigten und verzögerten Rezeptorbesetzungs-Effekt-Beziehung. Die Ergebnisse liefern weitere Hinweise für eine funktionelle Heterogenität der  $\text{Na}^+, \text{K}^+$ -ATPase und lassen vermuten, dass die durch KB-R7943 vermittelte Reduktion des Kalzium-Einstroms über den Na/Ca-Austauscher (reverse mode) der begrenzende Faktor in der Erzeugung des Digoxin-Effektes ist.

Ein weiteres Ziel der Arbeit war die Klärung der komplexen experimentellen Resultate über die veränderten inotropen Effekte von Herzglykosiden in hypertrophierten Herzen. Die Ergebnisse zeigen, dass eine Isoprenalin-induzierte Herzhypertrophie die Erzeugung des inotropen Effektes von Digoxin pro gehemmter Na-Pumpe reduziert. Die Dichte der  $\alpha_2$ -Rezeptoren war signifikant reduziert und die ihre Digoxin-Bindungsaffinität erhöht (in Folge eine Abnahme der Dissoziationsgeschwindigkeitskonstanten beider Rezeptortypen. Die inotrope Wirkung von Digoxin wurde auf zellulärem Niveau (Stimulus-Effekt-Beziehung) vermindert. Unter dem Einfluss von KB-R7943 wurde die Effektentwicklung bei höheren Digoxin-Dosen auf die gleiche begrenzende Stimulus-Effekt-Beziehung in beiden Gruppen reduziert. In durch Lipopolysaccharid (Endotoxin) induzierter Sepsis wurde die kardiale Kontraktilität und der inotrope Effekt von Digoxin vermindert. Die Abnahme des Stimulus-Effekt-Kopplungsfaktors und die Erhöhung der Rezeptoraffinität waren signifikant mit dem Ansteigen der Körpertemperatur (Fieber) korreliert.

Die Anwendung des mathematischen Modells in Kombination mit spezifisch geplanten Experimenten erlaubt eine quantitatives Verstehen der Konsequenzen einer abnehmenden Kalzium-Konzentration und einer Hemmung des Na/Ca-Austauschers auf den inotropen Effekt von Digoxin im normalen und erkrankten Rattenherzen. Die Methode gestattet eine Differenzierung zwischen den Effekten auf dem Rezeptor- und Postrezeptor-Niveau und liefert Parameter, die die funktionelle Heterogenität der  $\text{Na}^+, \text{K}^+$ -ATPase charakterisieren. Das Modell erlaubt außerdem erstmalig eine Erklärung der Effekte der kardialen Hypertrophy und Sepsis auf die Digoxin-Wirkung. Die Ergebnisse tragen zu einem besseren Verständnis der kardialen Pharmakokinetik und Pharmakodynamik von Digoxin in normalen und krankhaft veränderten Herzen bei.

### 7. References

- Askew GR, Lingrel JB, Grupp IL, and Grupp G. Direct correlation of Na<sup>+</sup>,K<sup>+</sup>-ATPase isoform abundance and myocardial contractility in mouse heart, in *The Sodium Pump Structure Mechanism, Hormonal Control and Its Role in Disease*. pp 718–721, Springer-Steinkopff, Darmstadt, Germany, 1994.
- Badenhorst D, Veliotes D, Maseko M, Tsoetsi OJ, Brooksbank R, Naidoo A, Woodiwiss AJ, Norton GR. Beta-adrenergic activation initiates chamber dilatation in concentric hypertrophy. *Hypertension*. 41:499-504 (2003).
- Benjamin IJ, Jalil JE, Tan LB, Cho K, Weber KT, Clark WA. Isoproterenol-induced myocardial fibers in relation to myocyte necrosis. *Circ Res*. 65:657-670 (1989).
- Berrebi-Bertrand I, Lelievre LG, Mouas C, Swynghedauw B. Inotropic effect of ouabain in hypertrophied rat heart. *Pflugers Arch*. 417:247-254 (1990).
- Bers DM. Cardiac excitation-contraction coupling. *Nature* 415:198-205 (2002).
- Bers DM, Barry WH, and Despa S. Intracellular Na<sup>+</sup> regulation in cardiac myocytes. *Cardiovasc Res*. 57:897-912 (2003).
- Bers DM. Cardiac Na<sup>+</sup>/Ca<sup>2+</sup> exchange function in rabbit, mouse and man: what's the difference? *J Mol Cell Cardiol*. 34:369-373 (2002).
- Bers DM. *Excitation-contraction coupling and cardiac contractile force*. Kluwer academic. Dordrecht, Netherlands, ed. 2, 2001.
- Billman GE. KB-R7943. Kanebo. *Curr. Opin. Investig. Drugs*. 2: 1740-1745 (2001).
- Blanco G and Mercer RW. Isozymes of the Na<sup>+</sup>,K<sup>+</sup>-ATPase: heterogeneity in structure, diversity in function. *Am J Physiol*. 275:F633–F650 (1998).
- Blaustein MP and Lederer WJ. Na<sup>+</sup>/Ca<sup>2+</sup> exchange: its physiological implications. *Physiol Rev*. 79: 763-854 (1999).
- Bolck B, Munch G, Mackenstein P, Hellmich M, Hirsch I, Reuter H, Hattebuhr N, Weig HJ, Ungerer M, Brixius K, Schwinger RH. Na<sup>+</sup>/Ca<sup>2+</sup> Exchanger Overexpression Impairs Frequency- and Ouabain-Dependent Cell-Shortening in Adult Rat Cardiomyocytes. *Am J Physiol Heart Circ Physiol*. 287:H1435-1445 (2004).
- Boluyt MO, Long X, Eschenhagen T, Mende U, Schmitz W, Crow MT, Lakatta EG. Isoproterenol infusion induces alterations in expression of hypertrophy-associated genes in rat heart. *Am J Physiol* 269:H638-647 (1995).
- Book CB, Moore RL, Semanchik A, Ng YC. Cardiac hypertrophy alters expression of Na<sup>+</sup>,K<sup>+</sup>-ATPase subunit isoforms at mRNA and protein levels in rat myocardium. *J Mol Cell Cardiol*. 26:591-600 (1994).
- Breimer DD and Danhof M. Relevance of the application of pharmacokinetic /pharmacodynamic modelling concepts in drug development. The “wooden shoe” paradigm. *Clin Pharmacokinet*. 32:259–267 (1997).
- Bridge JHB, Smolley JR, Spitzer KW. The relationship between charge movements associated with I<sub>Ca</sub> and I<sub>Na-Ca</sub> in cardiac myocytes. *Science*. 248:376-378 (1990).
- Briest W, Holzl A, Ressler B, Deten A, Leicht M, Baba HA, Zimmer HG. Cardiac remodeling after long term norepinephrine treatment in rats. *Cardiovasc Res*. 52:265-273 (2001).



## 7. References

---

- Bundgaard H, Kjeldsen K, Suarez Krabbe K, van Hall G, Simonsen L, Qvist J, Hansen CM, Moller K, Fonsmark L, Lav Madsen P, Klarlund Pedersen B. Endotoxemia stimulates skeletal muscle  $\text{Na}^+\text{-K}^+$ -ATPase and raises blood lactate under aerobic conditions in humans. *Am J Physiol Heart Circ Physiol*. 284:H1028-H1034 (2003).
- Caldwell JH, Kroll K, Li Z, Seymour K, Link JM, and Krohn KA. Quantitation of presynaptic cardiac sympathetic function with carbon-11-meta-hydroxyephedrine. *J Nucl Med*. 39: 1327-1334 (1998).
- Capogrossi MC, Kort AA, Spurgeon HA, Lakotta EG. Single adult rabbit and rat cardiac myocytes retain the  $\text{Ca}^{2+}$ - and species-dependent systolic and diastolic contractile properties of intact muscle. *J Gen Physiol* 88:589-613 (1986).
- Chambers DJ, Braimbridge MV, and Hearse DJ. Perfusate calcium: effect on cardiac stability and response to ischemia and reperfusion. *Can J Cardiol*. 7:410-418 (1991).
- Chaoshu T, Jung Y, Li-Ling W, Lin-Wang D and Maw-Shung L Phosphorylation of beta-adrenergic receptor lead to its redistribution in rat heart during sepsis. *Am J Physiol Regul Integr Comp Physiol* 274: R1078-R1086 (1998).
- Charlemagne D, Orłowski J, Oliviero P, Rannou F, Sainte Beuve C, Swynghedauw B, Lane LK. Alteration of  $\text{Na}^+\text{-K}^+$ -ATPase subunit mRNA and protein levels in hypertrophied rat heart. *J Biol Chem*. 269:1541-1547 (1994).
- Charlemagne D, Swynghedauw B. Myocardial phenotypic changes in  $\text{Na}^+\text{-K}^+$ -ATPase in left ventricular hypertrophy: pharmacological consequences. *Eur Heart J* 16 Suppl C:20-23 (1995).
- Chevalier B, Mouas C, Mansier C, Aumont MC, Swynghedauw B. Screening of inotropic drugs on isolated rat and guinea pig heart. *J Pharmacol Methods* 17:313-326 (1987).
- Chevalier B, Berrebi-Bertrand I, Mouas C, Lelievre LG, Swynghedauw B. Diminished toxicity of ouabain in the hypertrophied rat heart. *Pflugers Arch*. 414:311-316 (1989).
- Chorvatova A, Hart G, Hussain M.  $\text{Na}^+\text{-Ca}^{2+}$  exchange current ( $I(\text{Na}/\text{Ca})$ ) and sarcoplasmic reticulum  $\text{Ca}^{2+}$  release in catecholamine-induced cardiac hypertrophy. *Cardiovasc Res*. 61:278-287 (2004).
- Clausen T.  $\text{Na}^+\text{-K}^+$  pump regulation and skeletal muscle contractility. *Physiol Rev*. 83(4):1269-1324 (2003).
- Court O, Kumar A, Parrillo JE. Clinical review: Myocardial depression in sepsis and septic shock. *Crit Care*. 6:500-508 (2002).
- D'Argenio DZ and Schumitzky A. *ADAPT II User's guide: Pharmacokinetic/Pharmacodynamic Systems Analysis Software*. Biomedical Simulations Resource, Los Angeles, 1997.
- Derendorf H, Meibohm B, Modeling of pharmacokinetic/pharmacodynamic(PK/PD) relationships: concepts and perspectives. *Pharm. Res*. 16(2), 176-185 (1999).
- Dobson GP and Cieslar JH. Intracellular, interstitial and plasma spaces in the rat myocardium in vivo. *J Mol Cell Cardiol*. 29:3357-3363 (1997).
- Donahue JK, Kikkawa K, Thomas AD, Marban E, and Lawrence JH. Acceleration of widespread adenoviral gene transfer to intact rabbit hearts by coronary perfusion with low calcium and serotonin. *Gene Ther*. 5: 630-634 (1998).
- Dostanic I, Lorenz JN, Schultz Jel J, Grupp IL, Neumann JC, Wani MA, and Lingrel JB. The alpha2 isoform of  $\text{Na}^+\text{-K}^+$ -ATPase mediates ouabain-induced cardiac inotropy in mice. *J Biol Chem*. 278:53026-53034 (2003).

## 7. References

---

Eisner DA and Smith TW. The Na<sup>+</sup>,K<sup>+</sup> pump and its effectors in cardiac muscle, in *The Heart and Cardiovascular System* (Fozzard HA, Haber E, Katz AM, and Morgan HE eds.) pp 863–902, Raven Press, New York, 1992.

Elias CL, Lukas A, Shurraw S, Scott J, Omelchenko A, Gross GJ, Hnatowich M, and Hryshko LV. Inhibition of Na<sup>+</sup>/Ca<sup>2+</sup> exchange by KB-R7943: transport mode selectivity and antiarrhythmic consequences. *Am J Physiol Heart Circ Physiol*. 281: H1334-H1345 (2001).

Fauvel H, Marchetti P, Obert G, Joulain O, Chopin C, Formstecher P, Neviere R. Protective effects of cyclosporin A from endotoxin-induced myocardial dysfunction and apoptosis in rats. *Am J Respir Crit Care Med*. 15:165(4):449-455 (2002).

Fedorova OV, Talan MI, Agalakova NI, Lakatta EG and Bagrov AY Coordinated shifts in Na/K-ATPase isoforms and their endogenous ligands during cardiac hypertrophy and failure in NaCl-sensitive hypertension. *J Hypertens* 22:389-397 (2004).

Forester GV and Mainwood GW. Interval dependent inotropic effects in the rat myocardium and the effect of calcium. *Pflugers Arch*. 352: 189-196 (1974).

Gao J, Mathias RT, Cohen IS, and Baldo GJ. Two functionally different Na<sup>+</sup>/K<sup>+</sup> pumps in cardiac ventricular myocytes. *J Gen Physiol*. 106: 995-1030 (1995).

Gaszner B, Simor T, Hild G, and Elgavish GA. The effects of the NMR shift-reagents Dy(PPP)2, Dy(TTHA) and Tm(DOTP) on developed pressure in isolated perfused rat hearts. The role of shift-reagent calcium complexes. *J Mol Cell Cardiol*. 33: 1945-1956 (2001).

Golden KL, Ren J, O'Connor J, Dean A, DiCarlo SE, Marsh JD. In vivo regulation of Na<sup>+</sup>/Ca<sup>2+</sup> exchanger expression by adrenergic effectors. *Am J Physiol Heart Circ Physiol*. 280:H1376-1382 (2001).

Golovina VA, Song H, James PF, Lingrel JB, and Blaustein MP. Na<sup>+</sup> pump alpha 2-subunit expression modulates Ca<sup>2+</sup> signaling. *Am J Physiol Cell Physiol*. 284: C475-C486 (2003).

Grandel U, Fink L, Blum A, Heep M, Buerke M, Kraemer HJ, Mayer K, Bohle RM, Seeger W, Grimminger F, Sibelius U. Endotoxin-induced myocardial tumor necrosis factor-alpha synthesis depresses contractility of isolated rat hearts: evidence for a role of sphingosine and cyclooxygenase-2-derived thromboxane production. *Circulation*.102(22):2758-2764 (2000).

Grupp I, Im WB, Lee CO, Lee SW, Pecker MS, and Schwartz A. Relation of sodium pump inhibition to positive inotropy at low concentrations of ouabain in rat heart muscle. *J Physiol*. 360:149–160 (1985).

Guild S-J, Ward M-L, Cooper PJ, Hanley PJ, and Loiselle DS. Extracellular Ca<sup>2+</sup> is obligatory for ouabain-induced potentiation of cardiac basal energy expenditure. *Clin Exp Pharmacol Physiol*. 30: 103-109 (2003).

Harold F, Philippe M, Guillaume O, Olivier J, Claude C, Pierre F and Remi N Protective effects of Cyclosporin A from endotoxin-induced myocardial dysfunction and apoptosis in rats. *Am J Respir Crit Care Med* 165:449-455 (2002).

Harrison SM, McCall E, and Boyett MR. The relationship between contraction and intracellular sodium in rat and guinea-pig ventricular myocytes. *J Physiol*. 449: 517-550 (1992).

Hickerson TW, Grupp IL, Schwartz A, and Grupp G. The calcium dependence of the biphasic inotropic response to ouabain in the isolated rat heart. *Prog Clin Biol Res*. 258: 223-234 (1988).

Holford NHG and Sheiner LB. Understanding the dose-effect relationship. *Clin.Pharmacokinet*. 6:429-453 (1981).

## 7. References

---

- Houser SR, Margulies KB. Is depressed myocyte contractility centrally involved in heart failure? *Circ Res.* 92:350-358 (2003).
- Inserte J, Garcia-Dorado D, Ruiz-Meana M, Padilla F, Barrabes JA, Pina P, Agullo L, Piper HM, and Soler-Soler J. Effect of inhibition of  $\text{Na}^+/\text{Ca}^{2+}$  exchanger at the time of myocardial reperfusion on hypercontracture and cell death. *Cardiovasc Res.* 55: 739-748 (2002).
- Irlbeck M, Muhling O, Iwai T, Zimmer HG. Different response of the rat left and right heart to norepinephrine. *Cardiovasc. Res.* 31:157-162 (1996).
- Ishizuka N, Fielding AJ, and Berlin JR. Na pump current can be separated into ouabain-sensitive and – insensitive components in single rat ventricular myocytes. *Jap J Physiol.* 46: 215-223 (1996).
- James PF, Grupp IL, Grupp G, Woo AL, Askew GR, Croyle ML, Walsh RA, and Lingrel JB. Identification of a specific role for the  $\text{Na}^+,\text{K}^+$ -ATPase alpha 2 isoform as a regulator of calcium in the heart. *Mol Cell.* 3: 555-563 (1999).
- Kang W and Weiss M. Digoxin uptake, receptor heterogeneity, and inotropic response in the isolated rat heart: A comprehensive kinetic model. *J Pharmacol Exp Ther.* 302:577-583 (2002).
- Kenakin T. *Pharmacologic Analysis of Drug-Receptor Interaction.* Raven Press, New York, 1993.
- Khadour FH, Panas D, Ferdinandy P, Schulze C, Csont T, Lalu MM, Wildhirt SM, Schulz R. Enhanced NO and superoxide generation in dysfunctional hearts from endotoxemic rats. *Am J Physiol Heart Circ Physiol.* 283(3):H1108-H1115 (2002).
- Kitano H. Systems Biology: A Brief Overview. *Science* 295: 1662-1664 (2002).
- Kojima S, Wu ST, Wikman-Coffelt J, and Parmley WW. Acute effects of ethanol on cardiac function and intracellular calcium in perfused rat heart. *Cardiovasc Res.* 27:811–816 (1993).
- Kometiani P, Askari A, Liu J, Xie Z, and Askari FK. Downregulation of cardiac myocyte  $\text{Na}^+,\text{K}^+$ -ATPase by adenovirus-mediated expression of an alpha-subunit fragment. *Am J Physiol.* 280: H1415-H1421 (2001).
- Ladilov Y, Haffner S, Balsler-Schafer C, Maxeiner H, and Piper HM. Cardioprotective effects of KB-R7943: a novel inhibitor of the reverse mode of  $\text{Na}^+/\text{Ca}^{2+}$  exchanger. *Am J Physiol.* 276: H1868-H1876 (1999).
- Larsen JS, Schmidt TA, Bundgaard H, Kjeldsen K. Reduced concentration of myocardial  $\text{Na}^+,\text{K}^+$ -ATPase in human aortic valve disease as well as of  $\text{Na}^+,\text{K}^+$ - and  $\text{Ca}^{2+}$ -ATPase in rodents with hypertrophy. *Mol Cell Biochem.* 169:85-93 (1997).
- Laycock SK, McMurray J, Kane KA, Parratt JR. Effects of chronic norepinephrine administration on cardiac function in rats. *J Cardiovasc Pharmacol.* 26:584-589 (1995).
- Lelievre LG, Crambert G, Allen PD. Expression of functional  $\text{Na}^+,\text{K}^+$ -ATPase isozymes in normal human cardiac biopsies. *Cell Mol Biol.* 47:265-271 (2001).
- Lelievre LG, Maixent JM, Lorente P, Mouas C, Charlemagne D, Swynghedauw B. Prolonged responsiveness to ouabain in hypertrophied rat heart: physiological and biochemical evidence. *Am J Physiol.* 50:H923-H931 (1986).
- Levi AJ, Boyett MR, and Lee CO. The cellular actions of digitalis glycosides on the heart. *Prog Biophys Mol Biol.* 62:1-54 (1994).
- Levy RJ, Deutschman CS. Evaluating myocardial depression in sepsis. *Schock.* 22:1-10 (2004).
- Liu MS, Ghosh S. Myocardial sodium pump activity in endotoxin shock. *Circ Shock* 19:177-184 (1986).

## 7. References

---

- Liu MS, Xuan YT. Mechanisms of endotoxin-induced impairment in  $\text{Na}^+/\text{Ca}^{2+}$  exchange in canine myocardium. *Am J Physiol.* 251:R1078-R1085 (1986).
- Liu X, Songu-Mize E. Alterations in alpha subunit expression of cardiac  $\text{Na}^+, \text{K}^+$ -ATPase in spontaneously hypertensive rats: effect of antihypertensive therapy. *Eur J Pharmacol.* 327:151-156 (1997).
- Lopez LB, Quintas LE, and Noel F. Influence of development on  $\text{Na}^+/\text{K}^+$ -ATPase expression: isoform- and tissue-dependency. *Comp Biochem Physiol A Mol Integr Physiol.* 131: 323-333 (2002).
- Lucchesi PA and Sweadner KJ. Postnatal changes in  $\text{Na}^+, \text{K}^+$ -ATPase isoform expression in rat cardiac ventricle. Conservation of biphasic ouabain affinity. *J Biol Chem.* 266:9327-9331 (1991).
- Mager DE and Jusko WJ. Pharmacodynamic modeling of time-dependent transduction systems. *Clin Pharmacol Ther.* 70:210-216 (2001) a.
- Mager DE and Jusko WJ. General pharmacokinetic model for drugs exhibiting target-mediated drug disposition. *J Pharmacokinetic Pharmacodyn.* 28:507-532 (2001) b.
- Magyar CE, Wang J, Azuma KK, McDonough AA. Reciprocal regulation of cardiac  $\text{Na}^+, \text{K}^+$ -ATPase and  $\text{Na}^+/\text{Ca}^{2+}$  exchanger: hypertension, thyroid hormone, development. *Am J Physiol.* 269:C675-C682 (1995).
- Mathias RT, Cohen IS, Gao J, and Wang Y. Isoform-Specific Regulation of the  $\text{Na}^+ - \text{K}^+$  Pump in Heart. *New. Physiol Sci.* 15:176-180 (2000).
- McDonough AA, Velotta JB, Schwinger RH, Philipson KD, Farley RA. The cardiac sodium pump: structure and function. *Basic Res Cardiol.* 97 Suppl 1:119-124 (2002).
- McDonough AA, Wang J, and Farley RA. Significance of sodium pump isoforms in digitalis therapy. *J Mol Cell Cardiol.* 27:1001-1009 (1995).
- Minakawa M, Takeuchi K, Ito K, Tsushima T, Fukui K, Takaya S, Fukuda I. Restoration of sarcoplasmic reticulum protein level by thyroid hormone contributes to partial improvement of myocardial function, but not to glucose metabolism in an early failing heart. *Eur J Cardiothorac Surg.* 24:493-501 (2003).
- Muller-Ehmsen J, Nickel J, Zobel C, Hirsch I, Bolck B, Brixius K, Schwinger RH. Longer term effects of ouabain on the contractility of rat isolated cardiomyocytes and on the expression of  $\text{Ca}^{2+}$  and  $\text{Na}^+$  regulating proteins. *Basic Res Cardiol.* 98:90-96 (2003).
- Noel F and Godfraind T. Heterogeneity of ouabain specific binding sites and  $\text{Na}^+, \text{K}^+$ -ATPase inhibition in microsomes from rat heart. *Biochem Pharmacol.* 33:47-53 (1984).
- Nunez-Duran H, Riboni L, Ubaldo E, Kabela E, and Barcenas-Ruiz L. Ouabain uptake by endocytosis in isolated guinea pig atria. *Am J Physiol.* 255:C479-C485 (1988).
- O'Brian WJ, Lingrel JB, Fisher JE, Hasslgren PO. Sepsis increases skeletal muscle sodium, potassium-adenosinetriphosphatase activity without affecting messenger RNA or protein levels. *J Am Coll Surg.* 183:471-479 (1996).
- Pogwizd SM, Sipido KR, Verdonck F, Bers DM. Intracellular  $\text{Na}^+$  in animal models of hypertrophy and heart failure: contractile function and arrhythmogenesis. *Cardiovasc Res.* 57:887-896 (2003).
- Repke K, Est M and Portius HJ. On the cause of species differences in digitalis sensitivity. *Biochem Pharmacol.* 14(12):1785-1802 (1965).
- Reuter H, Henderson SA, Han T, Ross RS, Goldhaber JJ, and Philipson KD. The  $\text{Na}^+ - \text{Ca}^{2+}$  exchanger is essential for the action of cardiac glycosides. *Circ Res.* 90:305-308 (2002).

## 7. References

---

- Rona G, Chappel CI, Balazs T, Gaudry R, An infarct-like myocardial lesion and other toxic manifestations produced by isoproterenol in the rat. *Am Med Assoc Arch Pathol.* 67:99-111 (1959).
- Ruch SR, Nishio M, and Wasserstrom JA. Effect of Cardiac Glycosides on Action Potential Characteristics and Contractility in Cat Ventricular Myocytes: Role of Calcium Overload. *J Pharmacol Exp Ther.* 307:419-428 (2003).
- Sagawa T, Sagawa K, Kelly JE, Tsushima RG, and Wasserstrom JA. Activation of cardiac ryanodine receptors by cardiac glycosides. *Am J Physiol.* 282:H1118-H1126 (2002).
- Sahin-Erdemli I, Medford RM, Songu-Mize E. Regulation of Na<sup>+</sup>,K<sup>+</sup>-ATPase alpha-subunit isoforms in rat tissues during hypertension. *Eur J Pharmacol.* 292:163-171 (1995).
- Satoh H, Ginsburg KS, Qing K, Terada H, Hayashi H, and Bers DM. KB-R7943 block of Ca<sup>2+</sup> influx via Na<sup>+</sup>/Ca<sup>2+</sup> exchange does not alter twitches or glycoside inotropy but prevents Ca<sup>2+</sup> overload in rat ventricular myocytes. *Circulation* 101:1441-1446 (2000).
- Satoh H, Mukai M, Urushida T, Katoh H, Terada H, and Hayashi H. Importance of Ca<sup>2+</sup> influx by Na<sup>+</sup>/Ca<sup>2+</sup> exchange under normal and sodium-loaded conditions in mammalian ventricles. *Mol Cell Biochem.* 242: 11-17 (2003).
- Schornack PA, Song SK, Hotchkiss R, Ackerman JJ. Inhibition of ion transport in septic rat heart: 133Cs<sup>+</sup> as an NMR active K<sup>+</sup> analog. *Am J Physiol.* 272:C1635-C1641 (1997).
- Schultz Jel J, Glascock BJ, Witt SA, Nieman ML, Nattamai KJ, Liu LH, Lorenz JN, Shull GE, Kimball TR, Periasamy M. Accelerated onset of heart failure in mice during pressure overload with chronically decreased SERCA2 calcium pump activity. *Am J Physiol Heart Circ Physiol.* 286:H1146-H1153 (2004).
- Schwartz A and Petrashevskaya N. The importance of calcium in interpretation of Na<sup>+</sup>,K<sup>+</sup>-ATPase isoform function in the mouse heart. *Cardiovasc Res.* 51:9-12 (2001).
- Schwinger RH, Bundgaard H, Muller-Ehmsen J, Kjeldsen K. The Na<sup>+</sup>, K<sup>+</sup>-ATPase in the failing human heart. *Cardiovasc Res.* 57:913-920 (2003).
- Seki S, Taniguchi M, Takeda H, Nagai M, Taniguchi I, and Mochizuki S. Inhibition by KB-R7943 of the reverse mode of the Na<sup>+</sup>/Ca<sup>2+</sup> exchanger reduces Ca<sup>2+</sup> overload in ischemic-reperfused rat hearts. *Circ J* 66:390-396 (2002).
- Semb SO, Lunde PK, Holt E, Tonnessen T, Christensen G, Sejersted OM. Reduced myocardial Na<sup>+</sup>, K<sup>+</sup>-pump capacity in congestive heart failure following myocardial infarction in rats. *J Mol Cell Cardiol.* 30:1311-1328 (1998).
- Serikov VB, Petrashevskaya NN, Canning AM, Schwartz A. Reduction of Ca<sup>2+</sup> restores uncoupled b-adrenergic signaling in isolated perfused transgenic mouse hearts. *Circ. Res* 88:9-11 (2001).
- Shigekawa M and Iwamoto T. Cardiac Na<sup>+</sup>/Ca<sup>2+</sup> exchange: molecular and pharmacological aspects. *Circ Res.* 88: 864-876 (2001).
- Simor T, Lorand T, Gaszner B, and Elgavish GA. The modulation of pacing-induced changes in intracellular sodium levels by extracellular Ca<sup>2+</sup> in isolated perfused rat hearts. *J Mol Cell Cardiol.* 29: 1225-1235 (1997).
- Spiers JP, Kelso EJ, Allen JD, Silke B, McDermott BJ. Inotropic response to endothelin-1, isoprenaline and calcium in cardiomyocytes isolated from endotoxin treated rats: effects of ethylisothiourea and dexamethasone. *Br J Pharmacol.* 130:1275-1282 (2000).

## 7. References

---

- Stamm C, Cowan DB, Friehs I, Noria S, del Nido PJ, McGowan FX Jr. Rapid endotoxin-induced alterations in myocardial calcium handling: obligatory role of cardiac TNF- $\alpha$ . *Anesthesiology*. 95:1396-1405 (2001).
- Su Z, Sugishita K, Ritter M, Li F, Spitzer KW, and Barry WH. The sodium pump modulates the influence of  $[Na^+]_i$  on  $[Ca^{2+}]_i$  transients in mouse ventricular myocytes. *Biophys J*. 80:1230-1237 (2001).
- Sun X, Ng YC. Effects of norepinephrine on expression of IGF-1/IGF-1R and SERCA2 in rat heart. *Cardiovasc Res*. 37:202-209 (1998).
- Sweadner KJ, Herrera VL, Amato S, Moellmann A, Gibbons DK, Repke KR. Immunologic identification of  $Na^+,K^+$ -ATPase isoforms in myocardium. Isoform change in deoxycorticosterone acetate-salt hypertension. *Circ Res*. 74:669-678 (1994).
- Sweadner KJ. Multiple digitalis receptors. A molecular perspective. *Trends Cardiovasc Med*. 3:2-6 (1993).
- Szabo J, Nosztray K, Szegi J. Changes in sarcolemmal adenosine triphosphatase activity and in ouabain sensitivity of rat myocardium in isoproterenol-induced cardiac hypertrophy. *Pol J Pharmacol Pharm*. 41:553-559 (1989).
- Takeuchi K, del Nido PJ, Poutias DN, Cowan DB, Munakata M, McGowan FX, Jr, Vesnarinone restores contractility and calcium handling in early endotoxemia. *Circulation*. 102:III365-III369 (2000).
- Tavernier B, Mebazaa A, Mateo P, Sys S, Ventura-Clapier R, Veksler V. Phosphorylation-dependent alteration in myofilament  $Ca^{2+}$  sensitivity but normal mitochondrial function in septic heart. *Am J Respir Crit Care Med*. 163(2):362-367 (2001).
- Taylor PB and Tang Q. Development of isoproterenol-induced cardiac hypertrophy. *Can J Physiol Pharmacol*. 62:384-389 (1984).
- Thiemermann C The role of the L-arginine: nitric oxide pathway in circulatory shock. *Adv Pharmacol*. 28:45-79 (1994).
- Van der Graaf PH, Cox EH, Garrido KH, Van den Haak, Van Schaick, M. Danhof. *Measurement and kinetics of in vivo Drug effect: Advances in simultaneous pharmacokinetic/ pharmacodynamic modeling*. pp. 14-17, Leiden/Amsterdam Center for Drug Research, Leiden, Netherland 1998.
- Ver A, Szanto I, Banjasz T, Csermely P, Vegh E, and Somogyi J. Changes in the expression of  $Na^+/K^+$ -ATPase isoenzymes in the left ventricle of diabetic rat hearts: effect of insulin treatment. *Diabetologia* 40:1255-1262 (1997).
- Verdonck F, Volders PG, Vos MA, and Sipido KR. Intracellular  $Na^+$  and altered  $Na^+$  transport mechanisms in cardiac hypertrophy and failure. *J Mol Cell Cardiol*. 35:5-25 (2003).
- Vila Petroff MG, Palomeque J, and Mattiazzi AR.  $Na^+-Ca^{2+}$  exchange function underlying contraction frequency inotropy in the cat myocardium. *J Physiol*. 550:801-817 (2003).
- Wang J, Schwinger RHG, Frank K, Muelle-Ehmsen J, Martin-Vasallo P, Pressley TA, Xiang A, Erdmann E, McDonough AA. Regional expression of sodium pump subunits isoforms and  $Na^+/Ca^{2+}$  exchanger in the human heart. *J Clin Invest*. 98:1650-1658 (1996).
- Wang X, Yang J, Dong L, Pang Y, Su J, Tang C, Lin N. Alternation of  $Na^+-Ca^{2+}$  exchange in rat cardiac sarcolemmal membranes during different phases of sepsis. *Chin Med J(Engl)*. 113:18-21 (2000).
- Wang Z, Nolan B, Kutschke W, Hill JA.  $Na^+-Ca^{2+}$  exchanger remodeling in pressure overload cardiac hypertrophy. *J Biol Chem*. 276:17706-17711 (2001).

## 7. References

---

- Ward ML, Pope AJ, Loiselle DS, Cannell MB. Reduced contraction strength with increased intracellular  $\text{Ca}^{2+}$  in left ventricular trabeculae from failing rat hearts. *J Physiol.* 546:537-550 (2003).
- Weiss M and Kang W. P-Glycoprotein inhibitors enhance saturable uptake of idarubicin in rat heart: pharmacokinetic/pharmacodynamic modeling. *J Pharmacol Exp Ther.* 300:688-694 (2002).
- Weiss M, Kang W. Inotropic effect of digoxin in humans: mechanistic pharmacokinetic/pharmacodynamic model based on slow receptor binding. *Pharm Res.* 21:231-236 (2004).
- Weiss M. Cellular pharmacokinetics: Effects of cytoplasmic diffusion and binding on organ transit time distribution. *J Pharmacokin Biopharm.* 27:233-255 (1999).
- Willius FA, Keys TE, Withering W. An account of the foxglove and some of medical uses, with practical remarks on dropsy, and other diseases. *Classics of Cardiology*, New York NY Denver Publications Inc., 1:232-252 (1941).
- Wu LL, Tang C, Dong LW, Liu MS. Altered phospholamban-calcium ATPase interaction in cardiac sarcoplasmic reticulum during the progression of sepsis. *Shock.* 17(5):389-393 (2002).
- Xie Z and Askari A.  $\text{Na}^+/\text{K}^+$ -ATPase as a signal transducer. *Eur J Biochem.* 269:2434-2439 (2002).
- Yamamura K, Tani M, Hasegawa H, and Gen W. Very low dose of the  $\text{Na}^+/\text{Ca}^{2+}$  exchange inhibitor, KB-R7943, protects ischemic reperfused aged Fischer 344 rat hearts: considerable strain difference in the sensitivity to KB-R7943. *Cardiovasc Res.* 52:397-406 (2001).
- Yasuda S and Lew WY. Lipopolysaccharide depresses cardiac contractility and beta-adrenergic contractile response by decreasing myofilament response to  $\text{Ca}^{2+}$  in cardiac myocytes. *Circ Res.* 81:1011-1020 (1997).
- Zierhut W and Zimmer HG. Significance of myocardial alpha- and beta-adrenoceptors in catecholamine-induced cardiac hypertrophy. *Circ Res.* 65:1417-1425 (1989).

## **Publications**

Weiss M, Baek M., Kang W. Systems Analysis of Digoxin Kinetics and Inotropic Response in Rat Heart: Effects of Calcium and KB-R7943. *Am J Physiol Heart Circ Physiol.*287:H1857-H1867(2004).

Baek M and Weiss M. Downregulation of Na<sup>+</sup> pump  $\alpha_2$  isoform in isoprenaline-induced cardiac hypertrophy in rat: Evidence for increased receptor binding affinity but reduced inotropic potency of digoxin. *J Pharmacol Exp Ther.* 313:1-9(2005)

Baek M and Weiss M. Mechanism-based modeling of reduced inotropic responsiveness to digoxin in septic rat hearts. *Eur J Pharmacol.* (2005) *in press*

## **Abstract**

Baek M and Weiss M. Endotoxin-induced alterations in inotropic response to digoxin in the perfused rat heart; mechanistic PK/PD modeling. P1A-II-043 pp.115, "The Global Translation of Science into Drug Development in Advancing Therapy", *Pharmaceutical Sciences World Congress 2004*, Kyoto, Japan, May 30 – June 3. 2004



## **Acknowledgement**

I would like to express my sincere gratitude and appreciation to Professor Michael Weiss for providing me with the unique opportunity to work in the research area of *PK/PD* modeling, for his expert guidance and mentorship, and for his encouragement and support at all levels.

The financial support provided by 'Deutsche Forschungs Gemeinschaft' is greatly acknowledged.

I would like to express thanks to Mrs. Dagmar Günther and Sylvia Heidl for their great assistance and I also thank to my colleagues, Dr. Osama Abd Elrahman, Ms. Pakawadee Sermsappasuk for their kind assistance and help.

I wish to thank Prof. Ung-Kil Jee, at Chungnam National University, for his guidance and encouragement in the field of pharmaceutical research and also in my life.

To my beloved wife, Eunjin Cho, for being there to encourage me whenever I felt down on my way, and my two kids, Hyunwoong, Songiee, who serve joy of life, without their encouragement and understanding it would have been impossible for me to finish my work. I know that they have lost a lot due to my research abroad, I would like to give special thanks to my family and also to my father, brothers, sister and their families and parents-in-law in Korea for their love and encouragement.

Finally, I would like to give a special thanks to my mother in heaven for her endless love and sacrifices for me.

December 2004

Myoungki Baek

# Curriculum Vitae

## PERSONAL IDENTIFICATION

Name: MyoungKi Baek  
Address: Universitätsring 15  
06108 Halle (Saale), Germany  
Date of Birth: 1970.09.02  
Place of Birth: Daejon, South Korea  
Nationality: Korean  
Marital Status: Married, 2 children

## EDUCATION

03/1989 – 02/1994 Bachelor of Pharmacy at College of Pharmacy,  
Chungnam National University, Daejon, Korea  
03/1994 – 02/1996 Master of Science, Pharmaceutics at College of Pharmacy,  
Chungnam National University, Daejon, Korea  
Title: “Studies on the preparation of ketoprofen incorporated  
solid lipid nanoparticles (SLN) and the biopharmaceutical  
properties”  
08/2002 – 12/2004 Ph.D. Course at Section of Pharmacokinetics,  
Department of Pharmacology, Martin Luther University  
Halle-Wittenberg, Halle, Germany

## PROFESSIONAL EXPERIENCE

11/1999 – 07/2002 Senior Researcher, R&D Center of pharmaceuticals,  
Institute of Science & Technology, CJ Corporations Seoul, Korea  
01/1996 – 11/1999 Assistant Manager, Dept. of Manufacturing,  
Dongkook pharmaceuticals. Seoul, Korea

## License

04/1994 Pharmacist (Ministry of Health and Welfare, Korea)

## **Descloration**

I hereby declare that the work presented in this manuscript titled  
“Dynamic Systems Analysis of Receptor Interaction and Effectuation Mechanisms of  
Digoxin in the Rat Heart” is my own and was carried out entirely with help of literature  
and aid cited in the manuscript.

Halle, Germany

December 2004

Myoungki Baek